Proceedings of the

6th Oxford Tidal Energy Workshop

26-27 March 2018, Oxford, UK

Proceedings of the 6th Oxford Tidal Energy Workshop (OTE 2018)

26-27th March 2018

Monday 26th March

Session 1: Array Modelling (1)

Poster Presentations (1)

Session 2: Wake characteristics and turbulence (1)

Poster Presentations (2)

Session 3: Array Modelling (2)

EPSRC Engineering and Physical Sciences Research Council
UNIVERSITY OF OXFORD

27th March 2018

Session 4: Turbine Design and Performance (1)

Session 5: Turbine design and performance (2)

Poster Presentations (3)

Session 6: Wake characteristics and turbulence (2)

Workshop Organisers:

Richard H. J. Willden	(Chairman)	University of Oxford
Christopher R. Vogel	(Co-Chairman)	University of Oxford

Scientific Committee Members:

T. A. A. Adcock	(University of Oxford)	T. Stallard	(University of Manchester)
G. T. Houlsby	(University of Oxford)	P. K. Stansby	(University of Manchester)
I. Masters	(Swansea University)	C. R. Vogel	(University of Oxford)
T. Nishino	(Cranfield University)	R. H. J. Willden	(University of Oxford)

Sponsor:

Engineering and Physical Sciences Research Council (EPSRC)

EPSRC Engineering and Physical Sciences Research Council

UNIVERSITY OF OXFORD

Validation of an LES-ALM to simulate arrays of tidal turbines

Pablo Ouro*, Thorsten Stoesser
School of Engineering, Cardiff University, UK
Luis Ramirez
Group of Numerical Methods in Engineering, Universidade da Coruña, Spain
Magnus Harrold
College of Engineering, Mathematics and Physical Sciences, University of Exeter, UK

Summary: Co-location of turbines at sea sites requires careful attention to minimise wake-turbine interaction. Devices clustered too close may experience a detriment in power output and trigger loadings on those turbines operating in the wake of upstream turbines. High-fidelity computational models would allow to study the overall performance of tidal turbines arrangement. Combining Large-Eddy Simulation (LES) with Actuator Line Methods (ALM) allows to accurately predict the unsteady behaviour of turbine wakes, device loadings and thus helping to optimise wake-turbine interaction. An LES-ALM is herein well-validated with experimental results demonstrating its accuracy.

Introduction

Most tidal energy projects aim at deploying several devices in close proximity to each other to maximise the power output and to minimise the logistical challenges at selected offshore deployment sites. Tidal turbines convert the kinetic energy from fast-flowing tidal streams extracting momentum from the flow and consequently a low-momentum wake is generated behind each turbine. Turbines that operate in the wake of another turbine located upstream face several challenges in terms of high turbulence levels and lower approach flow velocity. Thus, the design of turbine farms requires knowledge of the turbine-turbine inter-play in order to avoid suboptimal performance and high hydrodynamic loads of turbines situated in the wake of others. In this context, accurate numerical methods are needed that allow studying different array configurations under varying flow conditions. In this research an LES-ALM approach is validated with experimental data and results show its adequacy to predict such flows.

Experimental setup

Stallard et al. [1] tested different arrays of Horizontal Axis Tidal Turbines (HATTs) in a hydraulic flume measuring 11.5m long (L), 5.4m wide (W) and 0.45m deep (h). The inflow velocity was measured along most of the water depth which followed a power law distribution with mean value (U_0) of 0.47m/s. A turbulence intensity of 12% in the flow direction was found with turbulence length scales $L_x = 0.56h$, $L_y = 0.33h$ and $L_z = 0.55h$. The scaled prototype had a diameter D=0.27m with blades designed with Göttingen 804 airfoil sections and rotated at a fixed tip speed ratio of 4.5 coinciding with the operation point of maximum performance. The blades are attached to a 0.05m long circular hub subsequently connected to a vertical tower that unites the rotor with the external support structure.

Large-Eddy Simulation – Actuator Line Method (LES-ALM)

The governing equations in LES (Eq. 1) are the spatially filtered Navier-Stokes equations for incompressible, turbulent, viscous flow. Staggered storage of velocities is adopted, and second order central differences are used to approximate flow derivatives. A fractional-step method with third order Runge-Kutta method are used to advance the simulation in time. WALE sub-grid scale model is used to calculate sub-grid stresses.

$$\Delta \cdot \mathbf{u} = 0 \quad ; \quad \partial \mathbf{u}/\partial t = -\nabla p + \nu \Delta \mathbf{u} - \nabla \tau - \mathbf{u} \cdot \nabla \mathbf{u} + f \tag{1}$$

An ALM is implemented in the open-source LES code Hydro3D, which has been previously validated for the simulation of HATTs adopting a geometry resolved method [2]. ALM divides each turbine blade into a number of sections of length Δr assuming constant chord length, c, and prescribed hydrodynamic characteristics, i.e. tabulated lift and drag coefficients (C_L,C_D). Each section is then represented by a single Lagrangian marker which moves freely along the computational mesh and delta functions [2] transfer velocities and forces between Lagrangian and Eulerian frameworks. At every time step, the relative velocity (V_{rel}) at each marker is calculated and used to compute the Lift (L) and Drag (D) forces to which a tip-loss correction term ($F1$ [3]) is also applied. These forces are projected onto the Cartesian coordinates of the Eulerian mesh obtaining the source term f (Eq. 2) present in the r.h.s. of the momentum equation and responsible for correcting the fluid velocities according to effect of the turbine. Note that both the turbine hubs and vertical support structures are modelled using the immersed boundary method [2].

$$f = (L,D) = 1/2 \cdot V_{rel}^2 \cdot (C_L\, e_L,\, C_D\, e_D) \cdot c \cdot \Delta r \cdot F1 \tag{2}$$

* Corresponding author.
Email address: ourobarbap@cardiff.ac.uk

Results

The computational domain is geometrically identical to the flume and is divided into 120 subdomains using three levels of local mesh refinement. The grid resolution is uniform and constant in the three spatial directions and Δx = 0.0045m is adopted on the finest mesh level in which the turbines are embedded, with 27 elements comprising each turbine blade. A fixed time step of Δt = 0.001s is adopted equating to approximately 2° of rotated angle per time step. The experimental velocity profile [1] is set at the inlet and an anisotropic synthetic eddy method superimposes turbulence fluctuations with the integral scales identical to those measured experimentally. Wall functions are imposed at the bottom channel bed and lateral walls while a shear-free slip condition is set at the top.

One configuration selected to firstly validate the LES-ALM considers 3 side-to-side turbines with hub-to-hub spacing of 1.5D. The prediction of power and thrust coefficient values are Cp=0.35 and Ct=0.87, respectively, which are in close agreement with the experimentally measured coefficients of Cp=0.32 and Ct=0.85. Contours of instantaneous streamwise velocity are presented in Fig. 1a and show how the turbines' wakes extend more than 20D downstream. The close intra-spacing between turbines generates a stream of high-velocity between the devices which progressively merges with the low-velocity areas.

Fig. 1b compares profiles of mean velocity deficit ($\Delta U=1-U/U_0$) at four sections in the wake between the present LES-ALM calculations and experimental results from Stallard et al. [1]. Overall, a good agreement is found with the computational model predicting well the flow behind the turbines. At x/D = 2, the computed flow field underestimates the peaks of velocity deficit due to fact turbines' geometry is modelled using a line which fails to resolve phenomena such as flow separation behind the blades or good resolution of tip vortices. Further downstream, at x/D = 8 and 12, the LES-predicted results still show a sinusoidal pattern whilst experiments indicate the individual turbine wakes have fully merged. Nonetheless, mean distribution of the velocity deficit is similar between numerical and experimental data.

Conclusions

The simulation results demonstrate the ability of the proposed LES-ALM to predict the wake developed downstream of tidal turbines as well as their performance and loadings. This computational model can accurately predict the wake behind the turbines and will serve to examine the behaviour of more arrays of turbines comprised of several rows of turbines with the aim of reducing negative inter-play between marine devices.

References:

[1] Stallard, T., Collings, R., Feng, T., Whelan, J. (2013) Interactions between tidal turbine wakes: experimental study of a group of three-bladed rotors. *Phil. Trans. R. Soc. A*. **371**, 20120159.

[2] Ouro, P., Harrold, M., Stoesser, T., Bromley, P. (2017). Hydrodynamic loadings on a horizontal axis tidal turbine prototype. *Journal of Fluids and Structures*.**71**, 78-95.

[3] Shen, W.Z., Sorensen J.N., Mikkelsen, R. (2005). Tip Loss Correction for Actuator/Navier-Stokes Computations. *ASME Journal of Fluids Engineering*.**127**, 209-213.

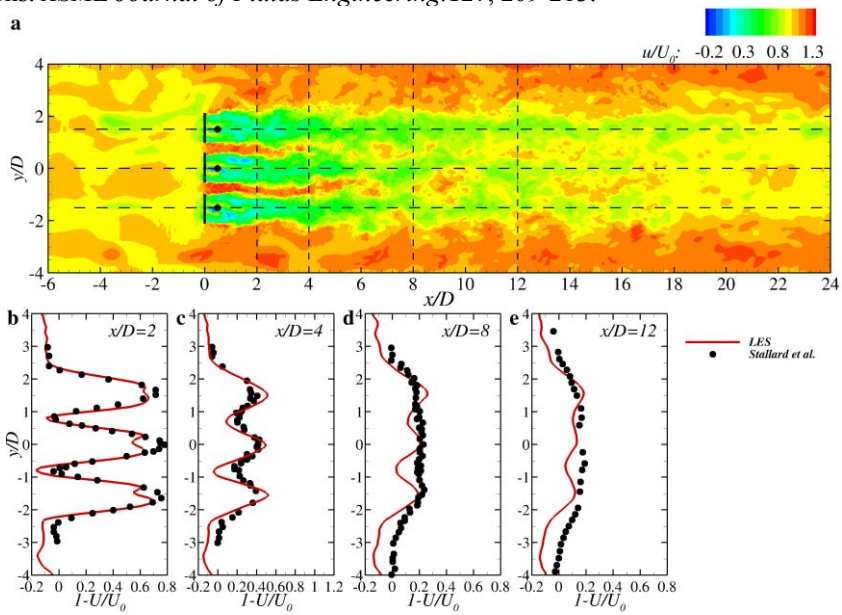

Fig. 1. Array of 3 in-line HATTs. Results of (a) instantaneous streamwise velocities and (b) validation of velocity deficit at four stages in the wake.

Arrays of non-uniform local blockage and resistance

Paul A. J. Bonar*, Vengatesan Venugopal, Alistair G. L. Borthwick
School of Engineering, University of Edinburgh, UK

Thomas A. A. Adcock
Department of Engineering Science, University of Oxford, UK

Summary: Depth-averaged simulations are used to investigate whether the performance of a tidal turbine array can be enhanced by varying either local blockage, local resistance, or both, across the array width. Results suggest that for an initially uniform flow field, the optimal array comprises turbines of equal size, spacing, and tuning.

Introduction

Theoretical models suggest that to maximise their combined power output, tidal turbines should be arranged in a single cross-stream row and optimally spaced to exploit local blockage effects [1-3]. However, because such models typically assume that the turbines within these arrays are identical, they do not consider the possibility that more power could be produced by exploiting spanwise variations in local blockage and resistance. In this abstract, numerical simulations are used to investigate whether array performance can be further enhanced by varying solely the local blockage, solely the local resistance, or both local blockage and resistance together, across the width.

Methods

The DG-ADCIRC model introduced at a previous workshop [4] is used to simulate steady, uniform, and depth-averaged flow through an idealised channel of low background roughness. A sub-grid-scale actuator disc model is then used to extend a cross-stream turbine array of global blockage 0.1 inward from one side of the channel. Turbines are defined by a local blockage ratio B_L and local wake velocity coefficient α_{4L}, and array performance is measured in terms of the global power coefficient C_{PG}, which is the ratio of available power to channel-scale kinetic energy flux. Starting with near-optimal uniform profiles (uniform $B_L = 0.5714$ and uniform $\alpha_{4L} = 0.583$, which combine to produce a near-peak C_{PG} of 0.966), the effects of non-uniform local blockage and resistance are explored by varying B_L and α_{4L} across the width of the array. In all cases B_L and α_{4L} are varied linearly, with non-uniform profiles denoted by the extreme values at the turbine edges nearest to (centre edge) and furthest from (end edge) the wall about which the array has reflectional symmetry (fig. 1).

Results & Discussion

Fig. 2 shows the variation in C_{PG} with non-uniform α_{4L} for near-optimal uniform B_L, and with non-uniform B_L for near-optimal uniform α_{4L}. The values obtained using these non-uniform profiles are lower than those obtained using the uniform profiles, but C_{PG} is shown to be relatively insensitive to local variations in B_L and α_{4L}. Given that turbine performance is a function of both B_L and α_{4L}, it is perhaps unsurprising that the performance of the array cannot be improved by varying these parameters independently across its width. However, it appears that neither can array performance be improved by varying these parameters together. Fig. 3 shows the variation in C_{PG} with non-uniform α_{4L} for arrays with higher B_L at their ends than at their centre, and higher B_L at their centre than at their ends. Certain non-uniform configurations are again shown to produce values of C_{PG} only slightly lower than that obtained using the uniform profiles, but their operation is found to be quite different at local-scale, requiring large and undesirable variations in local power and thrust coefficient.

These results suggest that for an initially uniform flow field, the optimal array comprises turbines of equal size, spacing, and tuning. This finding is encouraging because it is simpler and more cost effective to design each turbine to be the same and to operate in the same way. This finding agrees with Hunter et al. [5], who used 3D Reynolds-averaged Navier-Stokes simulations of porous discs to show that the C_{PG} of a cross-stream row of uniform B_L is maximised by a uniform α_{4L}. The finding does not agree, however, with Cooke et al. [6], who used a three-scale actuator disc model to show that a cross-stream row with uniform α_{4L} but non-uniform B_L can produce a higher peak C_{PG} than can be produced using the two-scale model of Nishino & Willden [1], for which both B_L and α_{4L} are uniform. That being said, it should also be noted that the third scale of wake mixing introduced by Cooke et al. [6] divides the single cross-stream row into multiple sub-rows within the same plane, thereby creating non-uniform B_L profiles much more complicated than the linear variations considered here.

* Corresponding author.
Email address: p.bonar@ed.ac.uk

Acknowledgements:
This paper is based on part of the first author's PhD studies, which were sponsored by the Energy Technology Partnership and Scotland's Saltire Prize Challenge competitors under Scottish Government Grant R43039 (Saltire Studentship). The authors thank Prof. Matthew Piggott, Prof. Paolo Perona, and two anonymous reviewers for providing helpful suggestions.

References:

[1] Nishino, T., Willden, R. H. J. (2012). The efficiency of an array of tidal turbines partially blocking a wide channel. *J. Fluid Mech.* **708**, 596-606.
[2] Draper, S., Nishino, T. (2014). Centred and staggered arrangements of tidal turbines. *J. Fluid Mech.* **739**, 72-93.
[3] Vogel, C. R., Houlsby, G. T., Willden, R. H. J. (2016). Effect of free surface deformation on the extractable power of a finite width turbine array. *Renew. Energ.* **88**, 317-324.
[4] Bonar, P. A. J., Venugopal, V., Borthwick, A. G. L., Adcock, T. A. A. (2016). Numerical modelling of two-scale flow dynamics. In *5th Oxford Tidal Energy Workshop*, Oxford, UK.
[5] Hunter, W., Nishino, T., Willden, R. H. J. (2015). Investigation of tidal turbine array tuning using 3D Reynolds-averaged Navier-Stokes simulations. *Int. J. Mar. Energ.* **10**, 39-51.
[6] Cooke, S. C., Willden, R. H. J., Byrne, B. W. (2016). The potential of cross-stream aligned sub-arrays to increase tidal turbine efficiency. *Renew. Energ.* **97**, 284-292.

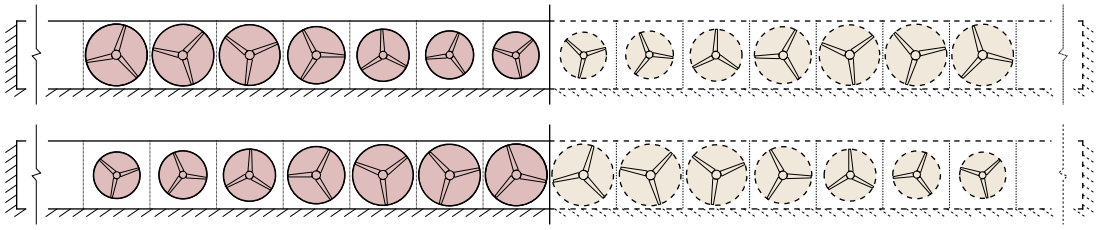

Fig. 1: (Online version in colour.) Schematic representations (streamwise cross-sectional views) of arrays with non-uniform local blockage profiles and their implied reflectional symmetries.

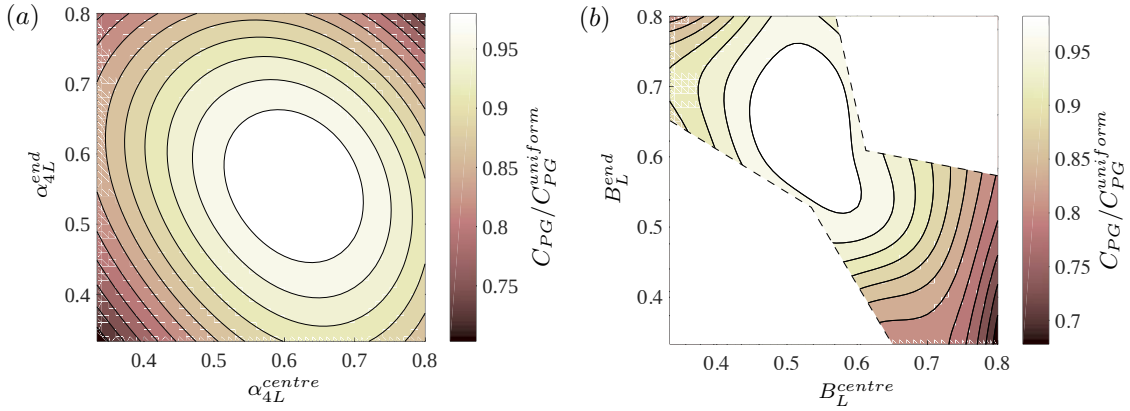

Fig. 2: (Online version in colour.) Variation in normalised global power coefficient C_{PG} with: (a) centre and end local tuning α_{4L} for arrays of near-optimal uniform local blockage ($B_L = 0.5714$), and; (b) centre and end local blockage B_L for arrays of near-optimal uniform local tuning ($\alpha_{4L} = 0.583$).

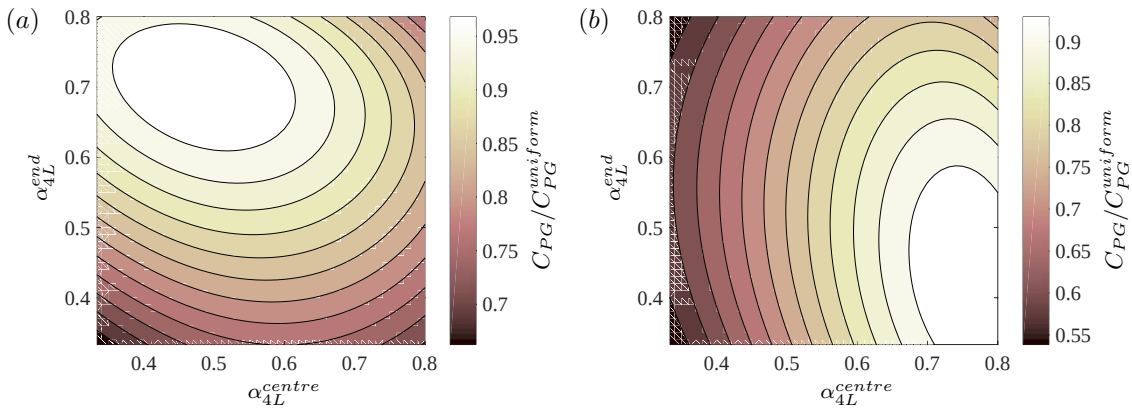

Fig. 3: (Online version in colour.) Variation in normalised global power coefficient C_{PG} with centre and end local tuning α_{4L} for arrays with: (a) higher local blockage at their ends ($B_L^{end} = 0.7$) than at their centre ($B_L^{centre} = 0.4$), and; (b) higher local blockage at their centre ($B_L^{centre} = 0.7$) than at their ends ($B_L^{end} = 0.4$).

Field observations of rotor thrust and bypass-acceleration at a tidal fence

Merel Verbeek*, Robert Jan Labeur, Wim Uijttewaal
Faculty of Civil Engineering and Geoscience, Delft University of Technology, NL

Summary: While various analytical and model studies have described the hydrodynamics of tidal turbines placed in close proximity to improve rotor performance, no comparison with field observations of full scale tidal fences have been reported to the author's knowledge. In this abstract, in situ measured turbine thrust and flow velocities downstream of a 1.2 MW five turbine tidal fence in the Eastern Scheldt (NL) are presented. The preliminary comparison to analytical approaches to describe flow past a tidal fence is promising.

Introduction

In the past decade, many studies underlined the importance of local flow blockage to improve performance of horizontal axis tidal turbines in channels. The peak turbine performance increases when the local blockage, namely the rotor swept area to channel area ratio, is optimized [1]. The same principle holds for a fence of turbines placed in close proximity and spanning over a part of a tidal channel [2]. Interestingly, not only rotor thrust increases as a result of this blockage, but also the velocity in between adjacent turbines increases [e.g. 3]. This so-called bypass speed-up influences turbine performance through interaction of downstream wakes. However, no field observations of this process have been reported to the author's knowledge.

From momentum theory it is known that the rotor thrust T [N] scales with the square of the ambient flow velocity u_0 [m/s] and hence linearly with the change in water level difference over the full length of the tidal channel Δh [m]:

$$T \sim u_0^2 \sim \Delta h. \quad (1)$$

The velocity change of the flow passing by and passing through the rotor plane may then be estimated using e.g. the thrust, Froude number and blockage ratio as described by [3] or by using numbers on wake mixing and rotor induction as described by [2]. However, up to now, these relations are only validated using numerical and experimental data.

In this abstract, the relation in [3] and Eq. 1 are compared to the velocity and load measurements of a full scale operating 1.2 MW tidal fence of Tocardo International BV. The fence is deployed in a gate of the Dutch storm surge barrier in the Eastern Scheldt (ES) basin. The five turbines are installed in close proximity, with an axis-to-axis spacing of 1.25 times the rotor diameter (D = 5.3 m) resulting in a local blockage ratio of 0.7 in the horizontal and 0.4 in the vertical allowing a comparison with blockage theory.

Methods

To get insight in the flow and turbine performance, rotor thrust and flow velocity are recorded during turbines operation both in stall conditions, at a minimal thrust coefficient C_T, and in normal conditions, at a high thrust

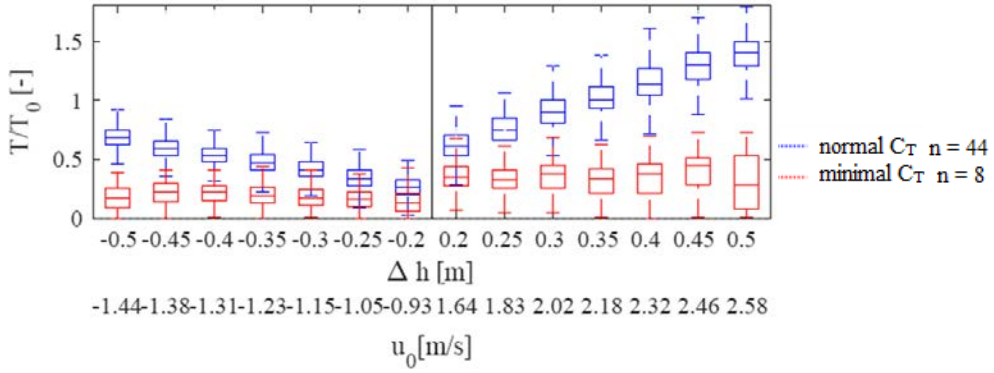

Fig.1. The normalised turbine thrust load as a function of water level difference Δh measured outside the turbine-influence area (u_0 is the corresponding upstream velocity measured 5 D upstream the rotor plane) for normal (blue) and minimal (red) turbine performance. The value of T_0 could not be disclosed.

* Corresponding author.
Email address: m.c.verbeek@tudelft.nl

coefficient, by adopting two tip speed ratios. The tip speed ratio (TSR) is a fixed ratio between the blade angular speed and the ambient velocity experienced one diameter (D) upstream the rotor plane. The velocity data is obtained from 5-beam ADCP transducers mounted in the strut and nacelle of the centre and outer turbines, recording the flow field up- and downstream of the fence up to 25 m in 50 bins. The along stream velocity component of centre- and side looking transducer beams are presented here. During the measurements, turbulence intensity amounted 0.06 at negative water level head and ±0.12 at positive head. The thrust was recorded with fibre optic instruments in the turbine struts. The water levels are measured in the tide gauges of the approach harbours up- and downstream of the Roompot barrier section with 31 gates, which implies that the calculated heads ($\Delta h = h_{sea} - h_{basin}$) [m] contain negligible influence of the turbines operated in one of these gates.

Results and discussion

The observations show that the thrust load of the turbine increases with the same rate as the water level head over the channel (Fig. 1). This linear relation, which is in line with Eq. 1, implies that the turbines deliver a scalable thrust at a fixed TSR. If the tidal currents flow past the fence, they experience rotor thrust and decelerate when aligned with a rotor plane and speed-up when in-between two rotor planes. These processes can be discriminated in the recorded velocity field (Fig 2, for Δh=0.3 m). The flow velocities in-between adjacent turbine wakes are higher when turbines are operated at normal C_T than at a minimal C_T. The bypass velocity ratio amounts +0.10 on time-average compared to +0.15 as calculated with the model of [3] for the reported operating conditions. The average wake velocity change is -0.6 compared to -0.53 calculated with the model of [3]. At half a fence width downstream (x=18 m), also fence-scale bypass speed-up and wake merging phenomena are observed in the data suggesting two scale dynamics as discussed by [2]. Noted should be that with the chosen data acquisition method, only minimal bypass speed-up and wake deceleration could be calculated, because a comparison is made to turbines operated at a minimal and not a zero thrust coefficient.

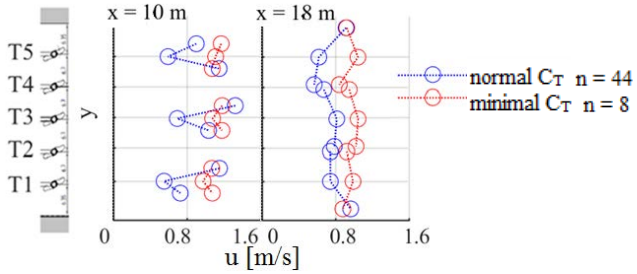

Fig. 2. Flow velocity at 10 m and 18 m downstream of the five turbine (T1-T5) fence for normal and minimal thrust at 0.3m water level head, which corresponds to an upstream velocity of 2.4 m/s.

Conclusions

As one of the first, this abstract presents field observations of the flow past a full scale tidal fence. The presented dataset suggests that turbine thrust and resulting wake deceleration and bypass speed-up downstream a five turbine tidal fence are scalable for different water level heads. The preliminary comparison of the data to analytical approaches to describe flow past a tidal fence is promising.

Acknowledgements:

This work is part of research programme The New Delta (869.15.008), which is financed by the Netherlands Organisation for Scientific Research (NWO). We are grateful to Tocardo International B.V. for the use of their velocity and load measurements. The European Regional Development Fund (ERDF) OP-Zuid 2014-2020 programme is acknowledged for their support.

References:

[1] Garrett, C., and Cummins, P. (2007). The efficiency of a turbine in a tidal channel. *J. Fluid Mech.* 588, 243-251.

[2] Nishino, T., Willden, R. H. (2013a). Two-scale dynamics of flow past a partial cross-stream array of tidal turbines. *J. Fluid Mech.* 730, 220-244.

[3] Edmunds, M., Malki, R., Williams, A., Masters, I., Croft, T. (2014). Aspects of tidal stream turbine modelling in the natural environment using a coupled bem-cfd model. *Int. J. Mar. Energy* 7, 20-42.

[4] Whelan, J., Graham, J., and Peiro, J. A (2009). Free-surface and blockage correction for tidal turbines. *J. Fluid Mech.* 624, 281-291.

An English Channel Model for the Optimisation of Tidal Turbines in the Alderney Race

Zoe L. Goss, Matthew D. Piggott, Stephan C. Kramer
Department of Earth Science and Engineering, Imperial College London, UK

Summary: Work by Coles et al [1] demonstrated the ability to optimise the location of devices within a tidal turbine array for a flood and ebb tide in the Alderney Race for a simplified shallow water model that featured adjoint optimisation capabilities. This study continues that work by experimenting with the impact that different functionals have on the array design and moving towards a more comprehensive approach. The model has been validated against tide gauge data and we are in the preliminary stages of testing the impact that different objective functionals, e.g. power or Levelised Cost of Energy, have on optimal array design.

Introduction

The regularity of the tides makes them an attractive option for renewable energy generation. The UK has around 50% of Europe's tidal energy capacity [2] and a technical resource supply of ~116 Twh/year [3], thanks to its bathymetry and coastline features which accelerates tidal currents in many locations. Our research focuses on the Alderney Race, a potential array location for both the French and the UK government. The Alderney Race contains the majority of the Channel Islands resource, with a maximum potential of 5.1 GW [4].

Since the tidal energy industry is very new, the first full sized arrays will only be developed if they can be shown to be viable from economic, engineering and environmental perspectives. Advanced numerical tools are needed to both predict and maximise power yields in arrays of up to hundreds of turbines, in order to prove viability of new sites and aid array design in this fledgling industry.

Methods

We started with the same set up as Coles et al [1] for a shallow water model of the English Channel using OpenTidalFarm. OpenTidalFarm is an open source software for the modelling of coastal flow combined with an adjoint solver and optimisation loop to enable tidal turbine array micro siting [5]. In this model a continuous turbine approach [6] was used to optimise the turbine density across the array area, which can be converted into a discrete number of turbines of a given diameter (16m used in this study).

This simplified model has a constant bathymetry of 50m across the whole domain and the optimisation was performed for two steady state flows; a flood tide (running from South-West to North-East) and ebb tide (running from North-East to South-West), with an inlet boundary velocity of 0.80 m/s and 4.24 m/s and an outlet elevation of 0m imposed on the East and West open boundaries respectively. The results below only show the array design for the flood direction. The mesh resolution used was 5km over the majority of the domain, 1km at the coastlines and 125m within Alderney Race.

Functionals which had a different weighting on power vs cost of devices were tested to demonstrate the impact that this balance had on array design. Four models with functionals; $J = P - 1600 \cdot c_t$, $J = P - 160 \cdot c_t$, $J = P - 16 \cdot c_t$ and $J = P$, were compared, where P is power in MW, c_t is the turbine drag coefficient, a function of the turbine density and area of the turbines. Only the foremost and latter model are discussed below.

Results

Figure 1 shows the optimal turbine density for the simplified OpenTidalFarm model when using functionals of $J = P - 1600 \cdot c_t$ and $J = P$ respectively. The former effectively has a break-even power that must be obtained in order to install more turbines, and results in a far sparser optimal layout. As shown in Table 1 this results in an array design which produces almost 5 times as much power per device, since fewer turbines in the array leads to reduced wake interactions. We also investigated the difference between the optimal array design in the Alderney Territorial Waters and the French Territorial Waters and found that the turbines in the FTW achieve a higher average power rating of 56.1 KW, as opposed to 38.6 KW in the ATW.

If $P - 1600 \cdot c_t$ can be viewed as a proxy for profit, where money is earned per power generated but also spent per device installed, it can be seen that if optimising for power alone, the optimal design would have so many turbines that the array would make a loss. In most of the array plot the turbine density reaches the maximum allowed (1 turbine diameter tip-to-tip lateral spacing and 8 for longitudinal spacing) which, along with the semi-idealised set-up, results in the impractically high total number of turbines shown in Table 1. This incentivises the development of more sophisticated and accurate economic models, to use as the functionals in these array optimisation tools.

Figure 2 shows the harmonic analysis for the Thetis model with just M2 forcing. It shows good agreement with the tide gauge data even for a very coarse model (5km over the majority of the domain and 1km at

coastlines) and spins up much quicker than the models forced by multiple constituents. This makes it appropriate for use in optimisation, where many iterations of the forward model must be run.

Conclusions

The impact that including the cost of devices can have on the optimal array layout demonstrates the need to develop more realistic economic models to aid array design. We are in the preliminary stages of implementing an optimisation with respect to Levelised Cost of Energy, using the more accurate portrayal of the English Channel developed in Thetis. We are also furthering our model validation using more detailed ADCP data in order to decide an appropriate resolution for best accuracy in the Alderney race, without compromising on computational speed.

References:

[1] D. Coles, S. C. Kramer, M. D. Piggott, A. Avdis, and A. Angeloudis, "Optimisation of tidal stream turbine arrays within Alderney Race," EWTEC, 2017
[2] Department for Business, Energy & Industrial Strategy, "Wave and tidal energy: part of the UK's energy mix," 2013.
[3] The Crown Estate, "UK Wave and Tidal Key Resource Areas Project Executive Summary," 2013
[4] D. S. Coles, L. S. Blunden, and A. S. Bahaj, "Assessment of the energy extraction potential at tidal sites around the Channel Islands," Energy, 2017.
[5] S. Funke and P. Farrell, "Tidal turbine array optimisation using the adjoint approach," Renewable Energy, 2013.
[6] S. W. Funke, S. C. Kramer, and M. D. Piggott, "Design optimisation and resource assessment for tidal-stream renewable energy farms using a new continuous turbine approach," Renewable Energy, 2016.

Functional \ Feature	$P - 16 \cdot c_t$	Power (MW)	Number of Turbines	Power per device (MW)
$J = P - 16 \cdot c_t$	527.4	1165.1	4,957	0.23
$J = P$	-3636.2	2149.0	44,971	0.048

Table 1 - Properties of the optimal solution for runs of the OpenTidalFarm model with two different functionals.

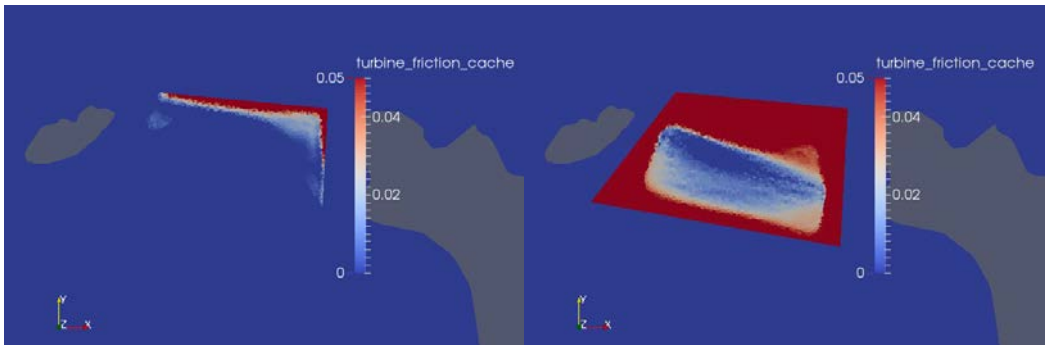

Figure 1 - The turbine friction, c_t, across the lease plot at the final stage of optimisation when using functionals of a) $J = P - 1600 \cdot c_t$ and b) $J = P$

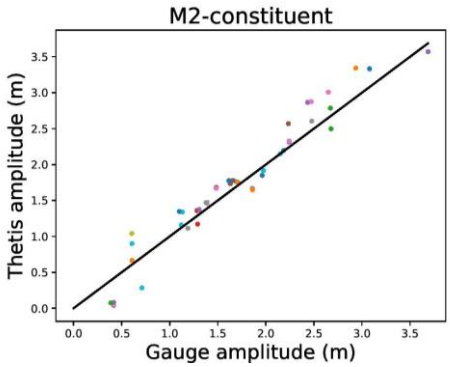

Figure 2 - Harmonic analysis of the Thetis model using only M2 forcing, compared to tide gauge data at 90 locations.

Tidal asymmetry and its effect on capacity factor of tidal resource

Ahmad Mukhlis Firdaus*, Thomas AA Adcock, Guy T Houlsby

Department of Engineering Science, University of Oxford, UK

Summary: This paper describes the aspects of power capping strategies in asymmetric tidal patterns. The capping strategies that are widely used in UK and Canada, where the tides are mostly semidiurnal and M_2 is the dominant component driving the tidal current, might not be applicable in an area with pronounced diurnal components resulting in tidal asymmetry. Using existing capping strategies in asymmetric tidal patterns may result in significant inefficiencies for turbine developers. This is addressed by analysing the Capacity Factor (CF) of the turbine in different tidal regimes, including symmetry and asymmetry.

Introduction

Tidal asymmetry arises when different tides occur on ebb and flood. Neill et al. [1] have examined the characteristics of tidal energy resources due to asymmetry. However, it is unclear what the direct impact of this phenomenon will be on tidal resource extraction. In their conclusion, Neill et al. [1] only mentioned that the asymmetric phenomenon is pronounced in certain tidal regimes. This is obvious due to power being a function of the cube of the flow velocity. Tidal asymmetry is therefore important for tidal resource extraction. Tidal asymmetry creates uneven flow during flood and ebb, which turbine developers need to consider for the design of support structures. Importantly, the asymmetry also affects the power-capping strategy to optimise the CF of the turbine.

Methods

Asymmetry arising from the interaction of the K_1, O_1 and M_2 components can be analysed by the comparison of joint amplitude $\frac{a_1}{a_2}$, see Hoithink *et al.* [2]. Their method is expanded here to include the an additional semidiurnal component S_2. This expansion is required as S_2 plays an important role in the neap-spring cycle. Moreover, a tidal stream generated by a combination of M_2 with K_1 and O_1 does not always create tidal asymmetry. Some specific combinations are needed to create the asymmetric tides. Using the same methods of solving as in [2] the joint amplitude for K_1 and O_1, joint amplitude of M_2 and S_2 (a_2) can be written as:

$$a_2(t) = \sqrt{A_{M_2}{}^2 + A_{S_2}{}^2 + 2A_{M_2}A_{S_2}\cos\left(\phi_{M_2} - \phi_{S_2} + 2\omega_2 t - 2\omega_3 t\right)} \tag{1}$$

and

$$\varphi_2(t) = \left(2\omega_1 t - \lambda_2\right) \tag{2}$$

where

$$\lambda_2 = \arctan\left(\frac{\left(A_{M_2}\sin\phi_{M_2} + A_{S_2}\sin\left(2\omega_3 t - 2\omega_2 t + \phi_{S_2}\right)\right)}{\left(A_{M_2}\cos\phi_{M_2} + A_{S_2}\cos\left(2\omega_3 t - 2\omega_2 t + \phi_{S_2}\right)\right)}\right) \tag{3}$$

In terms of tidal resource extraction, the capping strategy aims to optimise the utility of turbine and generator. By deliberately limiting the extracted power by changing the cut-out velocity, the CF is calculated based on the ratio of average power to the rated power. It is more economically advantageous to adopt a capping strategy than just to exploit the maximum velocity in the entire neap-spring tidal cycle. The choice of cut out velocity becomes a trade-off for the turbine developer. A higher cut-out velocity will give higher average power produced by the turbine, but the CF will be low. That means the turbine will be unable to produce at its optimum performance all the time, or will be over-designed for the particular site. A CF in range of 0.3~0.4 is usually adopted to give the optimum selection of turbines, with this factor arising partly from experience in the wind industry. However, in systems exhibiting tidal asymmetry a different strategy may be needed to obtain the optimum CF.

Tidal asymmetry effects are analysed by comparing the CF for different asymmetric conditions. The calculations of power extraction for the desired CF are done using 0-D linear momentum actuator disc theory (LMADT) [3] with a blockage ratio B = 0.1 and wake coefficient α_4 = 0.33. The model is run for 60 days for simplicity and in order to encompass a number of spring neap cycles. The CF is examined by comparing the ratio of cut-out velocity to the average velocity $U_{\text{cut-out}}/U_{\text{average}}$ and cut-out velocity to maximum velocity for the flow in the channel with a turbine array without capping.The Formzhal number (F) is used to enable comparison of amplitude between principal diurnal (AK_1 and AO_1) and principal semidiurnal (AM_2 and AS_2) tides. It is expressed as

$$\frac{AK_1 + AO_1}{AM_2 + AS_2} \tag{4}$$

* Corresponding author.
Email address: ahmad.firdaus@eng.ox.ac.uk

Results

Different cut-out velocities are introduced to investigate the effects of tidal asymmetry on the capacity factor of the turbine. Tidal velocities generated by different main tidal astronomical combinations create different types of symmetric or asymmetric tides (Fig. 1). The types can be classified into three different categories, constant (Fig. 1(a)), moderately fluctuated (Fig. 1(b)) and very-fluctuated (Fig. 1(c)).

In mixed diurnal conditions (F = 1), the desired CF= 0.35~0.40 is achieved by setting the cut-out velocities to 1.5~1.9 times the average velocity (Fig. 2(a)) for all categories. Meanwhile, if the cut-out velocities are compared to maximum velocity (Fig. 2(b)), there is a significant difference between the very-fluctuated cases and other cases (fluctuated and constant). In the constant and fluctuated cases the turbine array only needs to sacrifice 15~30% of available power from the maximum velocity, while the very-fluctuated cases have to exclude more than 40~55% of the potential production from the maximum tidal condition, to achieve the desired CF.

Conclusions

We have examined the power available for tidal stream energy production when both diurnal and semi-diurnal constituents are present in the tidal current. We find that to get a reasonable compromise between maximum power production and capacity factor we will need to use different strategies depending on the Formzhal number at a given site. In areas such as Indonesia, where there is a strong diurnal component to the tides, a very different capping strategy should be adopted compared with locations where semi-diurnal constituents dominate, such as around the UK.

References:

[1] Neill, S., P., Hashemi, M., R., Lewis, M., J. (2014). The role of tidal asymmetry in characterizing the tidal energy resource of Orkney, Renewable Energy 68 (2014) 337-350.

[2] Hoithink, A.J. F., Hoekstra, P. and van Maren, D. S. (2003) Flow Asymmetry, associated with astronomical tides: implication for the residual transport of sediment, Journal of Geophysical Research, Vol. 108, No. C10, 3315, doi: 10.1029/2002JC001539.

[3] Houlsby, G.T. and Vogel, C., R. (2016) The power available to tidal turbines in an open channel flow, Proc. ICE, Energy, Energy 2017 170:1, 12-21.

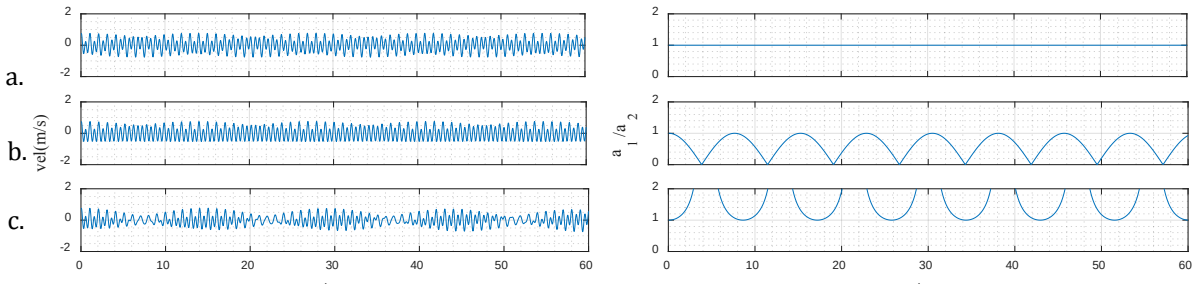

Fig. 1 Simulation using same Formzhal Number (F=1) in different S_2, M_2, K_1 and O_1 Composition.

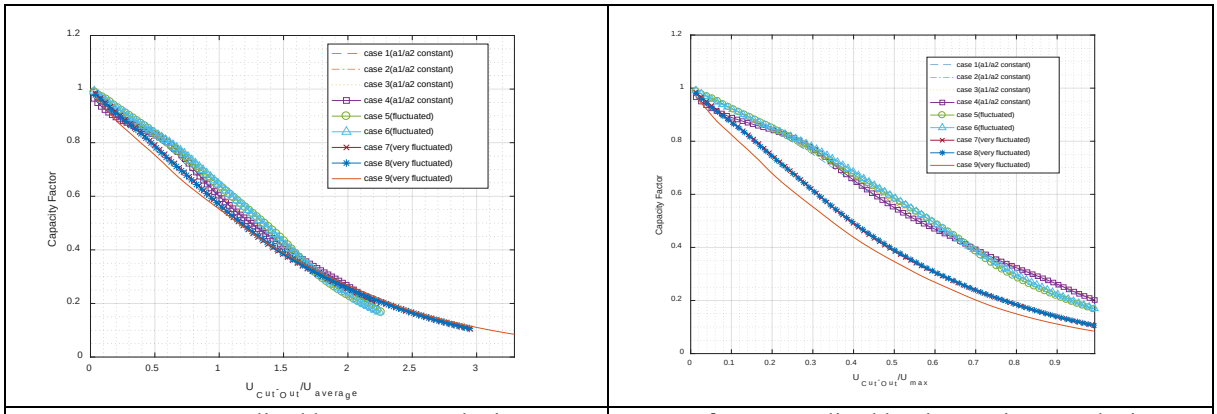

a. normalised by average velocity | b. normalised by the maximum velocity

Fig. 2 Relationship between the capacity factor (CF) and cut-out velocity normalised with average velocity and maximum velocity

Acquiring Flow and Movement Data on a Floating Tidal Energy Converter

Thomas Lake*, Alison J. Williams, Ian Masters
Marine Energy Research Group, College of Engineering, Swansea University

Summary: As part of the EPSRC SURFTEC project, measurements of the motion of a floating tidal energy converter alongside measurements of turbine performance and flow conditions are required to validate planned improvements to an existing BEMT model. Measurements have been acquired from a commercial prototype device during a test deployment using low cost commercial IMUs and a commercial ADV.

The design and configuration of this equipment is summarised here, along with a sample of the data acquired to date.

Introduction

As part of the **Su**rvivability and **R**eliability of **F**loating **T**idal **E**nergy **C**onverters (SURFTEC), work is ongoing at Swansea University to migrate an existing Blade Element Momentum Theory model[1] from MATLAB into C++, and to extend the model to support turbines mounted on a simplified representation of a floating platform.

Part of this work includes gathering data that can be used to validate this extended numerical model, which is being carried out with project partners Sustainable Marine Energy Ltd. using equipment mounted on their PLAT-I platform.

Data Acquisition

Based on the inputs and outputs of the existing BEMT model, it was determined that the motion of the platform, flow conditions and turbine operating parameters (specifically torque, thrust, and power) would need to be measured and recorded. For practical purposes, it was also desirable to record much of this data on a standalone system to minimise interference with the existing infrastructure and development of the PLAT-I platform.

To this end, a data acquisition system has been designed and deployed consisting of a central waterproof unit containing a central control and communications computer, commercial data logger (DL) and supporting hardware and some external sensors – specifically 2 separate Inertial Measurement Units (IMUs), a commercial Acoustic Doppler Velocimeter (ADV) and a GPS antenna.

The DL and ADV are both connected to the central unit, providing control, storage and remote access to the devices. A summary diagram showing the connection between components is shown in Figure 1**Error! Reference source not found.**.

Control Unit

The central waterproof unit consists of a Raspberry Pi (a low cost single board computer), Race Technology DL1 data logger (with built-in accelerometers and GPS) and supporting hardware. The Raspberry Pi runs control and monitoring software for the connected hardware, permitting remote access and monitoring with minimal configuration changes to the existing network on the SME platform.

The Race Technology DL1 data logger was chosen as it is a robust system used in the automotive industry to track vehicle position and acceleration (and from this, velocities). It also allows logging of external sensors and serial data, which has been used to connect the IMUs. This permits all position and movement data to be logged centrally against a single time source.

IMUs

The IMUs are bespoke units designed to be waterproof, robust and easy to integrate with the DL1 logger. These each incorporate 2 LSM9DS0 sensors - composed of 3 axis gyros, accelerometers and magnetometers. The use of 2 sensors in each unit allows them to be configured with different measurement ranges, as well as providing for redundancy. The internal architecture of these sensors limits the sensitivity that can be represented in the returned data based on the selected measurement range – for example configuring the accelerometer for $\pm 16g$ limits the sensitivity to $7\times10^{-4}g$, while the same sensor configured to measure $\pm 2g$ can represent

* Corresponding author.
Email address: t.lake@swansea.ac.uk

accelerations of $6\times10^{-5}g$ [2]. Using two sensors allows the representation of smaller accelerations to be maintained while also allowing a larger range to be measured on the second sensor. This configuration should permit any extreme events to be captured without clipping while still allowing smaller magnitude variations to be recorded.

The data from the IMU units are recorded at an average of 83Hz on the DL1 and an average of 20.8Hz on the Raspberry Pi. The measurement ranges were selected based on the results of scale tank tests presented previously in [3]. Each IMU is positioned ~15m from the central unit to better measure the motion of the outboard sections of the platform

ADV

The ADV used is a Nortek Vector, connected to and controlled by the Raspberry Pi. The ADV operates in 64Hz continuous data collection mode with a maximum velocity component range of $\pm4ms^{-1}$. It has onboard power and storage for standalone recording, but the planned 4-6 week deployment meant that this was insufficient. The ADV is powered from the central logging unit, with communication and power provided on a modified Nortek serial cable. The data is then stored directly by the Raspberry Pi (bypassing the storage onboard the ADV).

Future Work

Once the current deployment concludes, the next stage will be to process the data from the gathered motion rates into position and orientation data and investigate the correlations between platform accelerations and turbine loads. The data will then be used at Swansea to verify the extended BEMT model, as well as to investigate potential implications of the loads measured on component fatigue and device design life.

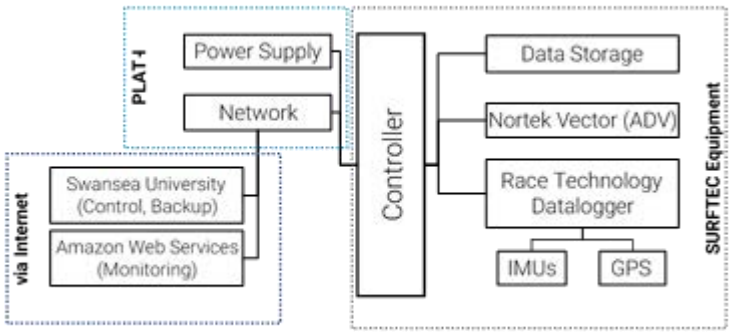

Figure 1: Data acquisition system overview diagram

Acknowledgements:

SURFTEC is a SuperGen grand challenge project, funded under EPSRC grant EP/N02057X/1. The assistance of project partners Sustainable Marine Energy Ltd is also acknowledged, for allowing the use of their platform to acquire this dataset.

References:

[1] Chapman, J.C., Masters, I., Togneri, M., Orme J.A.C (2013) The Buhl correction factor applied to high induction conditions for tidal stream turbines, *Renewable Energy* (60), pp 472 – 480, doi:10.1016/j.renene.2013.05.018

[2] STMicroelectronics, "iNEMO inertial module: 3D accelerometer, 3D gyroscope, 3D magnetometer". LSM9DS0 datasheet, revision 2, August 2013 - https://cdn-shop.adafruit.com/datasheets/LSM9DS0.pdf

[3] Jeffcoate, P., McDowell, J. (2017) Performance of PLAT-I, a Floating Tidal Energy Platform for Inshore Applications. In: *Proceedings of the 12th European Wave and Tidal Energy Conference*, Cork, Republic of Ireland

Investigating the fundamental nature of unsteady aerofoil response to gusts

Amanda Smyth*, Anna Young
Whittle Laboratory, Engineering Department, Cambridge University, UK
Luca Di Mare
Department of Engineering Science, University of Oxford, UK

Summary: This work uses a vortex lattice model and eigenmode decomposition to investigate the unsteady load response of tidal turbine blades to three-dimensional gusts. The gusts are found to interact with the blade aerodynamic modes, and the effect of three-dimensional geometry on these modes is found to be significant. The addition of rotation further deforms the modes. Early results indicate that the response of even a 2D aerofoil to 3D gusts will not be captured by 2D models, and it is therefore necessary to develop a new low-order method for accurate load evaluation. Eigenmodes have the potential to provide such a low-order, 3D analysis, and also give a direct link between geometry features and the unsteady response of the blade.

Introduction

The nature of tidal channel flows presents unique challenges to device designers due to the high level of unsteadiness, which results in time-varying angle of attack and therefore integrity and performance issues due to oscillating loads. Errors in unsteady load predictions will lead either to premature failure or over-cautious designs, and therefore higher costs. This means that it is vital to devise accurate methods to evaluate the unsteady load response of tidal turbines.

Current practice is to use unsteady transfer functions obtained from linear analytic theory [1], which allow the effect of unsteady flow to be estimated from the steady state turbine performance. These transfer functions are derived from 2D, inviscid, flat-plate models, and are readily used in conjunction with Blade Element Momentum Theory (BEMT). However, while this procedure is widely used in wind turbine design, simply transferring the method to tidal turbines raises a number of issues related in part to the inherently three-dimensional geometry of a tidal turbine [2]. Further to this, linear analytic functions are gust-specific; sinusoidal, uniform and step function gusts all have different transfer functions [3].

For designers, choosing the correct transfer function is a challenge given the highly random, 3D flow in the real ocean environment – a realistic gust will not correspond to any of the idealised gust definitions available. There is, therefore, a need for a generalised approach to modelling the interaction of tidal turbine blades with unsteady flow. Such a general method must be low-order for the sake of speed. The aims of this investigation are to explore the applicability of 2D linear analytic theory to 3D geometries and gusts, and to devise a generalised means of analysing the unsteady response of a range of turbine geometries. To achieve these aims, an inviscid vortex lattice method is used to calculate the unsteady response, and then the eigenmodes of the resulting influence matrix are analysed. The use of an inviscid model means that this study is limited to pre-stall conditions, where the unsteady load amplitude is changed little by viscous effects (see experimental validation outlined in [3], chapter 8).

Methods

The aerofoil is modelled as a solid boundary in the flow made up of a series of panels with associated vorticity. By applying Neumann's boundary condition of zero flow normal to the panel surface, and Kelvin's theorem that the time derivative of circulation must be zero, the vortex lattice equation is [4]:

$$\boldsymbol{A\Gamma} = \boldsymbol{gust} \tag{1}$$

$$\begin{bmatrix} a_{11} & \dots & a_{1N} & b_1 \\ \dots & \dots & \dots & \dots \\ a_{N1} & \dots & a_{NN} & b_N \\ i\omega & \dots & i\omega & 1/dt \end{bmatrix} \begin{bmatrix} \Gamma_1 \\ \dots \\ \Gamma_N \\ \Gamma_w \end{bmatrix} = \begin{bmatrix} u_1(x,y).n_1 \\ \dots \\ u_N(x,y).n_N \\ 0 \end{bmatrix} \tag{2}$$

At each point on the blade surface, a and b represent the influence of the blade and the wake circulation respectively. The full set of panel and wake circulation strengths Γ is found by inverting the influence matrix $\boldsymbol{A}$. However, instead of inverting $\boldsymbol{A}$ directly, the matrix can be decomposed into its eigenmodes. We then postulate that the circulation vector can be represented as a linear sum of the right eigenvectors of $\boldsymbol{A}$, i.e. $\Gamma=V_{R*}c$ [5]. Here c is a vector of weight parameters which determine how much of each mode contributes to the final circulation. The eigenmodes are low-energy modes, meaning the system will naturally respond using these modes, making

* Corresponding author.
Email address: asmms2@cam.ac.uk

them similar to the natural modes of a vibrating beam. The response to any unsteady forcing can be found by superposition of the eigenmodes.

The benefit of decomposing Γ into V_R and c is that the unsteady response can now be studied in terms of the properties of the two components: V_R is determined entirely by the geometry of the lifting surface, while the weight vector c results from the interaction of the gust with the eigenmodes. A larger value of c means that the gust is spatially similar to the corresponding eigenvector and therefore the load response of that mode will be increased.

Results

The simple case of a flat plate at zero incidence is considered in 2D, 3D, and in a three-bladed rotor configuration. In the rotor case the chord is uniform along the span, and the twist distribution ensures zero angle of attack at steady conditions, to make the geometry locally similar to a 2D case (chord, twist and camber can, however, be included in the model). The 3D geometries have a span/chord aspect ratio of 4.0, and the rotor is spinning with TSR = 4.0. Figure 1 shows a representative sample of eigenvectors for the three cases. The differences between the modes of an infinite 2D blade (Fig. 1(a)) and those of a blade of finite span (Fig. 1(b)) illustrate the effects of a finite span on the response behaviour. In both cases, there is a sinusoidal distribution across the chord, which increases in wavenumber for higher modes. However, while the modes of the 2D case are constant across the span, the 3D modes also have a spanwise sinusoidal variation. Adding rotation to the blade leads to further changes; due to the spanwise variation in relative speed in the rotor case (Fig. 1 (c)), the unsteady effects are intensified at the base of the blade. As stated above, the unsteady load response to a gust depends on its spatial similarity to the eigenmodes. These changes in modes therefore mean that the unsteady response to a given gust will be different in the case of a realistic 3D rotor from the idealised, infinite flat plate case.

References:

[1] C. L. Sequeira, "Hydrodynamics of Tidal Stream Turbines", PhD Thesis, Cambridge, 2014.
[2] A. I. Winter, "Differences in fundamental design drivers for wind and tidal turbines" *IEEE OCEANS* 2011.
[3] J. G. Leishman, *Principles of Helicopter Aerodynamics*. Cambridge University Press, 2000.
[4] J. Katz and A. Plotkin, *Low-Speed Aerodynamics*. Cambridge University Press, 2001.
[5] R. Florea and K. C. Hall, "Eigenmode Analysis of Unsteady Flows about Airfoils", *J.Comp. Phys.* 1998.

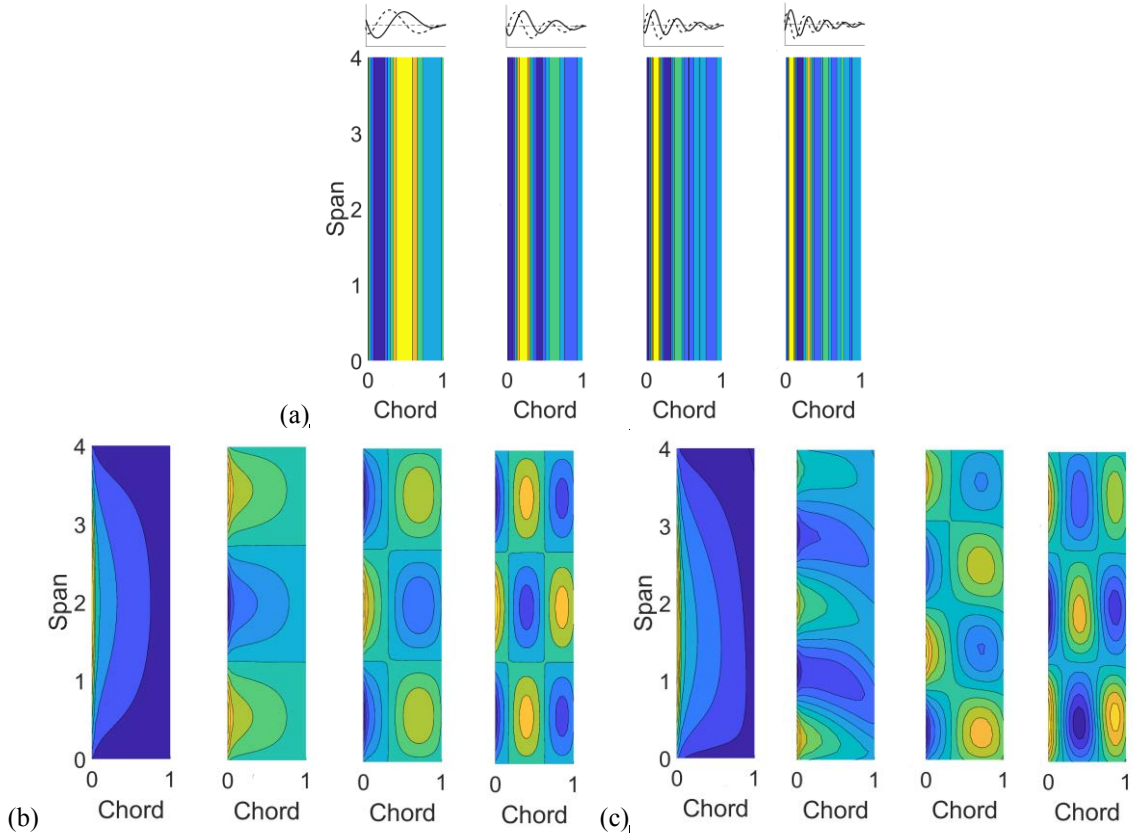

Figure 1: Examples of eigenvectors, representing surface distribution of circulation on the aerofoil. Each vector is normalised so that the maximum absolute value is 1. (a) 2D flat plate, (b) 3D flat plate, (c) rotor, TSR 4.0.

Unsteady hydrodynamics of full-scale tidal turbines

Gabriel T Scarlett[1], Ton van den Bremer[2] Brian Sellar[1] and Ignazio Maria Viola[1,*]
[1] *School of Engineering, Institute for Energy Systems, University of Edinburgh, UK*
[2] *Department of Engineering Science, University of Oxford, UK*

Summary: Due to the lack of full-scale measurements of the flow around tidal turbine blades, it is not clear if unsteadiness in the background flow can induce dynamic stall and the significance of this on the rotor's performance. To investigate, we develop a model that couples dynamic stall, rotational augmentation and blade element momentum theory with real flow measurements. We found that large, realistic waves lead to large fluctuations in power and thrust, mostly due to inviscid unsteady hydrodynamic effects near the blade tip. Conversely, flow fluctuations have little effect on the rotor's mean thrust and power.

Introduction

The marine environment is inherently unsteady due to waves and turbulence. When a rotor blade translates through unsteady flow, the rotation causes a time dependent flow field that can lead to load hysteresis, stall delay and dynamic stall (DS). To date, the quantification of unsteady loading on tidal turbine blades is an open question. Milne *et al*. [1] carried out experiments on a scaled turbine by oscillating it in a towing tank. At lower tip-speed ratios, they found the flow was largely separated over the blade span, which for high-frequency forcing caused the root bending moment to exceed the quasi-steady value by up to 25% due to DS. Galloway *et al*. [2] tested the effects of waves using a wave tank to generate linear waves. The experimental results showed that the median value of the root bending moment was exceeded by up to 175% during the presence of large waves. Contrarily to Milne *et al*., the authors concluded that the effect of DS was limited and, therefore can be neglected in some cases. Other than the work of Milne *et al*., no documentation of DS occurring on tidal turbine blades exists. Yet, it is known to occur on all types of horizontal-axis wind turbines, due to a combination of shear, turbulence, yaw misalignment and tower shadow effects [3]. Since tidal turbine blades will also experience these effects with the addition of waves, it is likely that dynamic stall occurs. In addition, the difference between the mean value and the steady state has yet to be quantified. The first aim of this work is to investigate if DS occurs in large, realistic waves. Secondly, it aims to quantify the differences between the resulting unsteady loads with those predicted with a commonly-adopted quasi-steady approach, which does not account for load hysteresis, stall delay and DS.

Method

A model has been developed, which couples a blade element momentum (BEM) [4], rotational augmentation [5] and DS models [6] to determine the unsteady blade loads. Induction factors are computed using a running average of the unsteady forces over a period of revolution. The rotor power and thrust are computed for a 3-bladed, 18 m diameter rotor. The blade profile follows that described by Gretton [7]. All blade sections comprise uniform thickness NREL S814 profiles. Velocity field measurements recorded during the ReDAPT project are used as an input to the model [8]. We consider a 256 s flow sample measured during a flood tide at the European Marine Energy Centre which includes an energetic wave train of ca. 5 m height and 10 s apparent wave period. The wave steepness, defined as the product of wave amplitude and wave number is approximately 0.17, indicating that the wave is weakly non-linear. The channel depth is 45 m and the hub depth is 27 m. The depth profile of the streamwise velocity (u) follows a power law with exponent 0.162, and it is 2.70 ms^{-1} at the hub. The magnitude of u averaged over the swept area and the sample period is $\bar{u} = 2.72$ ms^{-1}, while $\sqrt{\overline{u^2}}$ is 2.74 ms^{-1} and $\sqrt[3]{\overline{u^3}}$ is 2.77 ms^{-1}. The latter velocity is used for the steady simulation and to nondimensionalise forces, torque and power.

Results

The tip-speed ratio ($\lambda = 4.5$) and blade pitch ($\beta = 0.1°$) that maximise the power coefficient ($C_P = 0.47$) in a uniform constant current of velocity $\bar{u}$ are determined using the BEM model, where the static coefficients are corrected for rotation. All simulations are carried out using these parameters. Figure 1a-b show the power (C_P) and thrust (C_T) coefficients, respectively, over 10 rotational periods (T_r = 4.5 s). Results are presented for a uniform constant (steady) velocity and for the measured unsteady conditions. Unsteady fluctuations are clearly dominated by the period of the wave, with no discernible contribution from T_r. Fluctuations in C_P and C_T were found to exceed the steady value by almost 50% and 25%, respectively. Conversely, small changes are observed in the mean power and thrust coefficients, which both decrease by about 3%.

* Corresponding author.
Email address: I.M.Viola@ed.ac.uk

Time averaged, sectional lift ($\overline{C_L}$), drag ($\overline{C_D}$), thrust ($\overline{C_T}$) and torque ($\overline{C_Q}$) coefficients are shown in Fig. 2a-d, respectively. These coefficients are computed for steady, quasi-steady and unsteady conditions. The quasi-steady values are determined using static wind tunnel data [9] and, hence, do not take into account DS nor linear, inviscid, unsteady effects (*cf.* Theodorsen theory). The radial coordinate of the section (r) is normalised by the turbine radius (R). Each coefficient is maximum near the root, where the angle of attack is higher, and decreases towards the tip. Near the root, however, the unsteady values are significantly higher than the quasi-steady values, which more closely follow the steady values. This is due to the occurrence of DS. Conversely, near the tip, the unsteady values are lower than the quasi-steady values, which indicates that the unsteady effects are of a linear type. Compounded with the higher tangential velocity and longer moment arm, the lower sectional torque ($\overline{C_Q}$) and thrust ($\overline{C_T}$) near the tip lead to the reduction in the rotor's mean power and thrust, as observed in Fig. 1.

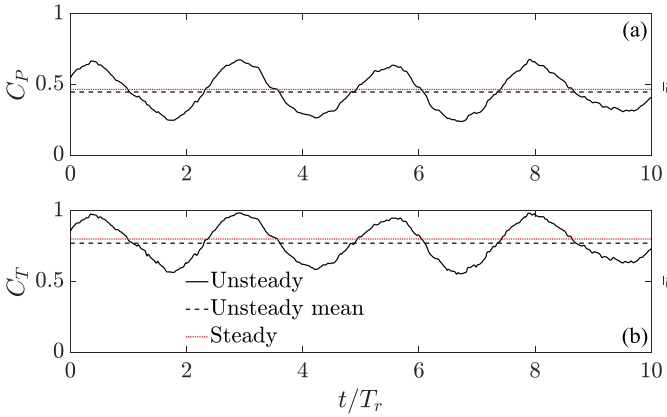

Fig. 1. Time series of (a) power coefficient and (b) thrust coefficient.

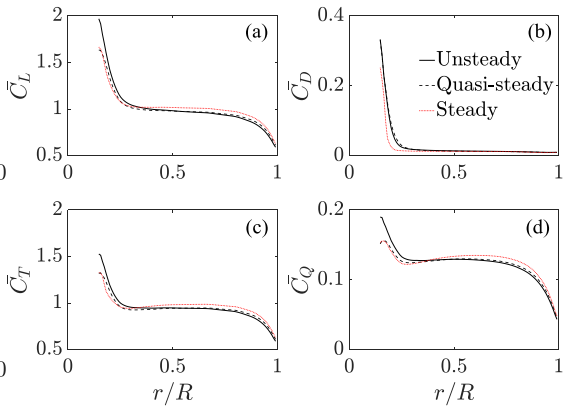

Fig. 2. Mean sectional coefficients of (a) lift, (b) drag, (c) thrust and (d) torque.

Conclusions

Large, realistic, waves conditions result in extreme fluctuations of the forces on the blade. The governing frequency is that of the wave, not the rotational frequency. The amplitude of the power and thrust variations are ca. 50% and 25% of their mean values. Dynamic stall occurs in the inner sections of the blade, but due to the low tangential velocity and small moment arm, it has a negligible effect on the rotor's performance. Conversely, linear, inviscid, unsteady effects at the tip result in a reduction of the maximum load fluctuations and of the rotor's mean power and thrust. These results show that large waves induce significantly large load fluctuations, however, there is little effect on the mean performance of the rotor.

Acknowledgements:

The first named author is supported by an Engineering and Physical Sciences Research Council studentship. Field measurements were acquired under the ReDAPT project, co-funded by the Energy Technologies Institute.

References:

[1] Milne I. A., Day A. H., Sharma R. N. and R. G. J. Flay, 2016. The characterisation of the hydrodynamic loads on tidal turbines due to turbulence, *Renewable Sustainable Energy Rev*, 56:851-864.

[2] Galloway P. W., Myers L. E. and A. S. Bahaj, 2014. Quantifying wave and yaw effects on a scale tidal stream turbine. *Journal of Renewable Energy*, 63:297-307.

[3] Butterfield C. P., D. Simms G. Scott and A. C. Hansen, 1991. Dynamic stall on wind turbine blades. No. NREL/TP-257-4510; CONF-9109112--7. National Renewable Energy Lab.

[4] Ning S. A, 2014. A simple solution method for the blade element momentum equations with guaranteed convergence. *Wind Energy*, 17:1327-1345

[5] Lindenburg C, 2004. Modelling of rotational augmentation based on engineering considerations and measurements, In European Wind Energy Conference, London, pp. 22-25.

[6] Sheng W, Galbraith R. A. M. and F. N. Coton, 2008. A modified dynamic stall model for low Mach numbers, *Journal of Solar Energy Engineering* 130: 031013.

[7] Gretton G. I, 2010. Development of a computational fluid dynamics model for a horizontal axis tidal current turbine. PerAWaT technical report, MA1003 WG3 WP5 D1.

[8] Sellar B, (2011 – 2014). Metocean data set from the ReDAPT project: http://dx.doi.org/10.7488/ds/1687

[9] Janiszewska, J. M., R. Reuss Ramsay, M. J. Hoffmann, and G. M. Gregorek, 1996. Effects of grit roughness and pitch oscillations on the S814 airfoil. No. NREL/TP--442-8161. National Renewable Energy Lab.

Unsteady Loading in an Array due to Simulated Turbulent Onset Flow

Hannah Mullings*, Tim Stallard, Imran Afgan
School of Mechanical, Aerospace and Civil Engineering, University of Manchester, UK

Summary: Unsteady loading due to environmental conditions and typical operation in an array is assessed. Load variations considered are due to onset turbulence and shear caused by both a theoretical seabed and wake onset for in-array positions. An investigation into the differences in loading cycles for a turbine in an upstream wake due to a turbulence and turbine position is shown. These differences are used to inform criteria for optimum set-up for a larger array of turbines. The objective is to standardise design life across an array based on damage equivalent loads and fatigue life.

Introduction

Maximising operating life is an important design objective for energy producing devices. This requires a thorough understanding of operational and environmental loads. Reliability of tidal stream turbines has previously been assessed for single turbine cases [1], typically with an emphasis on fatigue design of turbine blades. There has been little analysis of either the uncertainty on the loads due to either the method used for generating turbulent flow fields, with most studies employing spectral models, or the variation of load cycles due to in-array operation. This study examines in-array loading; with a focus on the effect of turbine positions within an array and turbulence generation methods on the effect of the uncertainty on the design life of turbines. The aim is to assess various operating points to establish consistent fatigue life across multiple turbines in the array, to work towards the standardisation of array operation.

Methods

For any working device the load cycles are dependent on time varying forces. This can be predicted using a range of methods of differing sophistication and computational cost, such as CFD and blade element type engineering models. Here, an interim approach is used which consists of synthesising alternative turbulent flow fields to obtain the time-varying velocity at a virtual blade point. Load cycles are determined from the resultant synthesised time history of rotor force using the Rainflow counting method [2] and a Damage Equivalent Load (DEL) obtained.

Blade forces and hence rotor thrust are obtained using two turbulent generation methods to establish inflow conditions. A domain of turbulent velocity has been generated using both a von Kármán spectra and a Synthetic Eddy Method [3]. For both of the generation methods a turbulence intensity of 3% and a length-scale of 0.6 m are used, representing a laboratory case. From these turbulent domains a helix of velocities for each of ten radii along a blade span and with the helix pitch defined by the tip speed ratio, see in Fig. 1. The turbulent velocity field considered here is taken as 'frozen' when it reaches each rotor point, no distortion effects have been investigated, as in [4], therefore the change in the turbulence ratio has been neglected. Relative velocities for each blade radii are input to a blade element calculation of rotor thrust. For turbines in an array, unsteady onset flow is superimposed with an upstream turbine wake profile following the semi-empirical wake equations in [5]. The total cycles are obtained for a specified target life for each turbine position case and operating point. The damage equivalent loads are defined as a repeating single magnitude load at a representative frequency; this frequency depends on the calculated initial load cycles. A comparison of loads is obtained by imposing the rotor frequency onto the calculation of damage equivalent loads for both generation methods.

Results

Spectra of the relative velocity incident to a blade segment are examined for three alternative inflow cases; (a) vertical shear applied ($1/7^{th}$ profile) and transverse shear from (b) in-line turbines, (c) offset (+/-0.5D) for one blade. The introduction of vertical shear leads to a peak at the rotor frequency f_0, this peak reduces with the inclusion of a wake for an in-line turbine and a second peak is observed at $2f_0$. By offsetting the downstream turbine the initial peak f_0 increases by a factor of 1.7 from the vertical shear case and the secondary peak is unnoticeable. The blade force at these harmonics differs by 20% for each flow field generation method with

* Corresponding author. *Email address*: Hannah.mullings@manchester.ac.uk

higher loading predicted by the SEM approach. However, for the frequency range greater than $3f_0$ the rate of decay of the load spectra is greater for the SEM inflow model than the von Kármán model. This is associated with lack of coherence of the SEM generated onset flow at higher frequencies, in agreement with conclusions drawn from [6]. As a consequence the frequency of the Damage Equivalent Load (DEL) for rotor thrust obtained with the SEM model is much smaller than for the von Kármán model but the magnitude is approximately double. However, the DEL magnitude is within 13% by both methods when the DEL frequency is considered as $3f_0$. As well as the turbulent flow with vertical shear (inflow (a)), Damage Equivalent Loads are also calculated for turbulent flow superposed with a wake profile (inflows b-c). The DEL magnitude for an imposed DEL frequency of $3f_0$ using the SEM method is shown in Fig. 2 and differs considerably with the transverse position of the downstream turbine due to difference of mean and transverse shear of the onset flow.

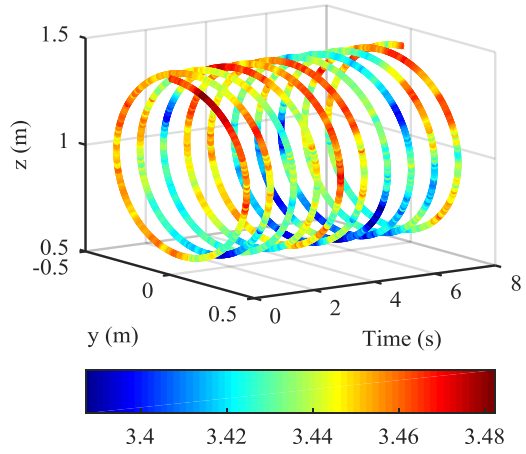

Figure 1: Helical variation of onset relative velocity at 70% radius with vertical shear profile applied.

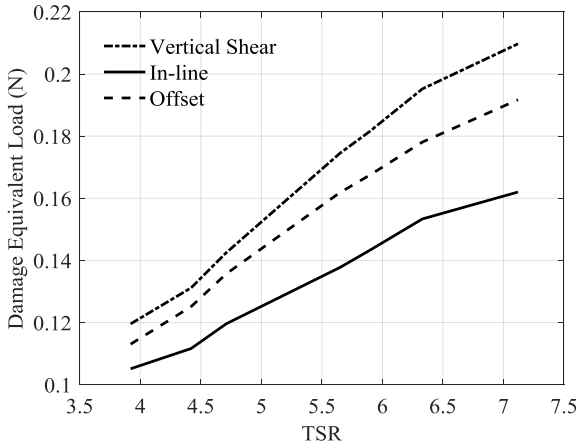

Figure 2: Variation of DELs with TSR using imposed repeating rotor frequency of $3f_0$, for the three onset flows defined by SEM, vertical shear and a semi-empirical wake.

Conclusions

The von Kármán and SEM methods for onset turbulent flow simulation generate load spectra that differ by around 20% at the rotor harmonics and with greater disparity for frequencies greater than $3f_0$. The Damage Equivalent Load (DEL) calculated from these load spectra with the same $3f_0$ imposed frequency across the TSR range considered are within 13%, with the synthetic eddy method generating higher loading. For an onset turbulent flow superposed with an upstream turbine wake, the DEL magnitude is reduced due to the decrease of the mean onset flow but with higher harmonics of loading occurring for the offset case. For all onset flow cases, the increase of TSR causes the DEL to increase. For the vertical shear and offset wake case this increase is 69-75%, for the in-line case the increase is only 54%. In this initial study, the effect of TSR on thrust coefficient and wake structure is not considered. The approach used here will be applied to examine the variation of DELs in a larger array, with comparison to experimental data. This work is part of a study investigating standardisation of load cycles and hence variation of loading for turbines in complex arrays, to achieve a similar design life.

References:

[1] Parkinson, S. G., Collier, W. J. (2016). Model validation of hydrodynamic loads and performance of a full-scale tidal turbine using Tidal Bladed. *International Journal of Marine Energy*, **16**, 279-297.
[2] Downing, S., Socie, D. (1982). Simple Rainflow Counting Algorithms. *Int. Journal Fatigue*, 31-40.
[3] Jarrin, N., Benhamadouche, S., Laurence, D., Prosser, R. (2006). A synthetic-eddy-method for generating inflow conditions for large-eddy simulations. *Int. Journal of Heat and Fluid Flow*, **27**, 585-593.
[4] Graham, J. M. R., Milne, I. (2017). Distortion Effects on Turbulence in a Tidal Flow due to the Mean Flow Field of a Horizontal Axis Tidal Turbine. In: *Proc. 12th EWTEC*, Cork, Ireland.
[5] Olczak, A., Stallard, Feng, T., T, Stansby, P. (2016). Comparison of a RANS blade element model for tidal turbine arrays with laboratory scale measurements of wake velocity and rotor thrust. *Journal of Fluids and Structures*, **64,** 87-106.
[6] Togneri, M., Masters, I, Carlier, C, Pinon, G. (2017). Comparison of synthetic turbulence approaches for two numerical tidal turbine models. In: *Proc. 12th EWTEC*, Cork, Ireland.

Dynamic Modelling of Floating Tidal Energy Converters

Jack Hughes[1], Alison J Williams, Ian Masters
College of Engineering, Swansea University, UK

Summary: Rigid Body Motion (RBM) modelling tools, used to predict the hydrodynamic loading and motions of floating bodies, are often coupled with additional codes to analyse operational performance of energy conversion devices. While existing open-source modelling tools serve this purpose for Wave Energy Converters (WECs) and Floating Offshore Wind Turbines (FOWTs), a tool for predicting the performance of Floating Tidal Energy Converters (FTECs) is yet to be established. Plans for developing a dynamic modelling tool for FTECs are presented, involving plans to couple established RBM and BEMT codes to model the overall performance of a FTEC.

Introduction

In order to achieve effective design of Tidal Energy Converters (TECs), in particular Tidal Stream Turbines (TSTs), it is necessary to predict the dynamic response of the system in its operational environment; this requires a multi-systems approach that considers the fluid-structure interactions as well as the performance of the turbine. The addition of a floating structure, thus the addition of a free surface in the model, adds an extra level of complexity. This has been recently explored in models of FOWTs such as NREL's aero-hydro-servo-elastic FAST model [1]. However no such model exists for modelling FTECs. Blade Element Momentum Theory (BEMT) has been used extensively in the wind energy sector to predict rotor performance and more recently, by the tidal energy industry for analysing TSTs. Swansea University's BEMT code has shown good agreement with experimental results when predicting rotor performance of fixed-TSTs in a range of operating conditions and may be run with a low computational demand [2, 3]. However, this method does not consider the fluid interaction and motions of a supporting structure.

RBM modelling is essential to many industries for hydrodynamic analysis of offshore structures and many modelling tools currently exist for this reason. Commercial dynamic analysis tools, such as ANSYS AQWA and PROTEUSDS, offer some significant benefits over open-source modelling tools, like adaptability to multiple industries, 1-to-1 support and all-in-one integrated packages. However, large licensing fees and limited flexibility can disaffect users with lower budgets and more specific needs. Open-source RBM tools are often industry-specific, especially when it involves energy conversion, for example wave energy related WEC-Sim and offshore wind related openFAST. An advantage of industry-specific code is that the Power-Take-Off (PTO) systems can be given more detailed consideration, for example, WEC-Sim provides the user with the ability to model PTO systems to determine the energy extraction of a given WEC [4]. Similarly, openFAST includes a BEMT aerodynamics module, which is part of a fully-coupled model, capable of predicting electrical power output of a FOWT in a range of operating conditions [1].

This study will consider the suitability of the aforementioned open-source RBM modelling tools for coupling with Swansea University's BEMT code to analyse the performance of a FTEC, as part of the EPSRC SUPERGEN Marine project "SURFTEC: Survivability and Reliability of FTECs". A simple moored buoy will be modelled, based on experimental work carried out by Ransley [5] in which a 6-DoF openFOAM model was validated against wave tank test data in decay tests and extreme wave events, with the aim of achieving comparable results at a fraction of the computational cost of CFD. This allows for the comparison of open-source modelling tools against validated wave tank test data.

Methods

To generate the moored buoy [5] experimental model in WEC-Sim, the following method will be used:

1. The CAD model and mesh of the moored buoy are generated in open-source CAD software, Salome, as shown in Fig. 1.

[1] Corresponding author.
Email address: 708774@swansea.ac.uk

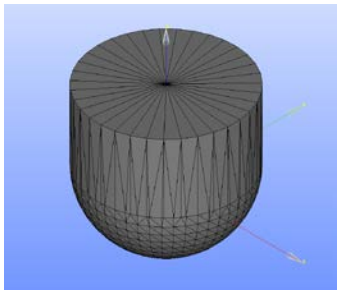

Fig. 1. Geometry of moored buoy, based on Ransley thesis dimensions [4].

2. The hydrodynamic coefficients; radiation damping, added mass, wave diffraction force, and wave excitation force, are generated in open-source Boundary Element Method (BEM) code, Nemoh and BEM pre- and post-processor code, BEMIO [6].
3. The wave tank experiments can then be reproduced in WEC-Sim by adjusting the code accordingly based on the methodology and description of tests conducted by Ransley [5].

Currently, steps 1 & 2 of the methodology have been completed, with WEC-Sim results to follow.

Future Work

In addition to the moored buoy experiments, plans for future work include testing a simplistic FTEC geometry, with the turbine modelled as an actuator disc [7], in WEC-sim and openFAST, as well as experimental wave tank testing. The testing of additional geometries is critical in determining whether the modelling tools are suitable for application to FTECs.

The compatibility of the established RBM tools will be analysed for coupling with the Swansea University BEMT code based on a number of criteria, the validity of results compared with the moored buoy experiments, computational expense, the ability to run relevant FTEC simulations and the relative complexity of coupling with the Swansea code.

The combined model will be validated using field data from the SURFTEC project, with the intention of further analysing the system behaviour of FTECs by modelling the operational stresses and fatigue.

Acknowledgements:
The author would like to thank Emilio Faraggiana for assisting in using Nemoh and WEC-sim.

References:

[1] Jonkman, J.M., 2007. *Dynamics modeling and loads analysis of an offshore floating wind turbine*. University of Colorado at Boulder.
[2] Masters I, Chapman JC, Willis MR, Orme JA (2011). A robust blade element momentum theory model for tidal stream turbines including tip and hub loss corrections. *Journal of Marine Engineering & Technology*. 2011 Jan 1;10(1):25-35.
[3] Masters I, Williams A, Croft TN, Togneri M, Edmunds M, Zangiabadi E, Fairley I, Karunarathna H. A comparison of numerical modelling techniques for tidal stream turbine analysis. *Energies.* 2015 Jul 30;8(8):7833-53.
[4] Code Structure — WEC-Sim documentation [Internet]. Wec-sim.github.io. [cited 7 February 2018]. Available from: https://wec-sim.github.io/WEC-Sim/code_structure.html
[5] Ransley E. Survivability of Wave Energy Converter and Mooring Coupled System using CFD [PhD]. Plymouth University; 2015.
[6] Boundary Element Method Input/Output (bemio) Documentation and Users Guide — bemio v1.0a0 documentation [Internet]. Wec-sim.github.io. [cited 7 February 2018]. Available from: https://wec-sim.github.io/bemio/index.html#
[7] Myers, L. E., & Bahaj, A. S. (2012). An experimental investigation simulating flow effects in first generation marine current energy converter arrays. *Renewable Energy*, *37*(1), 28-36.

Hydroelastic modelling of a composite tidal turbine blade

Federico Zilic de Arcos*, Christopher R. Vogel, Richard H. J. Willden
Department of Engineering Science, University of Oxford, UK

Summary: The traditional engineering approach to analyse and design turbines for energy extraction is based on decoupling the hydrodynamics from the structural design. Whereas this approach might be suitable for the analysis of a stiff structure, the use of composite materials to build cost-effective blades results in structures for which large deflections might occur, changing the hydrodynamic performance and the loads to which the structure is subjected. A coupled fluid-structure interaction approach must be taken to fully assess such devices.

Introduction

This poster describes the application of a fluid-structure interaction model based on a blade element momentum code (BEM) coupled with a finite elements static structural solver (FEM) to obtain the performance under different operating conditions of a generic 20m diameter tidal turbine based on the Risø-A1-24 aerofoil designed to operate at a tip speed ratio $\lambda = 5.5$. In this approach, the loads are transferred from the BEM to the FEM solver, and the angular deflections obtained from the FEM are then used as an input for the BEM solver, iterating until convergence is achieved.

BEM theory is a widely used method for analysing flow through a horizontal axis rotor in both tidal and wind energy application. The approach involves the solution of a system of equations comprising the momentum theory of a 1D flow passing through an actuator disc, and the blade element theory that describes the blades of a turbine as a collection of two-dimensional foil sections [1]. The present work implements the BEM method as described by Ning [2], which parametrises the system of equations into a single one depending on the inflow angle ϕ, instead of using two for the axial and tangential induction factors, guaranteeing a solution inside the range of operation.

Methods

The turbine blade structure was modelled using shell elements in the ANSYS® FEM software for steady structural simulations. The structure was designed following a traditional engineering approach, using carbon fibre and both woven and unidirectional laminates, applying the equivalent maximum thrust and tangential force at the rated flow velocity of 2m/s and maintaining a safety factor of 2. The blade was modelled as a cantilever beam, fixed at the root and the loads applied at the tip for the design scenario, and as pressure fields in the coupled model. A safety factor of 2 was employed.

The interface software was written in python. This code calculates the loads from the BEM, converts them into two two-dimensional pressure fields and then writes an ANSYS APDL file, based on the initial FEM model and includes the pressures for each iteration. The software then retrieves the deformed shape of the blade and uses that information as input for the BEM model, iterating as shown in Fig. 1. The convergence criteria were based on the integrated power and thrust coefficients, with a maximum of 20 iterations and taking around 5 minutes to solve per operational point on a standard workstation.

Experimental data [4] was employed for lift, drag and pressure coefficient distributions. The latter was converted into a dimensional pressure and distributed across the blade in the points defined by the grid.

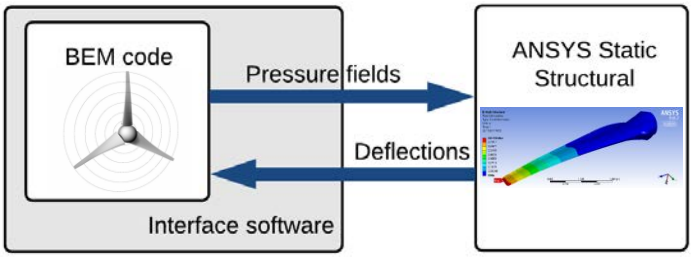

Figure 1. BEM-FEM code structure

* Corresponding author.
Email address: federico.zilic@eng.ox.ac.uk

Results

The turbine was analysed using the proposed model at three different flow speeds (2, 4 and 6 m/s) for $1 \leq \lambda \leq 10$ (Fig. 2). The maximum angular deflection of the blade was 0.5˚ at 2.0 m/s, 2.2˚ at 4m/s and 5.0˚ at 6m/s. Deformations, as can be seen in the extreme case, act passively to alleviate the loads on the turbine for most tip speed ratios.

Conclusions

Three different speeds were simulated to observe the behaviour at design and extreme conditions. Applying the loads at the tip is a conservative design case for a steady loading. The FSI results show that the turbine is capable of withstanding at least twice the design speed maintaining an adequate safety factor. Deformations act passively to alleviate the loads on the turbine for most tip speed ratios. In the future, a thorough assessment will be performed of how the turbine structural design influences its performance and understand how the structures and materials can be designed to react according to the local conditions.

Acknowledgments:
The first author would like to acknowledge the support of CONICYT PFCHA/BECAS CHILE DOCTORADO EN EL EXTRANJERO 2016 /72170292

References:

[1] Glauert, H. The elements of aerofoil and airscrew theory, Cambridge University Press, 1947.

[2] Ning, S. A.. A simple solution method for the blade element momentum equations with guaranteed convergence. *Wind Energy*, 2014, vol. 17, no 9, p. 1327-1345.

[3] Buhl, M. L. A New Empirical Relationship between Thrust Coefficient and Induction Factor for the Turbulent Windmill State. *Technical Report NREL/TP-500-36834*, 2005.

[4] Fuglsang, P., Dahl, K. S., & Antoniou, I. *Wind tunnel tests of the Risø-A1-18, Risø-A1-21 and Risø-A1-24 airfoils*. Risø National Laboratory, 1999.

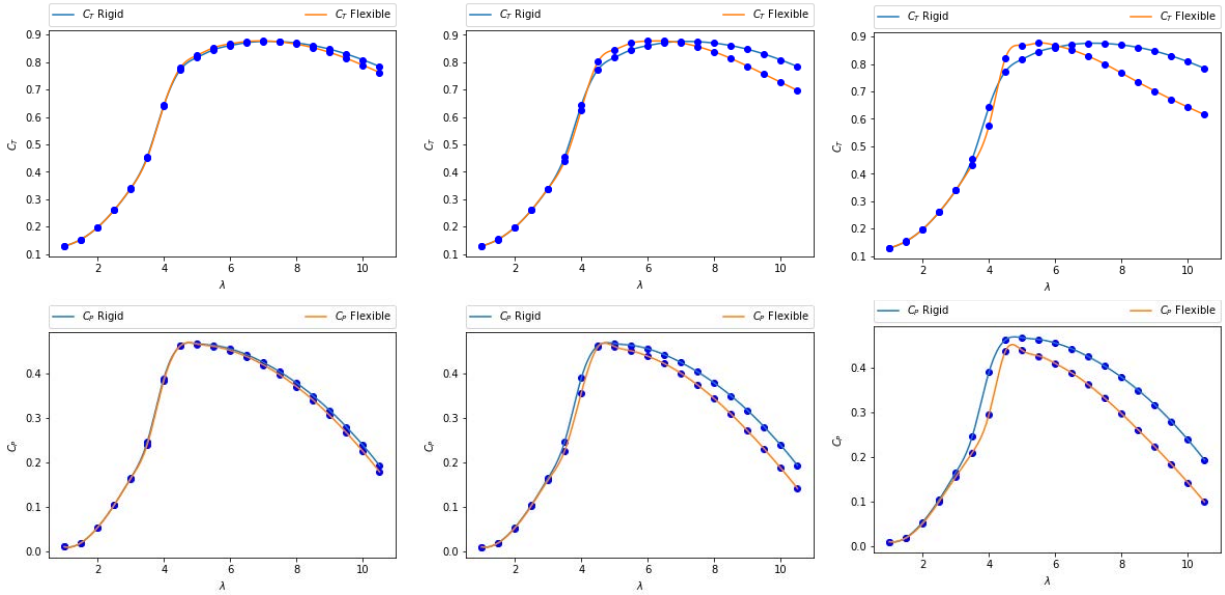

Figure 2: Thrust (top) and power (bottom) coefficients. From left to right, flow speeds of 2, 4, and 6 m/s. The graphs compare FSI (flexible – orange) and BEM (rigid – blue) results for the analysed turbine.

Coupling of WATTES and OpenFOAM codes for wake modelling behind close-packed contra-rotating vertical-axis tidal rotors

Ruiwen Zhao*, Angus Creech, Alistair Borthwick

Institute for Energy Systems, School of Engineering, University of Edinburgh, UK

Takafumi Nishino

Centre for Offshore Renewable Energy Engineering, Cranfield University, UK

Summary: This paper presents the preparatory set up of a numerical model to be used eventually to simulate flow past close-packed contra-rotating vertical-axis tidal rotors. The Wind and Tidal Turbine Embedded Simulator (WATTES) source code is used to represent turbines within the OpenFOAM CFD framework. Correct coupling of WATTES and OpenFOAM is a necessary prerequisite to device wake modelling.

Introduction

Salter et al. [1] compared vertical-axis transverse-flow tidal turbines with horizontal-axis axial-flow tidal turbines in terms of flow impedance, turbulence, blockage ratio, installation, pitch change, and navigation, with the Pentland Firth in mind. He found that high sweepage, vertical-axis, variable-pitch rotors lead to significantly higher potential power generation for high impedance flows and ducts [1]. Such vertical-axis transverse-flow turbines tolerate uneven seabeds and attain an even pressure drop by controlling the blade pitch, which contributes to low wake turbulence. Lower pitch-bearing loads are achieved and limited by adjusting the pitch angle and supporting blades at both ends. The device configuration saves plenty of space for power and pitch mechanisms. Thus, a group of close-packed contra-rotating vertical-axis rotors, shown in Fig. 1, has been designed by Stephen Salter to maximise the fraction of flow passage swept [2]. Access to the power take-off system is realised by means of a specialised quad ring-cam with digital hydraulics installed inside the annulus. The sweepage is estimated to increase to 80% given small gaps between the rotors, which are controlled by a hydraulic ram. The rotor diameter is recommended to be at least three times the water depth in order to provide stability in pitch and roll of a single rotor, and this should be doubled for a close-packed array. Following Buntine and Pullin [3], the design concept is based on two opposite-signed vortices cancelling each other out, and thus conditioning the flow though the turbine while lowering the turbulent kinetic energy in the wake. The turbine downstream area will then experience less stream-wise flow variation, enhancing energy extraction.

The vorticity magnitude distribution will be used to investigate the effect of wake turbulence on device performance; this in turn will be useful in assessing the merits and drawbacks of the vertical axis cross-flow turbine. The WATTES turbine model [4][5] (shown in Fig. 2) is presently under development for simulation of tidal flow interaction with a vertical axis turbine. The incompressible Navier-Stokes solver in OpenFOAM will be used to simulate the fluid flow around and through arrays of these turbines.

Methods

OpenFOAM is free open-source CFD software based on the finite volume method on general unstructured polyhedral meshes, and is written in C++. The WATTES code is an open library source written in Fortran 95 [6]. It uses both the dynamic torque-controlled actuator disc method and the actuator line technique with active-pitch correction to model wind and tidal turbines [4][5]. Compared with other momentum codes, WATTES predicts the dynamic response to the flow, where lift and drag force components are calculated from tabular aerofoil data instead of using axial induction factors, and included within the incompressible Navier-Stokes momentum equations as body force components. The wake modelling of close-packed contra-rotating vertical-axis tidal rotors will be built up based on the WATTES source using Fortran 95.

Before coupling the OpenFOAM and WATTES libraries of source code, an interface for linking C++ and Fortran subroutines has been integrated by calling the Fortran library from within OpenFOAM. WATTES is coupled to OpenFOAM via a dynamic library with wrapper functions. The coordinates and momentum sources of WATTES model are coupled so that they correspond correctly with those in OpenFOAM. A new fvOptions framework is introduced for run-time selectable physics, by representing the force components from the WATTES model as momentum sources in the governing equations in OpenFOAM. A simple simulation with an axial turbine configuration is undertaken for observing the wake profile behind model turbine.

* Corresponding author.
Email address: r.zhao@ed.ac.uk

Further modelling

The aim of this work is to model wakes behind close-packed contra-rotating vertical-axis tidal turbines. To accomplish this, the following tasks are necessary. First, a single vertical-axis turbine (VAT) will be modelled using actuator line theory to capture important flow features contributing to the fast wake recovery behind the VAT [7]. Tip-loss effects and dynamic stall should be investigated, and, if significant, can be incorporated in the model as corrections applied to the force terms in the actuator line method. However, the blade foils are quite short with different pitch angles at different depths. The bending stresses at both ends are decreased by a factor of nearly four. This means that the red rings (shown in Fig. 1) will suppress the tip-vortex losses caused by the adjacent foils at different angles. Although the rings experience drag, the spoked wheel could well be a more efficient load-bearing structure than a tower, which experiences vortex shedding as well as drag. Proper pitch control could solve the problem of dynamic stall. The actuator line method therefore offers a powerful technique by which to model VAT devices. Before progressing to tidal turbines, it is intended first to consider a vertical-axis wind turbine (VAWT) for which validation information is available (see e.g. Bachant et al. [7]). A pair of contra-rotating vertical-axis tidal rotors will then be modelled to examine the wake characteristics, and investigate the possibility of cancellation of opposite-signed vortices in the combined wakes behind the pair of rotors. Given the lack of experimental data on VAT tidal devices, the model will be validated using existing data from two vertical-axis wind turbines in a contra-rotating layout obtained by Parneix et al. [8]. Finally, a model of an array of close-packed contra-rotating vertical-axis tidal rotors will be tested using large eddy simulations (LES), and the wake dynamics and device performance analysed.

Acknowledgements:

The first-named author is supported by funding from the China Scholarship Council.

References:

[1] Salter, S. H. (2012). Are nearly all tidal stream turbine designs wrong? *4th International Conference on Ocean Energy*.

[2] Salter, S. H., Taylor, J. R. M. (2006). Vertical-axis tidal-current generators and the Pentland Firth. *IMechE Journal of Power and Energy*. **221**, 181-199.

[3] Buntine, J. D., Pullin, D. I. (1989). Merger and cancellation of strained vortices. *J. Fluid Mech.* **205**, 263-295.

[4] Creech, A. C. W., Fruh, W-G., Maguire, A. E. (2015). Simulations of an offshore wind farm using large-eddy simulation and a torque-controlled actuator disc model. *Surveys in Geophysics*. **36(3)**, 427 - 481. DOI: 10.1007/s10712-015-9313-7.

[5] Creech, A. C. W., Borthwick, A. G. L., Ingram, D. (2017). Effects of support structures in an LES actuator line model of a tidal turbine with contra-rotating rotors. *Energies*. **10**, 726.

[6] Creech, A.C.W. (2017). GitHub source code repository for Wind And Tidal Turbine Embedded Simulator (WATTES). Available online: https://github.com/wattes.

[7] Bachant, P., Goude, A., Wosnik, M. (2016). Actuator line modeling of vertical-axis turbines. *Wind Energy.* **00**, 1–17.

[8] Parneix, N., Fuchs, R., Immas, A., Silvert, F., Deglaire, P. (2016). Efficiency improvement of vertical-axis wind turbines with counter-rotating layout. *EWEA 2016*.

[9] Fraenkel, P. L. (2010). Development and testing of Marine Current Turbine's SeaGen 1.2MW tidal stream turbine. *3rd International Conference on Ocean Energy.*

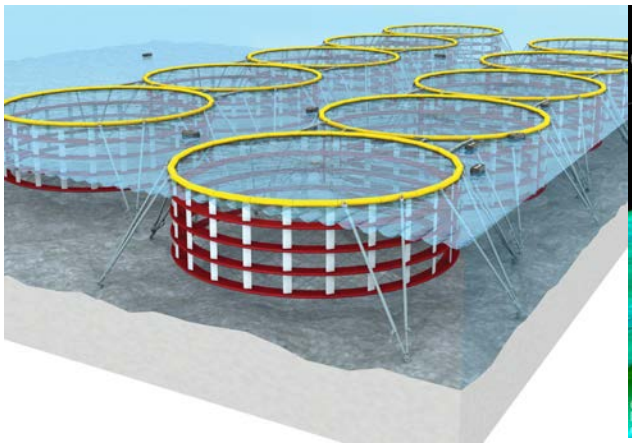

Fig. 1. An artist's impression of close-packed vertical-axis contra-rotating rotors (designed by Stephen Salter). © John MacNeill.

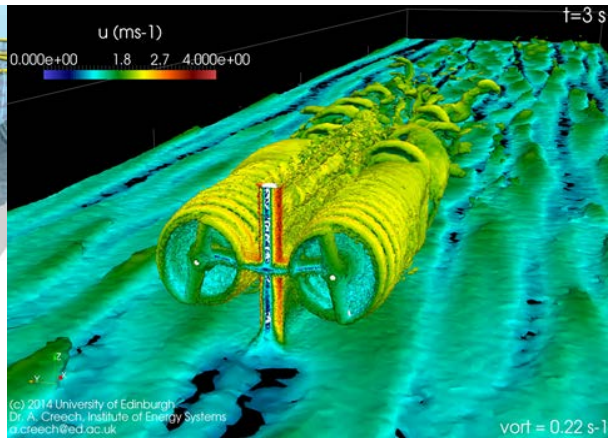

Fig. 2. A large eddy simulation using WATTES [5] of an axial-turbine installation [9] in Strangford Lough.

Characterising array performance for different operating points

Christoph Hachmann*, Tim Stallard, Peter Stansby
School of Mechanical, Aerospace, and Civil Engineering, The University of Manchester, UK

Binliang Lin
State Key Laboratory of Hydro-science and Engineering, Tsinghua University, Beijing 100084, China

Summary: The operating point of individual turbines within an array will vary through a tidal cycle. Hence, there is scope to select operating points for alternative design objectives such as maximising power generation or standardisation of turbine load ranges. A RANS CFD model of a multi-row turbine array is employed to establish variation of turbine loading, net power and drag for arrays in which each row of turbines is operated at a different operating point. This analysis informs design of an experimental campaign.

Introduction

Due to the predictability of the tidal stream resource arrays of tidal turbines could play a significant role in addressing future power network challenges as an auxiliary frequency balancing service. This would require a flexible operating strategy to achieve rapid rate of change of power supply. An option for this provision is through appropriate specification of the operating point of individual turbines, or subsets of turbines, within an array. This affects power generation of a larger group of turbines due to interactions within the array and due to feedbacks from the net resistance of the array to the coastal flow. Many studies have investigated maximum power availability [1,2] or the maximum power output from tidal arrays [3,4]. A study of a simplified tidal channel model by the authors [5] indicated that, compared to an array of identical turbines, application of a different rotor operating point for each row of an array can reduce the number of large variations of power ($\Delta P \geq$ 25% of the rated power, P_{rated}, within an hour) by 40% whilst decreasing the power output by only 13%.

Numerical Method

This paper focuses on the influence of a row-specific turbine operating strategy on the performance and loading of a multi-row array. The array configurations employed are comparable to an existing laboratory dataset of the wake and loading of tidal rotors [6] and the analysis informs an expanded experimental programme. A group of turbine rotors is modelled in the RANS-CFD solver Star-CCM+ with the k–ω SST turbulence model. The inflow is uniform and a slip condition is applied to the four plane stream-wise boundaries. Each rotor is modelled as a Constant Actuator Disc defined by a constant momentum sink term implemented across each disc:

$$\frac{F_x}{V} = \frac{\rho c_x u_D^2}{2 \cdot \Delta x} = \frac{\rho c_T u_0^2}{2 \cdot \Delta x} \quad (1)$$

Here, u_D, u_0, Δx as well as c_x and c_T refer to the disc and onset velocity, disc thickness as well as the local and global thrust coefficient, respectively. The simulation domain is set as a rectangular box with a length, width, and depth of 70D, 19D, and 1.68D, respectively, where D is the disc diameter. Applying Froude scaling to lab-scale dimensions, this configuration represents an 18 m diameter tidal stream turbine in a channel of 30 m depth The arrays studied comprise up to 12 rotors deployed in 3 rows with transverse and longitudinal spacing of 1.5D and 4D, respectively. We choose row-specific values for c_x of 1.2, 2.0, and 4.0 for rows 1, 2, and 3, respectively, to represent typical operating values of both turbine thrust and power coefficient developed within the range of onset flow speeds experienced by a turbine in-array with power output inferred as $F_x U_D$. The array performance coefficients reported are the sum of individual turbine performance coefficients. The three operating points and values for c_x follow from generic curves of thrust- and power-variation with velocity and tip-speed ratio: below rated speed where power is low but thrust high (c_x = 4.0), close to rated speed where power is maximum and thrust has decreased (c_x = 2.0), and above rated speed with sustained peak power and low thrust (c_x = 1.2).

Results

For an array with 3, 4, and 5 turbines in the first, second, and third row, respectively, two operating strategies are compared; a baseline strategy with constant operating point, c_x = 2.0, across the entire array and an adapted strategy with row specific operating point, $c_{x,row1}$ = 1.2, $c_{x,row2}$ = 2.0, $c_{x,row3}$ = 4.0.The choice of operating point

* Corresponding author.
Email address: christoph.hachmann@manchester.ac.uk

can have a substantial impact on the performance of the array. For a one-directional flow, the adapted operating strategy leads to a more sustained energy flux through the array and thus, smaller disparity of power generation between turbines. This results in an increase of thrust and power of 2.4% and 8.5%, respectively. For the reverse flow case, the adapted strategy decreases array power by 3.7%. This also reduces the net thrust by 3.5%, which would result in smaller changes to the coastal flow. The observation of a more sustained energy flux through the array is also shown quantitatively and qualitatively in form of performance coefficients and the surrounding flow field in Figure 1. An alternative strategy with high value of thrust and power generation along the upstream row leads to greater disparity of loads between turbines and lower power output.

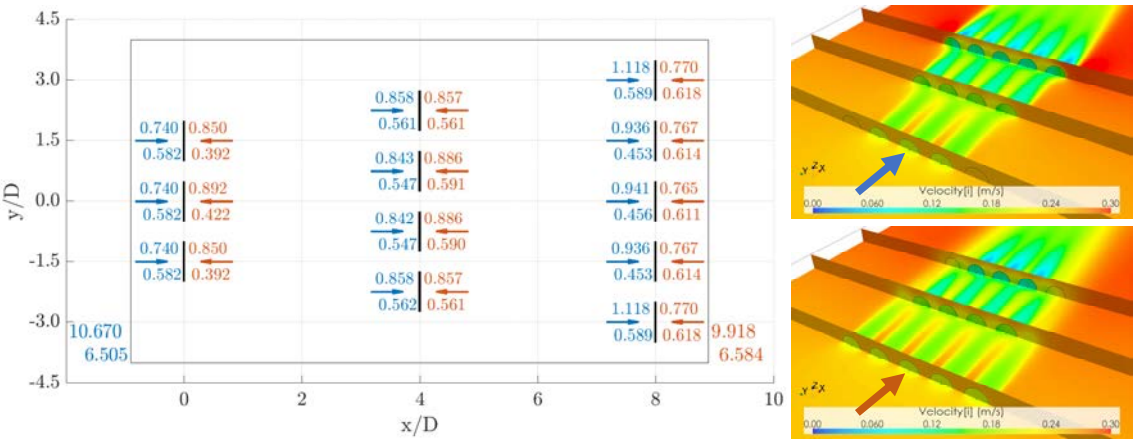

Fig. 1. Thrust (top text) and inferred power (bottom, indented text) coefficients for individual turbines and the whole array (left) and corresponding velocity field at mid-depth (right) of a 3-row array operating in flow in +ve (blue text on left) and –ve (orange text on right) directions when applying the adapted operating strategy.

Conclusions

This study aims to characterise the performance of an array for different operating points. Depending on the array configuration and in particular for larger arrays the choice of operating point for each row of turbines can have a significant impact on the performance of the array as a whole as well as the loading of individual turbines. Hence, array performance can be optimised which in turn will improve the operational flexibility of the array and the potential for reduced variation of power supply can be beneficial for grid integration.

Acknowledgements:

The author acknowledges financial support from EPSRC (EP/L016141/1) through the Power Networks Centre for Doctoral Training. The authors of this paper also received funding from the EU-China "IRES-8" Mobility Project under EU Contract Number No ICI+/2014/347-910. The contents reflect only the author's view and the European Union is not liable for any use that may be made of the information contained therein.

References:

[1] T.A.A. Adcock, S. Draper, G.T. Houlsby, A.G.L. Borthwick, S. Serhadlioglu. (2013). The available power from tidal stream turbines in the Pentland Firth. In: *Proc. R. Soc. A Math. Phys. Eng. Sci*. **469**.

[2] R. Vennell, S.W. Funke, S. Draper, C. Stevens, T. Divett. (2015). Designing large arrays of tidal turbines: A synthesis and review. *Renew. Sustain. Energy Rev*. **41**, 454–472.

[3] Y. Chen, B. Lin, J. Lin, S. Wang. (2015). Effects of stream turbine array configuration on tidal current energy extraction near an island. *Computers & Geosciences*. **77**, 20–28.

[4] P. Stansby, T. Stallard (2016). Fast optimisation of tidal stream turbine positions for power generation in small arrays with low blockage based on superposition of self-similar far-wake velocity deficit profiles. *Renew. Energy*. **92**, 366–375.

[5] C. Hachmann, T. Stallard, P. Stansby. (2017). Simulation of groups of tidal rotors with support structures. In: Proc. *12th European Wave and Tidal Energy Conference*. Cork, Ireland.

[6] A. Olczak, T. Stallard, T. Feng, P. Stansby. (2016). Comparison of a RANS blade element model for tidal turbine arrays with laboratory scale measurements of wake velocity and rotor thrust. *J Fluids Struct.* **64**, 87–106.

A basin-scale comparison of constrained BEM and actuator disc models

Lei Chen*, Christopher R. Vogel, Thomas A. A. Adcock
Department of Engineering Science, University of Oxford, UK

Paul A. J. Bonar
School of Engineering, University of Edinburgh, UK

Summary: In this abstract, we compare the basin-scale performance of tidal turbines represented using the volume flux-constrained actuator disc (AD) and blade element momentum (BEM) theories. For the more realistic BEM model, the available power is found to be at least 25% lower than that predicted by the AD model and the importance of 'tuning' turbines, i.e. optimising their resistance by adjusting the pitch or rotational speed of the turbine blades, is greatly reduced.

Introduction

Actuator disc theory provides what is perhaps the simplest representation of an axial flow turbine. Actuator disc models are widely used in the basin-scale modelling of tidal turbines, where they provide an inexpensive means of capturing blockage effects. Such models have been used to provide upper bound estimates of tidal stream energy resources and to demonstrate the need to 'tune' turbines to maximise their power output [1]. Here we compare the basin-scale performance of tidal turbines represented using the volume flux-constrained actuator disc (AD) and blade element momentum (BEM) theories. Though still idealised, the BEM model provides a more accurate description of turbine performance than does the AD model.

Methods

To model the turbines, we use the volume flux-constrained AD model of Garrett & Cummins [2] and the volume flux-constrained BEM model of Vogel [3], which extend the respective classical theories to incorporate blockage effects. For the BEM model, we use a fixed rotor design (a fixed number of blades and a fixed solidity) with the specifications of the Risø-A1-24: a 24% thickness aerofoil section that has been used to validate the model against the blade-resolved simulations of Wimshurst & Willden [4]. Basin dynamics are simulated using the simple channel model of Garrett & Cummins [5], for which we specify non-linear bed friction and employ a Runge-Kutta solver. Turbines are arranged in full-width, high blockage (B=0.4) rows and their performance characteristics are represented by the local resistance coefficient k (see figure 1).

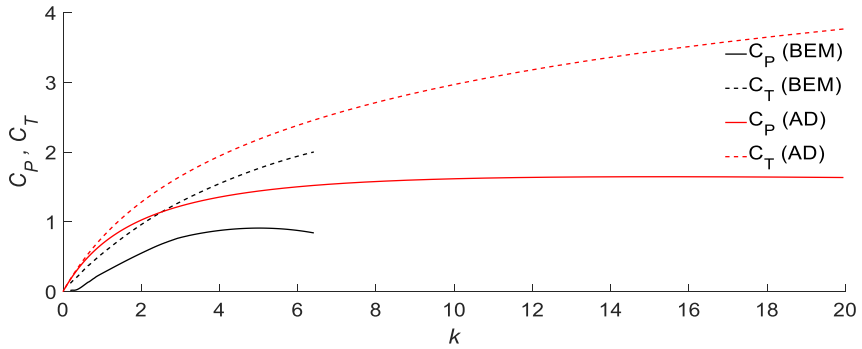

Figure 1: Variation of power and thrust coefficient for the highly blocked (B=0.4) BEM and AD models.

Results

We first consider the case in which the local resistance k is temporally fixed, i.e. does not vary over the tidal cycle. Figure 2*a* compares the maximum time-averaged power available to the BEM and AD models, and shows the power available to the BEM model to be at least 25% lower than that predicted by the AD model. Figure 2*b* shows how the optimal temporally fixed k varies with the channel's natural dynamic balance λ_0 [e.g. 5]. The importance of turbine tuning is greatly reduced for the BEM model because the more realistic turbines are unable to exert sufficient thrust on the flow for their resistance to become significant. It is worth noting, however, that these results may vary with the design of the rotor chosen for the BEM model.

* Corresponding author.
Email address: lei.chen@eng.ox.ac.uk

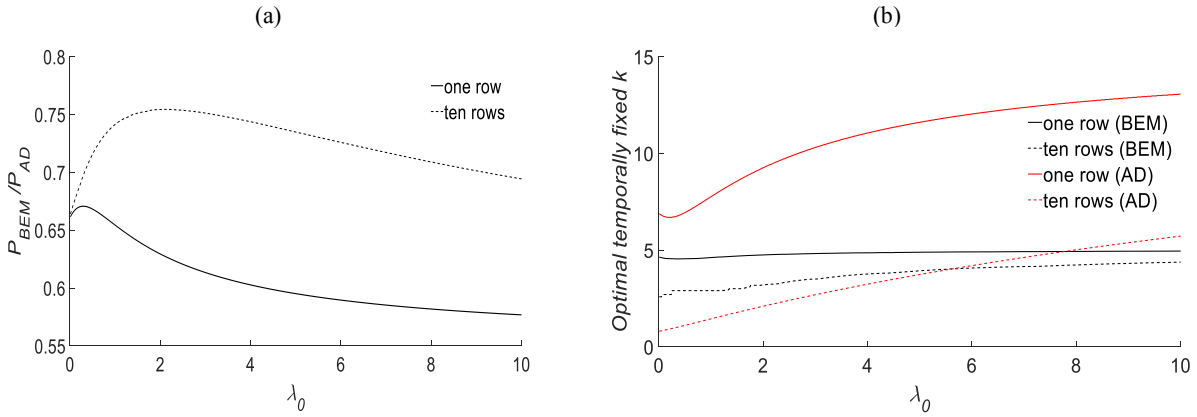

Figure 2: Comparison between BEM and AD models with temporally fixed local resistance k: variation of (a) maximum time-averaged available power, and; (b) optimal temporally fixed k.

Following Vennell & Adcock [6], we also consider the case in which the local resistance k of 5 uniform rows is varied over the tidal cycle. Calculating the optimal temporally variable k is a difficult optimisation problem and whilst we are confident that we have identified the key trends, we acknowledge that we may be slightly short of the global optimum. Figure 3*a* compares the (near) optimal temporal variation in k for the BEM and AD models, whereas figure 3*b* shows the potential increase in available power for both models relative to the case of temporally fixed k. The use of a temporally varying k is found to increase the power available to turbines in inertia-dominated channels but the benefits of time-varying tuning are shown to be relatively minor, particularly for the more realistic turbines.

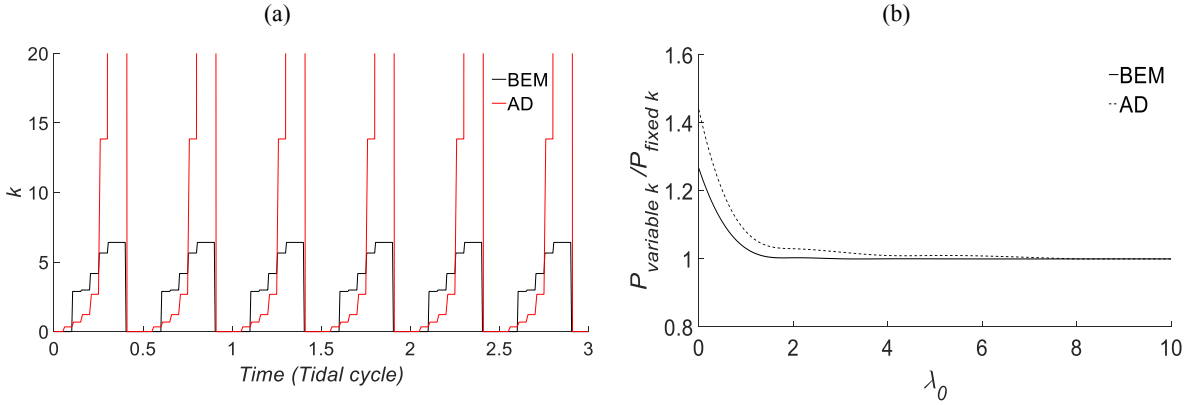

Figure 3: Comparison between BEM and AD models with temporally variable local resistance k: variation of (a) (near) optimal temporally variable k, and; (b) maximum time-averaged available power relative to temporally fixed k.

Conclusions

We have found that, as expected, actuator disc theory significantly overpredicts the amount of power available to more realistic models of tidal turbines. We have also shown turbine tuning to be relatively unimportant for more realistic turbines because they are unable to exert sufficient thrust on the flow for their resistance to become significant.

References:

[1] Vennell, R. (2010). Tuning turbines in a tidal channel. *J. Fluid Mech.* **663**, 253-267.
[2] Garrett, C., Cummins, P. (2007) The efficiency of a turbine in a tidal channel. *J. Fluid Mech.* **588**, 243-251.
[3] Vogel, C. (2014) Theoretical limits to tidal stream energy extraction. DPhil thesis, University of Oxford.
[4] Wimshurst, A., Willden, R.H.J. (2016) Computational analysis of blockage designed tidal turbine rotors. In: *2nd International Conference on Renewable Energies Offshore (RENEW), Lisbon, Portugal.*
[5] Garrett, C., Cummins, P. (2005) The power potential of tidal currents in channels. *Proc. R. Soc. A* **461**, 2563-2572.
[6] Vennell, R., Adcock, T.A.A. (2014) Energy storage inherent in large tidal turbine farms. *Proc. R. Soc. A* **470**:20130580.

The effects of uncertain bottom friction on estimates of tidal current power

Monika Kreitmair*, Alistair Borthwick
School of Engineering, University of Edinburgh, UK

Ton van den Bremer
Department of Engineering Science, University of Oxford, UK

Scott Draper
Oceans Institute, The University of Western Australia, Australia

Summary: The research to be presented at the workshop explores the impact of uncertainty in the value of bed roughness coefficient on estimates of the power that can be extracted from tidal streams. We introduce this uncertainty in two seminal theoretical models for tidal power potential and use perturbation methods to identify the leading-order effect of the uncertainty on the expected power dissipated and on the optimal turbine deployment in a tidal channel.

Introduction

Numerous sources of uncertainty affect estimates of the power potential of tidal currents, resulting in large ranges for the values reported for power estimates for a given site, such as the Pentland Firth, UK. We examine the role of one of the most important sources of uncertainty, namely regarding the magnitude of bottom friction. The bed roughness coefficient is commonly used as a tuning parameter in numerical basin-scale tidal energy models, with a single value for the coefficient being applied throughout the modelled domain. This value is altered until model predictions are in satisfactory agreement with observed values for water depth and flow velocities observed in the field. However, often no single value gives results that are in total agreement with field data and there remains uncertainty in the correct value to use [1]. We examine the influence of this uncertainty on the expected power dissipated by the turbines and optimal channel design.

Method

We consider two theoretical models for the extraction of power by turbines from tidal flow. The first is that of Garrett & Cummins (2005) [2] (henceforth GC05), which considers quasi-steady flow in a channel connecting two large basins. The second model is that of Vennell (2010) [3] (henceforth V10), an extension to GC05, where the assumption quasi-steady flow is relaxed by retaining the inertial term in the governing momentum-balance equation. In both of the channel models turbines are deployed across the whole cross-section of the channel such that the presence of the turbines may be represented by a global increase in bed roughness. The models find an analytical, closed-form solution for power dissipated, given in terms of a bed roughness parameter λ_0 and a turbine drag parameter λ_T.

Uncertainty in the value of background roughness coefficient is introduced by perturbing the bed roughness parameter about its mean value and expanding the solution for power as a Taylor series in terms of this perturbation about the deterministic case. By taking the expectation of the series, an expression for expected power is obtained, in terms of the mean of the bed roughness parameter μ_{λ_0}, its variance $\sigma_{\lambda_0}^2$, and the turbine drag parameter λ_T. As we are concerned with leading-order behaviour, we truncate the series at second order and hence do not consider higher-order statistical moments of the bed roughness parameter, but only variance. The expected power is maximised with respect to the turbine drag to obtain an expression for the optimum turbine drag under uncertainty $\lambda_T{}^*$, again as a function of the statistical moments of the bed friction parameter (mean and variance). Similarly, the standard deviation in power is determined.

Results

In the channel models GC05 and V10, the bottom friction parameter λ_0 is a measure of the dynamic balance in the channel, as it represents the ratio of the combination of the natural drag losses and exit separation to acceleration in the channel, normalised by the driving amplitude. Large values of λ_0 correspond to channels in which the dynamics are dominated by the effect of friction and small values to channels where inertia dominates. In the quasi-steady limit of GC05 (large λ_0 such that the inertial term may be neglected), uncertainty in λ_0 is

* Corresponding author.
Email address: m.kreitmair@ed.ac.uk

found to have the effect of increasing the expected power for all values of mean background friction and turbine drag λ_T. That is to say, the power determined from a distribution of values for the bed roughness parameter is greater than that calculated from the mean value for λ_0. This may be seen in Figure 1a which shows the change in expected power $\Delta E[P] = E[P] - P_{det}$ normalised by deterministic power P_{det} and the relative variance in the bed friction parameter $\hat{\sigma}^2_{\lambda_0} = \sigma^2_{\lambda_0}/\mu^2_{\lambda_0}$, and as a function of the turbine drag scaled by μ_{λ_0}. Here, the black line is positive for all values of $\lambda_T/\mu_{\lambda_0}$. The effect of uncertainty on the expected power is a result of neglecting the inertial term and the consequent inverse relationship between the non-dimensional flow rate Q' (and hence power) and λ_0 in this quasi-steady limit. This results in a positive second derivative with respect to λ_0 and thus a positive change in expected power. Furthermore, the turbine drag at which the expected power is maximised is reduced by a constant factor independent from the mean background friction μ_{λ_0}, as shown in Fig. 1b. This figure shows the change in the optimum turbine drag value, normalised by the optimum drag of the deterministic case and per unit relative variance $\hat{\sigma}^2_{\lambda_0}$, and as a function of mean background friction.

By retaining the inertial term in V10, the change in the expected power $E[P]$ now depends on the relative magnitude of turbine drag to mean background friction, as seen in Fig 1a. Because the driving head is balanced by both the acceleration of the flow as well as the dissipation due to drag in the channel, the flow rate Q' is bounded as $\lambda_0 \to 0$ (see inset in Fig. 1a). As a result, for sufficiently small values of μ_{λ_0}, the change in expected power becomes negative for small values in turbine drag as the power curve changes from convex to concave in the transition from a friction to an inertia dominated regime. The effect on the optimal turbine tuning changes also, with the decrease in the value of $\lambda_T{}^*$ now depending on the value of mean background friction (see Fig. 1b), and is generally reduced.

Conclusions

The effect of uncertainty in bed roughness on power extracted by turbines has been found to be sensitive to the dynamic balance of a tidal channel. For a friction-dominated channel, there is an increase in the expected power. This behaviour changes as the channel becomes more inertia dominated and the expected power increases by less and can even reduce due to the effects of uncertainty in the inertial regime. However, regardless of dynamic balance, it is always beneficial to reduce the turbine drag under uncertainty, as larger amount of expected power may be extracted with a smaller deployment of turbines.

References:

[1] Adcock, T. A. A., Draper, S., Houlsby, G. T., Borthwick, A. G. L., Serhadlioğlu, S. (2013) The available power from tidal stream turbines in the Pentland Firth. Proc. R. Soc. A **469**.
[2] Garrett, C. & Cummins, P. (2005) The power potential of tidal turbines in channels. Proc. R. Soc. A **461**, 2563-2572.
[3] Vennell, R. (2010) Tuning turbines in a tidal channel. J. Fluid Mech. **663**, 253-267.

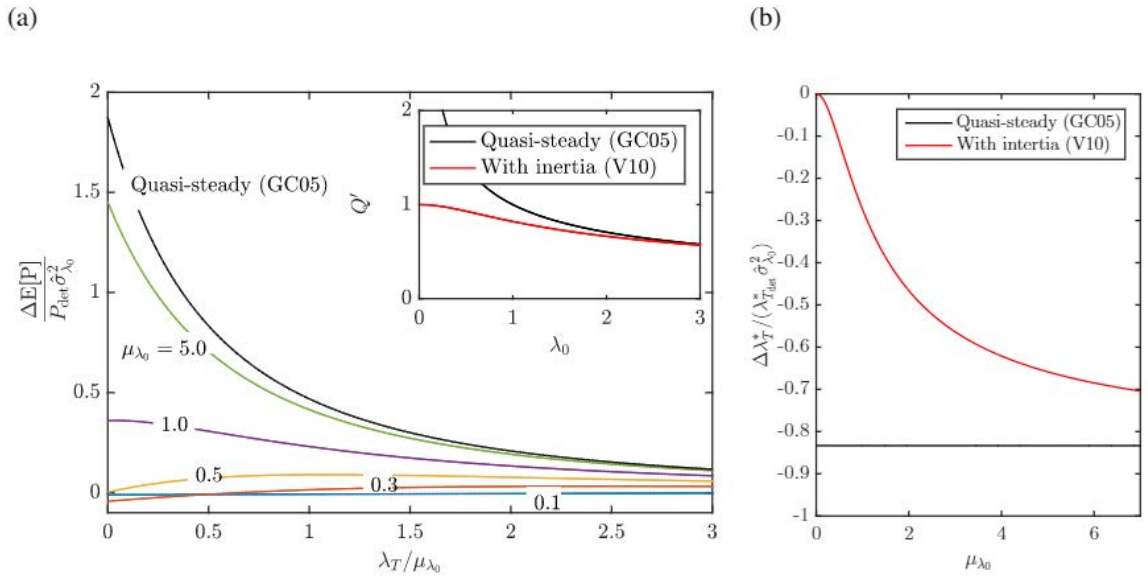

Fig. 1. Relative change in expected power as a function of the turbine drag λ_T (scaled by mean bed friction parameter μ_{λ_0}) per unit relative variance in λ_0, determined from the GC05 and V10 models (a) and relative change in the optimal turbine friction in the presence of uncertainty in the background friction parameter (b). The inset in panel (a) shows the non-dimensional flow rate in the channel as a function of λ_0 for an undisturbed channel, i.e. $\lambda_T = 0$.

An Experimental Evaluation of Blockage Corrections for Cross-Flow Current Turbines

Hannah Ross*, Brian Polagye
Department of Mechanical Engineering, University of Washington, USA

Summary: Blockage corrections are applied to experimental data collected over a range of blockage ratios for a laboratory-scale cross-flow turbine. As the blockage ratio increases, turbine performance is significantly augmented. Several corrections, based on linear momentum actuator disk theory, are found to be reasonably effective at adjusting power and thrust to match unconfined conditions.

Introduction

The performance of a current turbine can be significantly affected by flow confinement. The magnitude of this effect is related to the blockage ratio (β) [1], defined as the projected area of the turbine and supporting structure (A_T) divided by the cross-sectional area of the channel (A_C). Previous studies have shown that increasing the blockage ratio for a given turbine while holding the turbine rotation rate and free-stream velocity constant leads to a higher flow speed through the turbine, larger forces, and a greater power output [1-3]. These effects present both opportunities and challenges. High-blockage arrays can be used to augment individual turbine performance. However, blockage effects make it difficult to relate laboratory results produced at moderate to high blockage ratios to unconfined performance. To account for these effects, analytical corrections are often applied to data collected at blockage ratios greater than 5−10% [1]. Many of these corrections are based on linear momentum actuator disk theory, and there has been no published systematic, experimental verification of their effectiveness for cross-flow turbines. To explore the performance of analytical corrections for cross-flow turbines, several formulations found in the literature are applied to data from a laboratory-scale cross-flow turbine collected at multiple blockage ratios.

Methods

To characterize turbine performance at multiple blockage ratios, channel width was varied while attempting to hold all other significant parameters constant, such as the chord-based Reynolds number (Re_c), Froude number (Fr), and submergence depth (d). Here, the Reynolds and Froude numbers are defined as

$$Re_c = \omega R c / \nu, \quad Fr = V / (gh)^{1/2} \tag{1-2}$$

where ω is the angular velocity of the turbine, R is the turbine radius, c is the blade chord length, ν is the kinematic viscosity of the fluid, V is the free-stream velocity, g is the acceleration of gravity, and h is the undisturbed water depth. Experiments were performed in three facilities: the Tyler Flume at the University of Washington in Seattle, WA, the Bamfield Marine Sciences Centre (BMSC) flume in Bamfield, Canada, and the Chase Ocean Engineering Lab Tow Tank at the University of New Hampshire in Durham, NH. Removal of a false wall at the BMSC flume allowed two different channel widths to be tested, resulting in a total of four blockage ratios ranging from 3−36%. The lowest blockage ratio was taken as the unconfined reference case. The turbine was tested at $Re_c \approx 3.0\text{x}10^4$ $-7.5\text{x}10^4$ (varying ω, constant V) and $Fr \approx 0.2$.

The turbine was characterized by measuring the power (C_P) and thrust (C_T) coefficients over a range of tip-speed ratios (λ), defined as

$$C_P = P / 0.5\rho A_T V^3, \quad C_T = T / 0.5\rho A_T V^2, \quad \lambda = \omega R / V \tag{3-5}$$

in which ρ is the fluid density, P is the mechanical power produced by the turbine, and T is the thrust force on the turbine. The coefficients of power and thrust were corrected for blockage using the methods proposed by Barnsley & Wellicome (BW) [4], Mikkelsen & Sørensen (MS) [5], and Houlsby et al. [6]. The BW method was popularized in the marine energy research community by Bahaj et al. [7]. Although the model developed by Houlsby et al. is not explicitly presented as a blockage correction, the equations can be rearranged and solved in a manner similar to the method given by [4].

* Corresponding author.
Email address: hkross@uw.edu

Results

The power coefficients for a range of blockage ratios are given in Fig. 1. Fig. 1(a) shows the uncorrected measurements as a function of tip-speed ratio. Figs. 1(b) and (c) present the curves as corrected by the BW and MS methods, respectively. The MS method requires wake measurements, which are time-intensive to collect. Therefore, only a single tip-speed ratio corresponding to the maximum power output was tested at each blockage. The analogous uncorrected measurements, and the results computed using the BW correction, are given as a reference. The method presented by Houlsby et al. was also applied, but the results are not shown as they are similar to those given in Fig. 1(b). Also not presented are the C_T results, which follow the trends shown in Fig. 1.

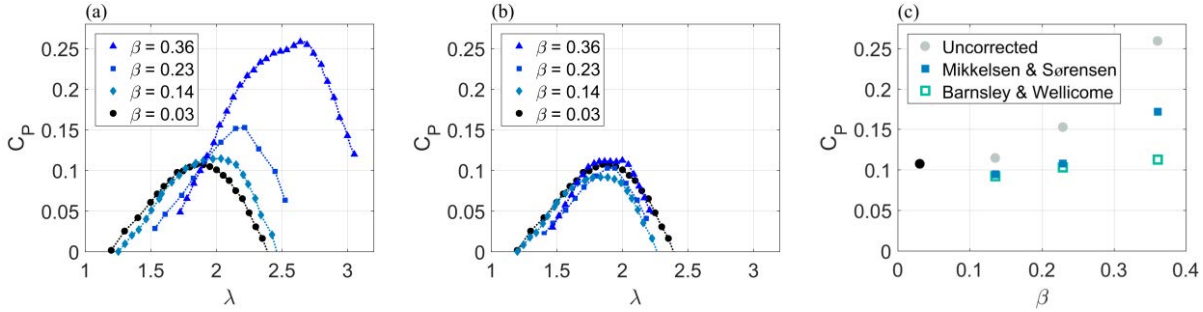

Fig. 1. Cross-flow turbine power coefficients, plotted as a function of tip-speed ratio and blockage ratio. Uncorrected (a) measurements are compared to results of the BW (b) and MS (c) corrections.

The effectiveness of each method was evaluated by calculating the percent error of the corrected curves compared to the unconfined reference case (3% blockage in the University of New Hampshire tow tank). Averaged across all blockage cases and tip-speed ratios, the BW method produced an error of approximately 15%, while the MS method performed somewhat worse with an error of 24%. It should be noted that, although significant effort was made to hold all other parameters constant while changing blockage, small variations in water temperature (ν has a strong temperature dependence), inflow profile, and turbulence intensity between facilities produced some uncertainty in the measurements that has yet to be fully quantified but likely accounts for a portion of the error.

Conclusions

The results of this work suggest that some analytical blockage corrections are effective when applied to cross-flow turbines under certain operating conditions. If thrust measurements are available, it is recommended that the correction developed by Barnsley & Wellicome [4] be applied, as it yields the least error. For high Froude number flows, it may be advantageous to employ the model derived by Houlsby et al. [6].

Acknowledgements:

This material is based upon work supported by the National Science Foundation Graduate Research Fellowship Program under Grant No. DGE-1256082 and the US Department of Defense Naval Facilities Engineering Command. The authors would like to thank the Bamfield Marine Sciences Centre, the Center for Ocean Renewable Energy at the University of New Hampshire, and the Alice C. Tyler Trust.

References:

[1] McTavish, S., Feszty, D., Nitzsche, F. (2014). An experimental and computational assessment of blockage effects on wind turbine wake development. *Wind Energy* **17**, 1515-1529.

[2] Consul, C. A., Willden, R. H. J., McIntosh, S. C. (2013). Blockage effects on the hydrodynamic performance of a marine cross-flow turbine. *Phil. Trans. R. Soc. A* **371:20120299**.

[3] Kinsey, T., Dumas, G. (2017). Impact of channel blockage on the performance of axial and cross-flow hydrokinetic turbines. *Renewable Energy* **103**, 239–254.

[4] Barnsley, M. J., Wellicome, J. F. (1990). Final report on the 2nd phase of development and testing of a horizontal axis wind turbine test rig for the investigation of stall regulation aerodynamics. *Report No. E.5A/CON5103/1746*, ETSU.

[5] Mikkelsen, R., Sørensen, J.N. (2002). Modelling of wind tunnel blockage. In: *Global Windpower Conference*, Paris, France.

[6] Houlsby, G. T., Draper, S., Oldfield, M. L. G. (2008). Application of linear momentum actuator disc theory to open channel flow. *Report No. OUEL 2296/08*, Department of Engineering Science, University of Oxford.

[7] Bahaj, A. S., et al. (2007). Power and thrust measurements of marine current turbines under various hydrodynamic flow conditions in a cavitation tunnel and a towing tank. *Renewable Energy* **32**, 407–426.

A reduced order model to predict flows around cross-flow turbines

Soledad Le Clainche and Esteban Ferrer*
ETSIAE-UPM (School of Aeronautics), Universidad Politécnica de Madrid

Summary: We develop a reduced order model to represent the complex flow behaviour around cross-flow turbines. First, we simulate cross-flow turbines using an accurate high order discontinuous Galerkin-Fourier Navier-Stokes (NS) Large Eddy Simulation solver with sliding meshes and extract flow snapshots in time. Subsequently, we build a reduced order model based on a high order dynamic mode decomposition approach that selects modes based on flow frequency. We show that only a few modes are necessary to reconstruct the solution with high fidelity, even for rotating blades in turbulent regimes. Additionally, we compare the reduced order model based on the high order NS solver to fast 2D simulation (using a Reynolds Averaged NS turbulent model) to prove the higher fidelity of the proposed method.

Introduction

The simulation and prediction of the temporal evolution of flows around cross-flow turbines is difficult. This difficulty is caused, on the one hand, by the blade motion, which leads to unsteady flow features and dynamic effects, but also to the turbulent flow regime in which these devices operate (i.e. high Reynolds numbers). Turbulent flows require modelling to be simulated at an affordable cost (e.g. RANS or LES).

In this text, we simulate a cross-flow turbine with an expensive 3D high order numerical method that resolves the geometry and blade movement explicitly. Only the small scales in the turbulent flow (LES approach) are modelled in these simulations. Since these computations are expensive, we propose to devise a Reduced Order Model (ROM) using snapshots extracted from the accurate high order simulation. To the authors' knowledge, our work is the first to propose a ROM for cross-flow turbines.

We show that combining high order simulations with ROM enables accurate solutions with high fidelity, and outperforms cheaper 2D Navier-Stokes simulations (using a simpler turbulent model: based on a Reynolds Averaged Navier-Stokes approach -RANS). Furthermore, we show that even when the number of snapshots is small (e.g. do not cover an entire turbine rotation), the ROM is capable of predicting the temporal behaviour at any time or blade azimuthal location.

Methods

High order LES solver: High order (>2) numerical methods (e.g. discontinuous Galerkin) have seen an increased popularity over the last decade. These methods are characterised by low numerical errors (i.e. dispersion and diffusion). In this work, flow solutions of the non-linear incompressible Navier-Stokes (NS) equations, are obtained from the 3D unsteady high order h/p Discontinuous Galerkin (DG)-Fourier solver developed by the second author [1,2]. The solver has been validated for a variety of flows, including blade aerodynamics under static and rotating conditions [1], instability analysis and turbulent regimes [2].

DMD based ROM: Higher Order Dynamic Mode Decomposition (HODMD) [3] is an extension of the Dynamic Mode Decomposition (DMD) approach that has been introduced as a tool to analyse complex and noisy flows. The ROM uses a new criterion selection method that has been recently introduced by Kou & Zhang [4] to select the most relevant DMD modes to construct reduced order models.

Results

We perform numerical simulations for a one bladed turbine [5] and compare 3D simulated results issued from the high order Navier-Stokes solver (for polynomial order 3) with experimental data and also to fast 2D simulations computed using the commercial finite volume solver Ansys-Fluent-16.2 modelled using 2D Reynolds Average (uRANS) Navier-Stokes solutions and a k-omega SST turbulence model. Both high order and low order solvers use sliding meshes and rotate the mesh as time evolves. The high order solver computes 3D simulations (as required by LES type turbulent models) whilst Fluent (using uRANS) allows cheaper 2D simulations. The former provides more expensive simulations, which are typically more accurate. We have compared the simulated results to experimental tests [5] for the normal non-dimensional blade force. These results are not shown for lack of space. We have observed very good agreement between 3D high order DG computations and experiments. We also compare the low order 2D Fluent-Ansys solution to the experimental values and observe good overall agreement but less accuracy than when the high order solver is used. In general, a more complex flow with multiple vortices emanating from the training edge is observed, when using the high

* Corresponding author.
Email address: esteban.ferrer@upm.es

order LES approach and a smoother flow (with fewer flow details) when simulating using the uRANS model. Both the time evolution of the forces and the flow fields suggest that the high order LES solver is more accurate that the low order uRANS model.

Now, we compare velocity components: streamwise (Ux) and normal (Uy), on a horizontal line close to the blade (at y=-4) for a fixed simulation time, in figure 1. We observe, in figure 1-top, that the low order uRANS solver provides similar trends that the high order LES simulation, but does not capture all details. Finally, figure 1-bottom, compares the original high order solution to the ROM prediction at y=-4, for an increasing number of DMD modes. We observe enhanced accuracy as the number of modes increases but also good predictions even when only 3 modes are retained (top figure).

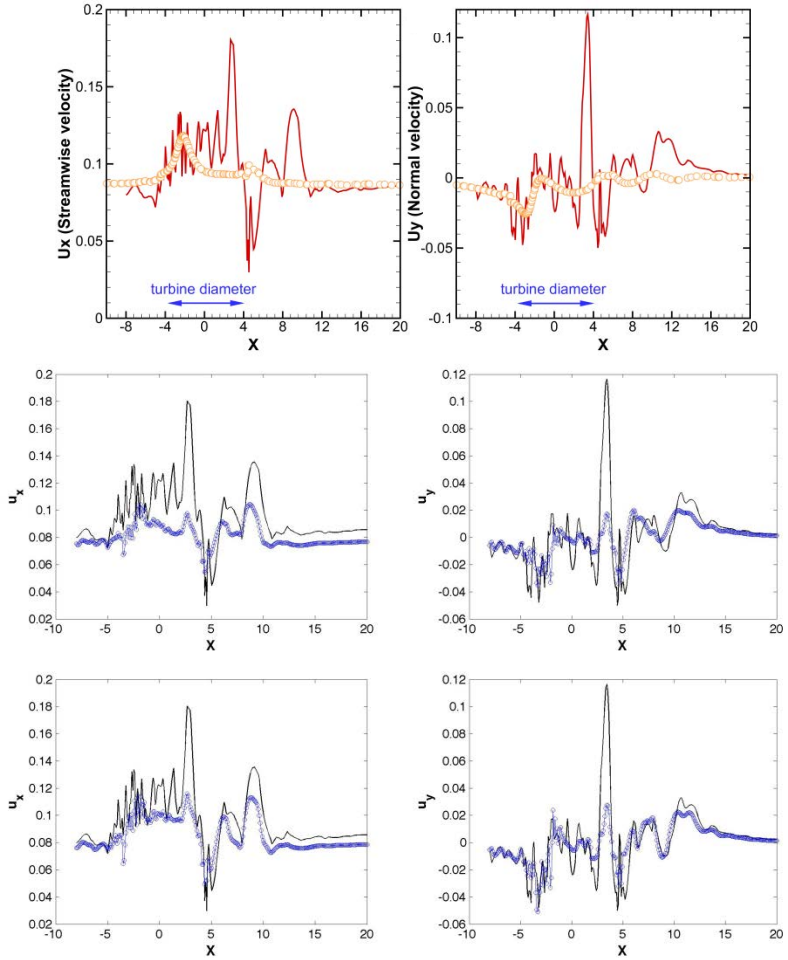

Fig. 1. Ux and Uy velocity at line y=-4: (top) high order (red) vs low order (orange) solvers and (bottom) high order (black) vs ROM (blue) for 3 (left) and 5 (right) retained modes.

Conclusions

We have developed a reduced order model (ROM) to mimic the behaviour of the flow around cross-flow turbines in turbulent regimes. The novel approach requires the simulations of the turbine rotation using a 3D high order solver with a turbulent model of LES type. From this simulation, we extract snapshots to construct the ROM. It has been shown that this method can be more accurate than low order solvers with simpler turbulent models.

References:

[1] E. Ferrer and R.H.J.Willden, A high order discontinuous Galerkin - Fourier incompressible 3D Navier-Stokes solver with rotating sliding meshes. *J. of Comp. Physics*, **231**(21):7037–7056, 2012.

[2] E. Ferrer, An interior penalty stabilised incompressible discontinuous Galerkin-Fourier solver for implicit Large Eddy Simulations. *J. of Comp. Physics*, **348**:754–775, 2017.

[3] S. Le Clainche, and J.M. Vega, Higher Order Dynamic Mode Decomposition. *SIAM J. on Appl. Dyn. Systems*, **16**(2), 882-925, 2017.

[4] J. Kou, and W. Zhang, An improved criterion to select dominant modes of dynamic mode decomposition. Eur. *J. Mech. B/Fluids*, **62**, 109-129, 2017

[5] J.W. Oler, J.H. Strickland, B.J. Im, and G.H. Graham, Dynamic stall regulation of the Darrieus turbine. *Sandia Technical Report* SAND83-7029 UC-261, 1983.

Size matters: Investigation into "full scale" and geometry scaling of the Helical Gorlov marine turbines

Esther R Quaintmere*, Professor Phil Rubini
Department of Engineering and Computer Science, University of Hull, UK

Summary: In this paper, aspects of geometric symmetry and their effect on the fidelity of CFD simulations of Gorlov turbines are investigated. The results make a significant contribution to an assessment of the required geometric resolution for future performance simulations when large numbers of individual simulations are required, for example as part of a Design Of Experiments (DOE) analysis. Large scale parallel simulations were undertaken for a full scale marine turbine, during which, a range of geometry sections were investigated to ascertain the sensitivity of approximations employing geometric symmetry. It was established that a quarter section turbine is able to satisfactorily replicate the torque of a full scale turbine. This is a significant conclusion and will allow a significant saving in overall compute time for DOE investigations.

Introduction

The conclusion from many research papers, for example (1-3), imply that the power coefficient of a vertical axis marine turbine decreases with the helical angle, thus Darrieus turbines are more efficient than Gorlov. Two notable papers (4, 5) contradict this, stating an increase in power with the increase in helical angle. Due to the discrepancy in these reports about how the helical pitch angle effects the power coefficient, this parameter is one of a number where further investigation would be valuable, as part of a parametric Design of Experiments approach. The computational resource required for such a DOE exercise would be considerable, hence warranting an investigation into the possibility of employing reduced geometric sections.

Chao Li et al. (6) presented a method referred to as 2.5D modelling, widely applied to Darrieus turbines. In this method a reduced section of a blade, in the span wise direction, is simulated using a translational periodic boundary to transform flow parameters from one boundary and apply it to another. Chao Li et al. (6) concluded that 2.5D URANS provides similar results to 2D URANS, for a Darrieus turbine and that 2.5D LES simulations are comparable to 3D experimental results. Gorlov turbines, due to their helical shape cannot be simply represented in two dimensions by applying geometric symmetry. This paper investigates the potential of applying reduced geometry assumptions, similar to the 2.5D approach proposed by Chao Li et al. (6), to represent full turbine simulations of a Gorlov vertical axis marine turbine.

Methods

The commercial code, Star CCM+ V.12.06.011 was employed for this work. A series of simulations were undertaken of a Gorlov turbine, including both full turbine simulations, and simplified geometries, achieved by splitting the blades into reduced geometry sections (with periodic boundaries top and bottom) of varying height's ($1/8^{th}$, $1/6^{th}$, 1/4, 1/2). All simulations were undertaken on the HPC facility at the University of Hull, this has 180 compute nodes each with 2x14 core (5,040 cores) and 4 high memory nodes each with 4x10 (40 cores). The simulations were allowed to reach a steady state solution, typically after ten full revolutions of the turbine. Torque data from the reduced geometry simulations was then post processed, by summing over the appropriate periodic sections, to generate representative torque data of a full turbine. The resultant data was then compared with published experimental data (2) and prior CFD simulations (7).

After conducting grid dependence studies, the optimal mesh for this simulation was found to be a polyhedral grid structure. The boundary layer around the hydrofoils requires prism layers (near wall structured mesh) in order to resolve the complex flow phenomena. This prism layer thickness should be 16% of the chord length. The final grid resolution was 25 million cells for a full turbine and 1 million cells for a $1/6^{th}$ section. The resultant reduction in compute time clearly demonstrates the potential of applying 2.5D modelling to Gorlov turbines, which would then also allow further refined meshes time accurate simulations. In the present work, Unsteady RANS (URANS) simulations were undertaken, where the literature indicates that the turbulence model best suited to the hydrokinetic vertical axis turbines is the k-ω SST(8). After conducting time convergence studies it was established that for accurate results a time step resolution equivalent to 1.2 degrees rotation should be applied.

* Corresponding author.
Email address: E.R.Bruce@2012.hull.ac.uk

Results

Large scale parallel simulations were conducted and it can be observed in figure 1 that for a four-bladed turbine, the full turbine shows good agreement with the full scale turbine, thus indicating that the simulation is validated. It can be observed from the graph that sections of 1/8th and 1/6th show considerable improvement over earlier published CFD simulations (7) they are not however, comparable with the experimental data (2). The results indicate that the 1/8th and 1/6th section is inaccurate in predicting the torque, this is due to the sections being too small to accurately predict the flow which is being angled by the helical shape of the blade. A section size of ¼ or greater does accurately represent a full turbine's torque curve. In Figure 3 shows a visualisation of a Gorlov turbine and the representation of the flow over the helical blades, and closer snapshot of the hydrofoil.

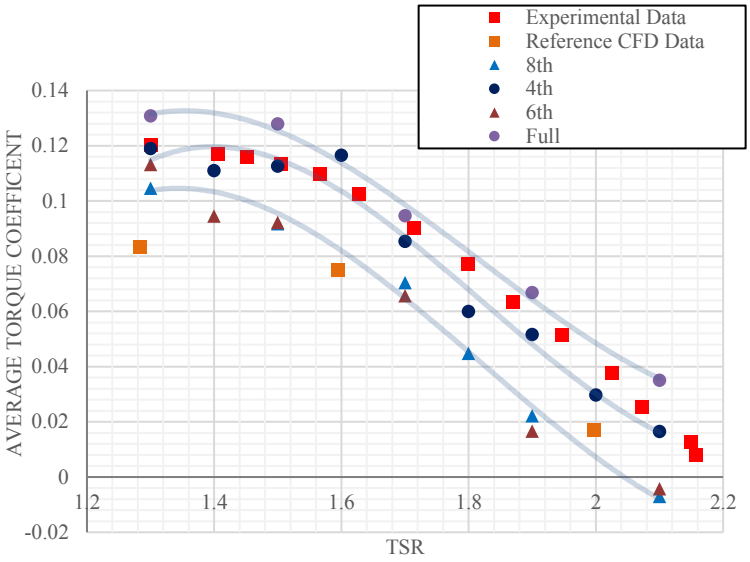

Figure 1Average Torque for a four-bladed Gorlov turbine

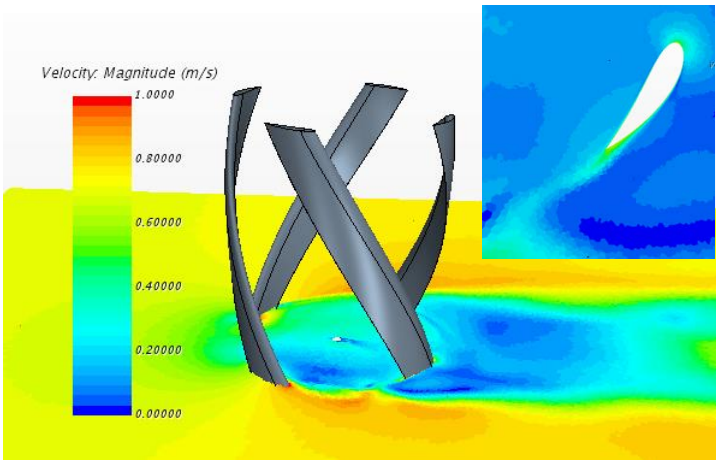

Figure 2 Instantiates Velocity Field around a Gorlov turbine

Conclusions

This investigation has established that although there is no geometric symmetry in a Gorlov turbine, the 2.5D approach as proposed by Chao Li et al.(6) can be applied. The results depend on the size of the section selected. A 1/4 section was found to accurately represent the torque curve of a full scale Gorlov turbine. This work has demonstrated that, the 2.5D approach adequately represents the physical phenomena and is therefore acceptable for parametric investigations where large numbers of simulations would be undertaken.

References:

1. Marsh P, Ranmuthugala D, Penesis I, Thomas G. Numerical investigation of the influence of blade helicity on the performance characteristics of vertical axis tidal turbines. Renewable Energy. 2015;81:926-35.
2. Niblick AI. Experimental and Analytical Study of Helical Cross-Flow Turbines for a Tidal Micropower Generation System: University of Washington; 2012.
3. Mitsuhiro S, Katsuyuki S, Seiji K, editors. Output Characteristics of Darrieus Water Turbine with Helical Blades for Tidal Current Generations. The Tweifth International Offshore and Polar Engineering; 2002; Kitakyushu, Japan.
4. Gorlov A, editor The Helical Turbine and its applications for hydropower without dams. ASME International mechanical engineering congress and exposition; 2002; New Orleans, Louisiana, USA.
5. Chen L, Lam W-H. Slipstream between marine current turbine and seabed. Energy. 2014;68:801-10.
6. Li C, Zhu S, Xu Y-l, Xiao Y. 2.5D large eddy simulation of vertical axis wind turbine in consideration of high angle of attack flow. Renewable Energy. 2013;51:317-30.
7. Hall TJ. Numerical Simulation of a Cross Flow Marine Hydrokinetic Turbine: University of Washington; 2012.
8. Maître T, Amet E, Pellone C. Modeling of the flow in a Darrieus water turbine: Wall grid refinement analysis and comparison with experiments. Renewable Energy. 2013;51(0):497-512.

Modelling Tidal Stream Turbine and Array Interaction

Matt Edmunds*, Alison J. Williams, Ian Masters.
College of Engineering, Swansea University, UK

Summary: This work introduces a revised technique for predicting lift distribution along a foil, and incorporations to the model for capturing the effects of changing Reynolds number and foil section profile. The model verification process is under way and results look promising. Verification against three traditional benchmarks (Bahaj et al, Mycek et al, and NREL wind turbine experiments) demonstrate the model's robustness and flexibility in predicting a range of scenarios under controlled scaled experiments. The verified GAD-CFD model will be used to investigate how unsteady tidal flows propagate and evolve through a tidal array field, i.e. sea bed mounted, mid water column located and surface floating.

Introduction

This abstract discusses the verification of a Generalised Actuator Disc (GAD) embedded CFD Model, based on Blade Element Momentum CFD (BEM-CFD) [2], for the modelling of horizontal axis marine and wind turbines. This model builds on previous work and includes additional features for improving the robustness, accuracy, and performance of a wider range of case studies/scenarios. The new features are divided into two main parts; the first includes a foil geometry linked analytical solver (derived from Prandtl's lifting line theory) replacing the elliptical lift distribution first introduced in [2], the second introduces the ability to provide lift and drag data for a range of foil profiles and Reynolds numbers for a given turbine geometry. This work also considers the importance of how the assembly structure can effect downstream wake characteristics. The model is designed to reduce computational cost i.e. workstation level rather than cluster level computational requirements. The aim of this work is the introduction of a more complete model for studying; multiple device interactions, automated load balancing, bathymetry interactions, and general site wide environmental implications.

Results

Verification of the revised model is conducted utilising experimental results from Bahaj et al. [1], Mycek et al. [4] (see Figures 1 and 2), and experimental work conducted on wind turbine design at NREL [3]. Although full validation of these techniques are still required, the model is complete and the verification process is progressing well. The model achieves improvements over previous work in terms of accuracy under a more varied range of operating conditions. This includes downstream wake prediction (Figure 2), and power/thrust characterisation (Figure 1). Figure 1 demonstrates the improved predictive capability under low Reynolds number conditions, in this case relatively low velocities. In addition improvements to tip loss corrections, from the revised lift distribution method and variable foil cross section lift/drag data, support the improved power prediction . With improvements to; tip loss corrections from the revised lift distribution method, handling of variable foil cross section lift/drag data, and the addition of the nacelle and tower assembly structures, downstream wake characterisation a shown in 2 compare favourably with the downstream wake structures presented in [4].

Conclusions

The GAD-CFD model verification process demonstrates good correlation in controlled experimental conditions at flume scale. This process will be extended to capture the ongoing work with Edinburgh as part of Supergen 3+/4 to calibrate/verify the model using results from experiments conducted at the FloWave facility. The aim is to include measurements of turbulence intensity to calibrate the base model under higher turbulent conditions, also the study and verification of multiple rotor interactions. This work will then be extended to include: a study of lift and drag input data with emphasis on turbulent effects; stall and pitch control power limiting allowing insight into site wide loading dynamics; understanding of downstream wake dynamics when power limiting, and understanding potential site wide optimisations to improve power yield.

*Corresponding author.
Email address: m.edmunds@swansea.ac.uk

Acknowledgements:

The Authors wish to acknowledge the financial support of the Welsh Assembly Government, the Welsh European Funding Office, and the European Regional Development Fund Convergence Programme. The work was also supported by the EPSRC funded "Extension of UKCMER Core Research, Industry and International Engagement" project (EP/M014738/1). The Author(s) acknowledge(s) the financial support provided by the Welsh Government and Higher Education Funding Council for Wales through the Sêr Cymru National Research Network for Low Carbon, Energy and Environment. (C001822).

References:

[1] AS Bahaj, AF Molland, JR Chaplin, and WMJ Batten. Power and thrust measurements of marine current turbines under various hydrodynamic flow conditions in a cavitation tunnel and a towing tank. *Renewable energy*, 32(3):407–426, 2007.

[2] M. Edmunds, Alison J. Williams, I. Masters, and T. N. Croft. An enhanced disk averaged CFD model for the simulation of horizontal axis tidal turbines. *Renewable Energy*, 101:67 – 81, 2017.

[3] P. Giguere and M. S. Selig. Design of a Tapered and Twisted Blade for the NREL Combined Experiment Rotor.

[4] Paul Mycek, Benoît Gaurier, Grégory Germain, Grégory Pinon, and Elie Rivoalen. Experimental study of the turbulence intensity effects on marine current turbines behaviour. Part I: One single turbine. *Renewable Energy*, 66(0):729 – 746, 2014.

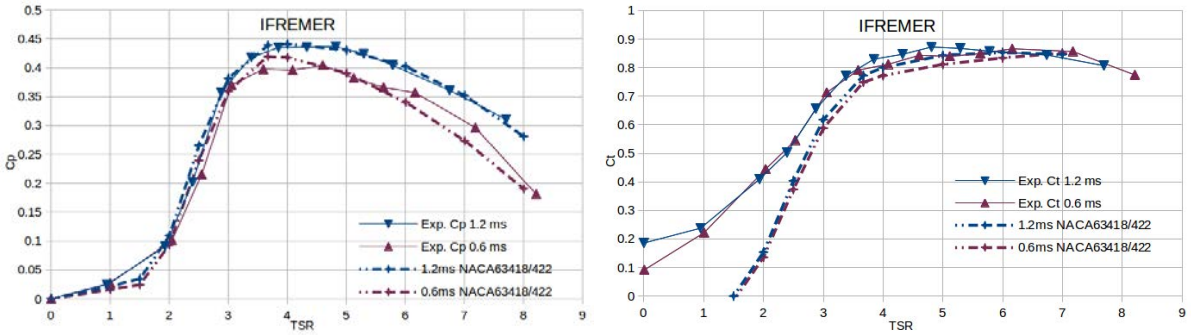

Figure 1: Coefficient of power and thrust plotted against TSR for the Mycek et al [4] work. The variation due to foil section geometry change and Re is captured in the GAD model.

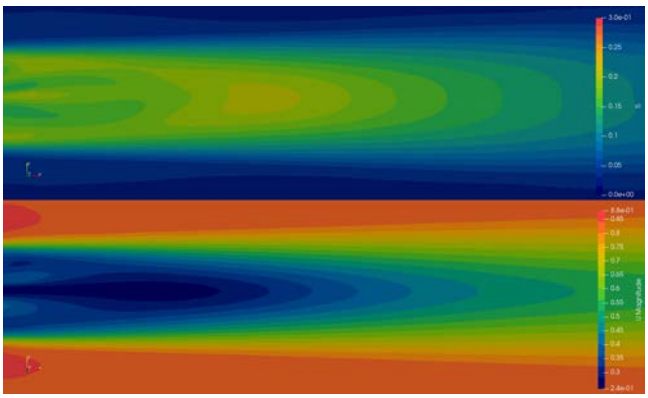

Figure 2: Turbulence intensity (TOP) and velocity (BOTTOM) plots at TSR3.67 and 0.8m/s for the Mycek et al [4] work at 3% Ti. These plots represent the importance of getting not only the rotor characteristics correct, but also the assembly geometry.

Influence of support structures on tidal turbine power output

Subhash Muchala, Richard H. J. Willden*
Department of Engineering Science, University of Oxford, UK

Summary: A blade resolved computational fluid dynamics (CFD) model with a Reynolds-Averaged Navier Stokes (RANS) formulation using the *k-ω* SST turbulence model was used to study the performance of a horizontal axis tidal stream turbine in the presence of two different support structures: cylinders with circular and elliptical cross-sections. The integrated rotor force coefficients were higher in the presence of the circular support structure than the elliptical support due to the higher opposing thrust from the cylinder, resulting in an increased local flow velocity near the top half of the rotor.

Introduction

The energy available for extraction from a tidal channel is affected by the resistance presented by the turbines and associated infrastructure, as shown for example by Garrett and Cummins [1]. Locally, the presence of support structures can also influence the energy available to individual tidal turbines. The focus of this abstract is to study the influence of different support structure designs on a full-scale (18 m diameter) tidal turbine in a shear flow. McNaughton [2] implemented a sliding mesh method within a larger, stationary domain, with a fully blade resolved turbine inside the sliding mesh in order to study the forces on a full-scale tidal rotor. Mason-Jones *et al*. [3] have shown the influence of shear profile and support structures on a tidal turbine using a fully resolved blade model. By using a fully resolved model, it was possible to study the interaction effects between the rotor and the support structure, and the variation in force coefficients as a blade completes one rotation was presented to demonstrate this.

In the current paper, the influence of support structure shape on the turbine rotor forces and its wake is discussed. As a real tidal channel has a sheared velocity profile, all the simulations were performed in a shear flow profile. The shear flow model in the present work was implemented using the model of Fleming *et al.* [4]. Also, the change in the forces experienced by the support structures due to the presence of the tidal rotor is also discussed.

Method

A fully blade resolved CFD model with a RANS formulation using the *k-ω* SST turbulence model [5] was used to study the tidal turbine performance. The rotor itself was placed inside a cylindrical inner domain and the support structure is in the outer rectangular domain. A structured mesh was used in both the inner and outer domains. To mesh the cylindrical inner domain, a 120^o wedge of the domain was meshed first to achieve $y^+ > 30$, and this block was copied twice to form the whole inner domain. The inner domain mesh was rotated during the simulations to capture the unsteadiness in the wake which was important to study the forces on the support structure. Following a mesh convergence study, approximately 4.77 million cells were required in the inner domain, and 1.05 million in the outer domain. The turbine simulations were performed for 10 rotor revolutions in order to allow the wake to propagate downstream. The depth-averaged flow velocity was 2 ms^{-1} with an inlet turbulent intensity of 6%, and a shear flow profile was specified following Fleming *et al*. [4].

Results

The integrated rotor force coefficients were higher in the presence of the circular rather than the elliptical support structure due to the higher opposing thrust from the cylinder. This resulted in an increased local flow velocity near the top half of the rotor. The variation in the force coefficients over a single blade rotation was also higher in the presence of support structures as they influence the pressure distribution around the blade when it passes in front of the support structure; see Figure 1. As a result, the minimum value of the force coefficients does not occur at exact bottom position 180^o. The minimum power coefficient occurs at 166^o and 170^o for the cylinder and ellipse respectively, whereas the minimum thrust coefficient occurs at 170^o and 175^o.

The angle of attack on the blade decreases as it approaches the support structure due to the reduction in streamwise flow velocity just upstream of the support structure. This drop is higher for cylindrical support than

* Corresponding author.
Email address: richard.willden@eng.ox.ac.uk

the elliptical support due to its larger opposing thrust, causing a greater drop in stream-wise velocity; see Figure 2. The drop in the angle of attack due to the presence of the support structure causes a significant drop in the blade sectional forces as it approaches the support structure.

The presence of rotor also causes a drop in the forces on the support structure. The mean streamwise force coefficients of the circular and elliptical support structures are 0.21 and 0.12 respectively, which are much lower than if they were in open water without the rotor present. For both of the support structure designs, the streamwise sectional forces behind the rotor swept area are lower than that in open water, whereas the mean cross-stream forces are higher.

Conclusions

A full scale tidal turbine was simulated in the presence of two different support structures, with cylindrical and elliptical cross-sections, to study the flow interaction between the rotor and the support structure. The variation and magnitude of the rotor blade forces was different compared to the case without support structures, which may have design implications for the fatigue life of the rotor blades.

The swirl from the rotor induces a mean cross-stream force component on the support structure which is much higher in the case of an ellipse than the cylinder. This is because a small change in the angle of attack of the flow on the support structure causes a larger difference in the forces on the elliptical structure than on the cylindrical structure. This could be an important factor in the design of elliptical cross-section supports.

In case of both the support structure designs, the stream-wise sectional forces behind the rotor swept area are lower than that in open-water whereas the mean cross-stream forces are higher. This should be considered when designing the dimensions of the support structures.

References:

[1] C Garrett and P Cummins. *The power potential of tidal currents in channels*. Proceedings of the Royal Society A **461**:2563-2572, 2005.

[2] J McNaughton. *Turbulence Modelling in the near-field of an axial flow tidal turbine using Code Saturne*. PhD thesis, University of Manchester, UK, 2013.

[3] A Mason-Jones, D M O'Doherty, C E Morris, and T O'Doherty. *Influence of a velocity profile and support structure on tidal stream turbine performance*. Renewable Energy, **52**:23-30, 2013.

[4] C Fleming, S C McIntosh, and R H J Willden. *Tidal turbine performance in sheared flow*. In Proc. 10th European Wave and Tidal Energy Conference, pages 147 – 158, September 2013.

[5] F R Menter *Two-equation eddy-viscosity turbulence models for engineering applications*. AIAA Journal **32**(8):1598-1605, 1994.

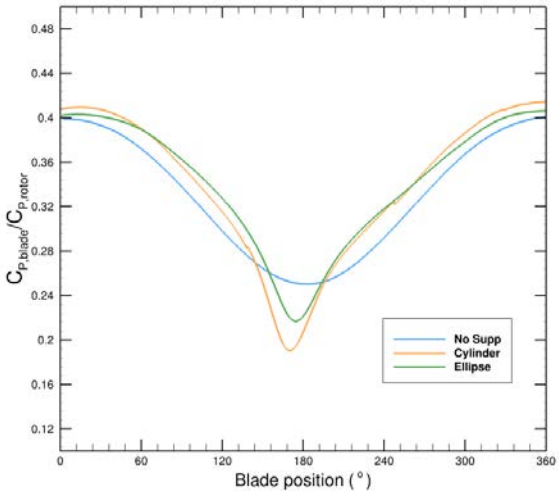

Fig. 1. Blade power coefficient normalized with respect to the rotor power coefficient for different support structures, cylinder and ellipse, at 10° blade pitch angle during one rotation cycle.

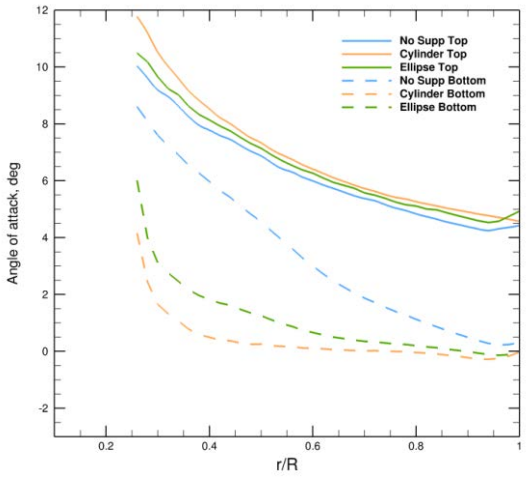

Fig. 2. Angle of attack variation along the span of a turbine blade in the presence of different support structures for 10° blade pitch angle, at the top (solid line) and bottom (dashed line) angular position in a rotational cycle.

CFD Analysis of Tidal Range Turbine Draft Tube Wakes

Ross Gwenter*, Ian Masters, Alison Williams
College of Engineering, Swansea University, Bay Campus

Summary: We report on experimental OpenFoam Computational Fluid Dynamics results from tests designed to investigate the hydrodynamics of low head tidal range turbines, singularly sectioned and in a quadruple grouping. The objective is to provide a preliminary estimate and characterisation of the flow behaviour exiting from the turbine draft tube. Particular attention was paid to the flow velocity, the wake length, and the bed shear stresses.

Introduction

Large scale tidal range schemes have the potential to modify the hydrodynamic environment of intertidal regions with sediment transport, mixing, and localised scour effects. Depth-averaged Shallow Water Equations (SWE) models are used to simulate far-field coastal hydrodynamics. Coastal models typically have large domains to capture far-reaching interactions. For practical computation purposes, grid sizes often are larger than the length-scales of either the natural topographic variation or the hydraulic structures in tidal range schemes. The result being the inability to capture the complex near-field 3D flow and adequately assess the impact of such. 3D Computational Fluid Dynamics (CFD) models are capable of simulating complex 3D flow characteristics, and can be used to improved the near-field predictions of shear stresses, bed scour and wake characteristics. However, CFD simulation is not suitable for coastal region scales.

The aim of this academic research is to couple the 2D depth-averaged modelling and the 3D CFD simulations, through inserting a CFD model into a sub-grid within the 2D depth-averaged coastal model. The intention being to improve the near-field simulation of turbine wakes in coastal models. This abstact details a preliminary CFD model of the Swansea Bay Tidal Lagoon turbine housing, with design emphasis on limiting the computational intensity with simple geometry.

Methods

The domain extent is 400x200x30m in x, y and z directions respectfully, with the intention to span beyond where the wake will interact with the side and downstream boundaries. The model geometry consists of either a single Turbine Draft Tube (TDT) with the anticipated incline slope of the scour mattress surface (the turbine housings are below the natural bed level) or a quadruple coupling. The mesh was structured to be finest around the TDT and Scour Mattress surfaces, then gradually coarsening with perpendicular distance over four distinct levels, each three cells across until the base level. The mesh grade levelling was specified as a subdivision of the base cell, with the finest being 0.09m. A hierarchical hexahedral mesh structure was used as within the model, large areas of relatively straight flow require little refinement, while the smaller areas of more complex flow require significant refinement.

The domain was forced by a plug flow inlet velocity condition of 7m/s across the TDT cross-section boundary surface, flowing parallel to the +x-axis in direction. The input flow was intended to represent the maximum flow velocity scenario, which only occurs briefly over the generation cycle.

The TDT, bed and scour mattress boundaries were fixed at 0.0 m/s, while the +y and -y side boundaries along with the ceiling surface were set to slip. The downstream boundary was set to a zero-gradient. The kinetic energy and dissipation rate were set similarly to 0.0 values, and use smooth wall function to compute the boundary layer. The turbulence model used was the RNG $K - \varepsilon$ model.

Results

Figure 1 shows the domain vertically sectioned along the y-normal plane. The jet flow after exiting the tube expands while simultaneously decreasing in velocity as the TDT jet diffuses into the ambient fluid. The Coanda effect is present with two apparent cases of flow attachment. One being along the TDT filleted exit, the other along the scour mattress and bed. The incline slope of the scour mattress can reduce the wake length by $\approx 125m$ or 37%. At $\approx 250m$ from the TDT exit, the flow velocity magnitude has reduced to $0.1m/s$. A slight blocking effect leading an altered velocity profile before the incline is also present.

Bed shear stress magnitudes are shown in Figure 2, and were attained from the 3D CFD flow, Reynolds stress on the bottom surface. Magnitudes of 0.0039 Pa in the region adjacent to the TDT exit were reached, and $\approx> 0.003$ Pa over areas that will be covered by the scour mattress. Shear stresses of 0.001 Pa were shown at $190m$ away from the TDT exit. The blocking effect from the incline slope, causing greater wake width expansion coincidently produces a wider stress profile.

*Corresponding Author
Email: 881656@swansea.ac.uk

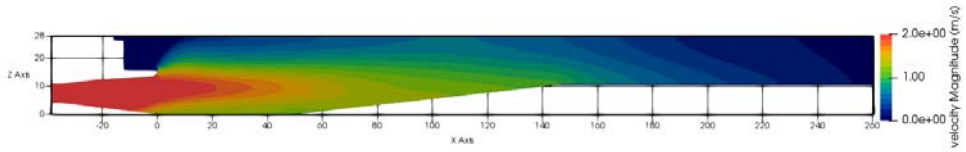

Figure 1: *Velocity magnitude (m/s) plot of a single TDT wake flow. A section cut of a y-normal plane, intersecting the TDT centreline*

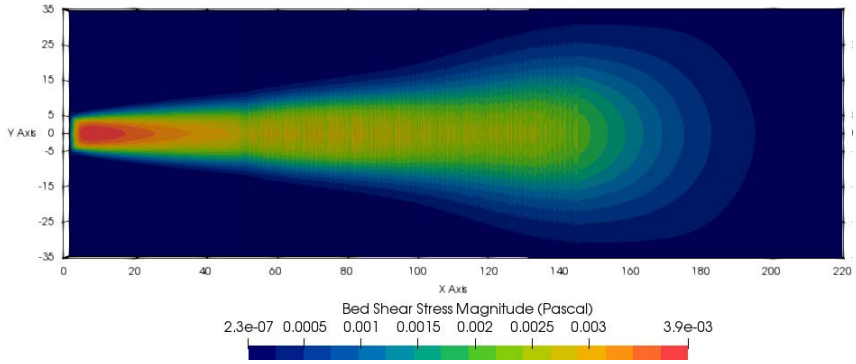

Figure 2: *Shear Stress magnitude (Pa) profile plot on the Scour Mattress and bed surface.*

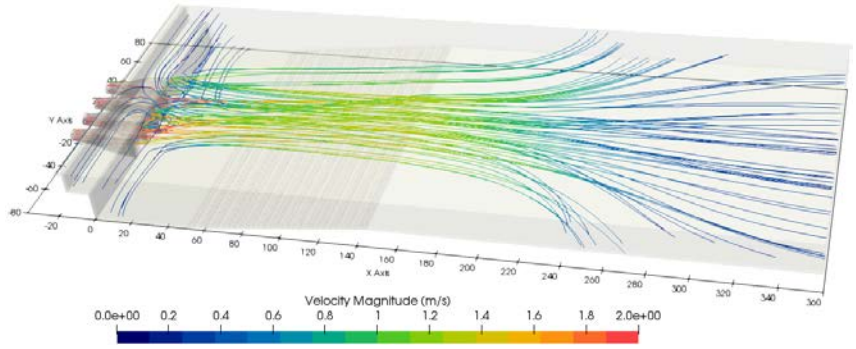

Figure 3: *Velocity magnitude (m/s) streamlines plot from four TDT's.*

Figure 3 shows the velocity magnitude streamlines from the quadruple TDT coupling. Jet streams can be seen exiting the TDT with a comparably high velocity flow, inducing entrainment flows from the surrounding fluid. A vortex can be seen forming between the middle TDT's adjacent to the exit. The wake expansion rate increases 200m downstream, as the flow velocity nears that ambient fluid.

Conclusion

While the flow characteristics are not validated by any physical experiments, the flow profiles are relatable to what is seen in other investigations such as those carried out by P.Jeffcoate *et al* [1], featuring characteristics such as the Coanda effect; which is suspected to have been utilized in the design to aid the initial wake expansion and shorten the downstream wake dissipation length. The wakes appear to form a shear boundary layer between the jet flow and the near stagnant ambient fluid in the downstream region. The wake boundary layer zones contain the highest turbulent kinetic energy of the flow, outside of the TDT. They also act as a shield layer to the main jet body. When multiple wakes are present, the two inside wake jets are protected by the outer wakes from the shearing effects of ambient fluid interaction. This aspect is thought to lead to increased momentum conservation within the wake, resulting in longer wake lengths. The inclined gradient in the scour mattress can have a substantial impact on the wake dissipation rate, being able to reduce the worst-case flow velocities to $\approx 0.2m/s$ in 260m (Figure 3). If combined with an intelligent scour mattress design, the rate in which the wake dissipates could be substantially increased even further.

Acknowledgements:
Authors would like to acknowledge the funding from the European Social Fund via the Welsh Government, M2A and Tidal Lagoon Power that has made this research possible.

References:

[1] P. Jeffcoate, P. Stansby, and D. Apsley, "Flow and bed-shear magnification downstream of a barrage with swirl generated in ducts by stators and rotors," *Journal of Hydraulic Engineering*, vol. 143, no. 2, pp. 1–20, 2017.

Implementation of a Tidal Barrage Boundary in DG-ADCIRC

Tulio Marcondes Moreira*, Thomas A. A. Adcock, Guy T. Houlsby
Department of Engineering Science, University of Oxford, UK

Tidal range power plants have been considered for large scale electricity generation for their potential ability to produce highly predictable energy without the emission of greenhouse gases. In this work, a 2D model for tidal impoundment is implemented in DG-ADCIRC and verified. Sequentially, the barrage boundary is utilized to model the Swansea Tidal Lagoon project in a two-way generation scheme. Power predictions derived from the 2D model are further compared to a 0D model and back-of-the-envelope calculations.

Introduction

Tidal Lagoons (and barrages) extract power by artificially inducing a head difference between the ocean and an impounded area. By allowing water to flow through sluice gates and turbines to an artificial impoundment, the high tide is confined until a minimum operational head is established between the ocean and basin [1]. The large impounded body of water that forms the tidal lagoon will inevitably cause environmental impacts, affecting intertidal regions and changing the natural velocity fields in and out of the lagoon. Also, the sudden high flow-rates, developed when turbines start operating, can significantly perturb water velocity and elevation at the vicinity of the hydraulic structures (e.g. turbines and sluice gates) [2]. To consider these interactions is crucial to understand (i) differences of power output predictions for different dimensional models (0D, 2D), (ii) how barrage operation/design choices can relate to the intensity of near field environmental impacts.

In order to consider these interactions, it is necessary to model the hydrodynamic structures at the basin scale. In 2D models, this can be done by approximating turbines and sluices through simple 0D equations or charts that parametrize the flow-rate as a function of the head difference between the ocean and the impounded lagoon.

Numerical Model Implementation

For including the effects of sluices and turbines inside DG-ADCIRC, modifications were made to an existing culvert model. The culvert boundary incorporates an internal barrier into the mesh that connects pairs of nodes across the “barrier” segment. The flow between these pairs is found from the water level difference between "Front" and "Back" sides, according to flow direction. In order to simulate a tidal barrage behaviour, the culvert equations are substituted by appropriate sluice and turbine equations, along with a control switch for starting and ending power generation. For modelling the turbines, a parametrization by experiments from Andritz Hydro is utilized, where the power output is related to the turbine unit speed n_{11}, and the turbine unit discharge Q_{11} by:

$$Q_{11} = (0.0166)n_{11} + 0.4861; (for\ n_{11} \leq 255) \quad (1)$$

$$\mathrm{Q}_{11} = 4.75; (for\ n_{11} > 255) \quad (2)$$

and,

$$n_{11} = \left(S_p D/\sqrt{H}\right)^2, \quad (3)$$

where the total turbine flow-rate is $Q_t = Q_{11}D^2H^{0.5}$. Here, S_p, and D are respectively the turbine rotation (rpm) and diameter, while H is the head difference between the ocean and the impounded lagoon.

Flow-rate through sluices is modelled through the “orifice” equation $Q_o = C_d A_s \sqrt{2gH}$, where C_d is the discharge coefficient, A_s the sluice area and g the gravity constant. Ramp functions following the hyperbolic tangent increase are used to avoid abrupt variations in flow, aiding in the model stability.

Results and Discussion

After verifying mass conservation through a rectangular mesh domain (Fig. 1), the Swansea Tidal Lagoon (Fig. 2) is included inside a large model from the West Coast of UK (Fig. 3). Design details (e.g. number of sluices,

* Tulio Marcondes Moreira.
Email address: tulio.marcondesmoreira@eng.ox.ac.uk

number of turbines) and operational starting and finishing heads for the turbines are obtained from [3]. Utilizing the M2 tide as the single forcing input, comparisons of power predictions between 2D and 0D model are shown to have good agreement (Fig.4), with 0D predictions of mean power output higher than numerical results by about 1.8%. An upper bound for power production for the Swasea Lagoon is obtained by applying an 80% turbine efficiency to the expected power output by Prandle [1] (i.e. 37% of the total energy extracted by instantaneously filling and emptying a tidal lagoon during a cycle at peak Ebb and Flood tides respectively). The back-of-the-envelope prediction surpasses the 2D model by 9%, as expected from an upper bound.

Conclusions

A boundary condition for simulating the operation of a two-way tidal lagoon was successfully implemented into DG-ADCIRC, and verified against a 0D model and analytical results. For the verification process, two domains were studied: a simple rectangular model and the Swansea Tidal Lagoon included in the West Coast of UK. Evaluation of the rectangular model allowed verification of mass conservation across the interior barrier. Simulations with the more complex Swansea model showed the accuracy of the numerical method when compared with either analytical or back-of-the-envelope predictions.

Acknowledgements:

TMM would like to thank the Brazilian funding agency CAPES, for financing the current research.

References:

[1] Prandle, D. (1984). Simple theory for designing tidal power schemes, *Advances in water resources* 7(1), 21-27.

[2] Zhou, J., Pan, S., Falconer, R. A. (1984). Optimization modelling of the impacts of a Severn Barrage for a two-way generation scheme using a Continental Shelf model. *Advances in water resources*. **7(1)**, 21-27.

[3] Angeloudis, A., Falconer, R. A., Bray, S., and Ahmadian,R. (2016). Representation and operation of tidal energy im-poundments in a coastal hydrodynamic model. *Renewable Energy*, **99**, 1103–1115.

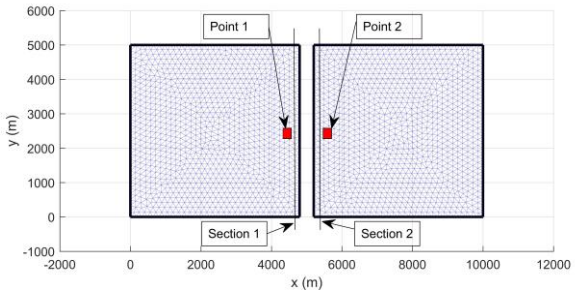

Fig. 1. Rectangular model for mass conservation.

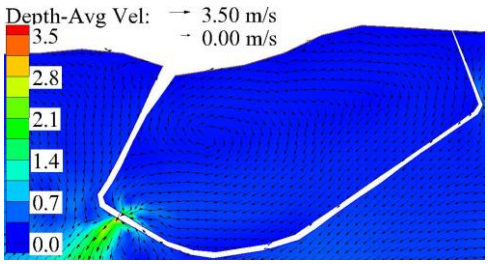

Fig. 2. Ebb-Stage Swansea Tidal Lagoon.

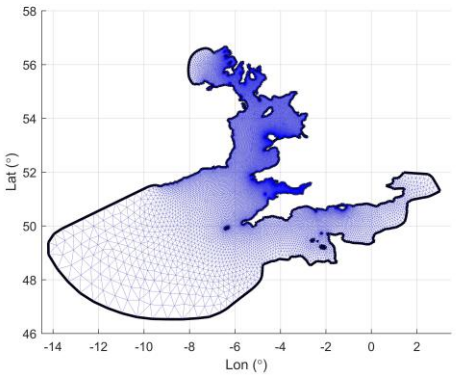

Fig. 3. West Coast of UK model.

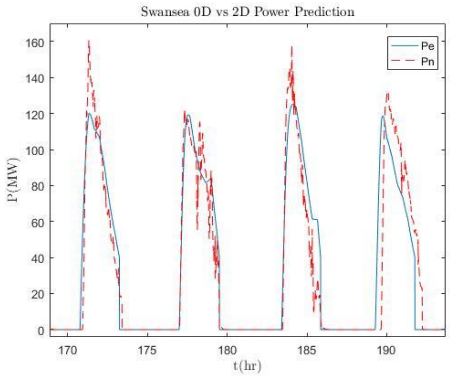

Fig. 4. Swansea Power (2D vs 0D) models.

Misalignment of currents and waves at tidal energy sites

Matt Lewis*, Simon Neill, Peter Robins, Alice Goward-Brown
Bangor University
*m.j.lewis@bangor.ac.uk

Tim Stallard
Manchester University

Summary: To date, tidal energy research has assumed that waves travel in-line with tidal currents; with either waves following or opposing the tidal current. We hypothesize tidal currents generally follow bathymetric contours, whilst waves propagate perpendicular to these contours due to refraction. Waves co-existing obliquely to a current, and misalignment between the flood and ebb tidal direction, were observed in a 2 month ADCP deployment at a tidal-stream energy site (Northwest Anglesey Demonstration Zone, UK). Therefore, studies of device performance and resilience should consider misalignment in their experiment design beyond channelized or rectilinear flow assumptions (e.g. in flume facilities and CFD model formulations).

Introduction

Tidal energy investor confidence requires improved predictions of electricity generated and device reliability. It is desirable to mitigate load variation to maximise reliability of components, such as blades. Therefore, realistic oceanographic conditions, especially wave-tide interaction and oblique wave events, are essential to understand to inform resilient and efficient tidal energy devices designs. Likely loadings on tidal turbines during operating conditions, and potential shut-down limits to avoid damage, due to waves is of crucial importance to turbine device developers.

Typically, devices-scale studies of performance or resilience use scaled tank experiments or high-fidelity computational fluid dynamics (CFD) studies; with realistic ocean conditions parameterised and imposed at the boundaries (e.g. [1]). For example, the misalignment of flow between the flood and ebb tidal-direction plane has been hypothesized [2], and effect to device performance studied [3], allowing designs of yaw devices (to face the direction of flow). However, little research has investigated wave-current malalignment at tidal energy sites.

To date, research on tidal turbine loading in waves has largely addressed waves that travel in-line with tidal currents (waves following or opposing the current). Tidal currents typically follow bathymetric contours, whilst waves propagate obliquely to these contours due to refraction; hence waves may propagate out-of-line (obliquely) to the tidal current. Waves co-existing obliquely to a current could be an important design condition at tidal stream sites [4]; therefore, our aim is to use observations of wave and current fields to determine their existence and frequency.

Methods

Data was collected using a 600kHz 5-beam ADCP, with nearby waverider buoy, both of which were located at the Crown Estate tidal-stream demonstration zone Anglesey UK (53.32°N 4.78°W) during a 2 month (Sept – Nov 2014). The wave climate, and the directional wave climate relative to tidal current direction, was studied to prove the existence of oblique wave events proposed in [4], and to add further knowledge to the wave climate of tidal energy sites. This wave and current climate data is compared to other tidal energy site surveys around the Irish Sea, and Pentland Firth (see [4]); with wave-current misalignment, and flood-ebb directional misalignment quantified.

Results

Significant misalignment of wave and current fields observed in the two month record was observed (see Fig. 1), and misalignment in flood-ebb direction also observed. Only 8% of the 61 day record was found to contain waves “inline” (±20° tolerance for error and measurement uncertainty) to the ADCP observed tidal current. Analysis of the wave climate showed the oblique wave climate (>20° to tidal current direction) to be larger than the inline wave climate. Indeed, “fully” oblique (waves propagating at angles of ~90° to tidal current direction) were observed for significant wave events (significant wave height, *Hs*, above 1m) and the largest wave events (*Hs*>4m) were observed to be oblique. Our observations are compared to observations from the Pentland Firth in 2012 (considered a more channelized tidal energy site [4]), where oblique wave events were also observed: >65% of waves propagate at >20° to the flow (mean Hs of 1.29 m) with a maximum wave event (*Hs* = 9.48 m and *Tz* = 7 s) shown to be 28° out-of-line to the direction of tidal flow (from [4]). These observations of a significant wave

climate at tidal energy sites, including oblique wave events, indicates wave-current and wave-tidal energy device interaction is an important research topic.

Conclusions

To inform resilient and efficient tidal energy device designs, it is essential to understand realistic oceanographic conditions. Here, we demonstrate the occurrence of large and oblique (to the current) wave conditions. These oblique wave events are likely to have significant influence of waves on turbine loading. Therefore, methods and tools must be developed to fully investigate realistic environmental conditions at turbine scale; such as oblique wave event methods in CFD. Furthermore, the fundamental problem of intermediate water depth waves, propagating over turbulent, sheared flow, is essential to remove barriers to industry development.

References:

[1] Apsley, D, Stallard, T. and Stansby, P.K. Actuator line CFD modeling of tidal-stream turbines in arrays with experimental evaluation. Renewable Energy, 2017 (in review).
[2] Lewis, M., Neill, S., Robins, P. E., & Hashemi, M. R. 2015. Resource assessment for future generations of tidal-stream energy arrays. Energy, 83, 403-415.
[3] Frost, C.H., Evans, P.S., Harrold, M.J., Mason-Jones, A., O'Doherty, T. and O'Doherty, D.M., 2017. The impact of axial flow misalignment on a tidal turbine. Renewable Energy, 113, pp.1333-1344.
[4] Lewis M, Neill S, Hashemi, MR. 2014. Realistic wave conditions and their influence on quantifying the tidal stream energy resource. Applied Energy, 136; 495 – 508.

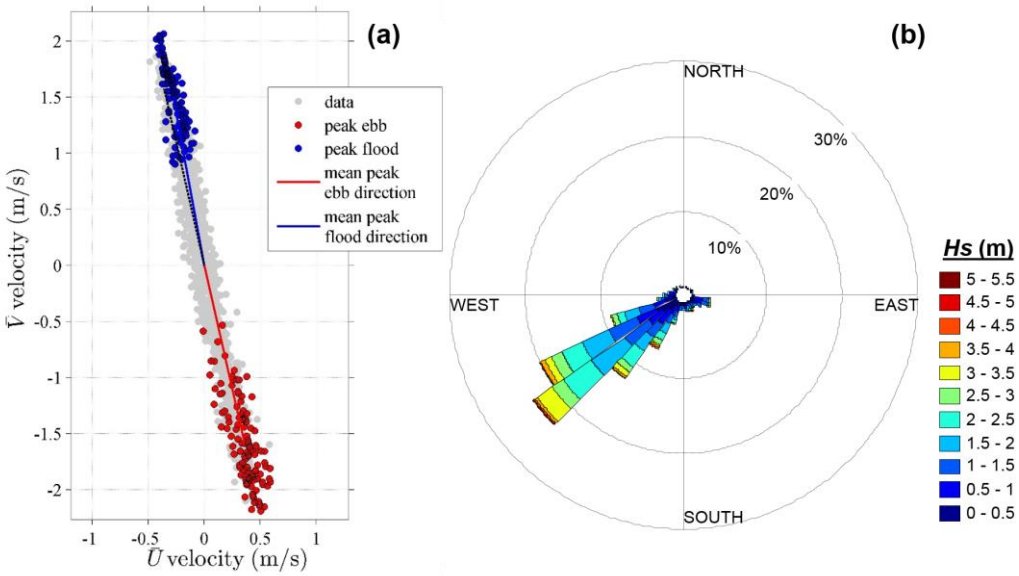

Fig. 1. Oceanographic conditions observed with a 5-beam ADCP deployed the Crown Estate tidal-stream demonstration zone, Anglesey UK. Depth-averaged tidal current (a) and the directional wave climate (b), shown here for direction and significant wave height (*Hs*), used to estimate wave-current misalignment occurrence.

Optimization of Tidal Turbines Blades for Low Velocity Flow

Job Immanuel Encarnacion*, Cameron Johnstone
Department of Mechanical and Aerospace Engineering, University of Strathclyde, UK

Summary: The renewable energy in the Philippines has a very low share in the country's power generation. However, the renewable energy plan of the country aims to increase the production of power from renewable energy and included in the targets is the addition of a 75GW ORE capacity. It is then determined that the total potential of tidal in-stream energy in the Philippines is more than 80GW. Although, the tidal flow around the country is very low, averaging at about 0.40-0.80m/s. This inhibits the development of tidal turbine technology since TSTs are currently very expensive and the low velocity flow will translate to very low energy captured per turbine. Current efforts in the country to assess the possible generation from TSTs deals with inappropriate matching of current technology to low velocity flow. Thus, a blade design that is optimized for low velocity flow is created. Initial results show that a high tip speed ratio blades such as the NACA 63-8XX series is appropriate for low velocity flows since the low Ct value at the peak Cp occurring at higher TSRs. This should lessen the cost of manufacturing and material. Integration of the design methodology is being done as of the moment.

Introduction

As of 2016, the energy mix of the Philippines is still dominated by coal accounting for 47.7% of the total generation. The renewable sector only accounts for 24.2% of the energy mix with 12.2% coming from geothermal generation [1]. This is an indication of low utilization of renewable energy resources in the country although the National Renewable Energy Program has set a roadmap to achieve an additional 15,236MW RE by 2030 from the 2010 generation of 5,369MW. The roadmap includes an addition of 75MW of ocean energy by 2025 [2].

It is estimated that the total potential of tidal in-stream energy in the Philippines is more than 80GW [3]. However, as of today, ocean energy devices harnessing this huge potential are yet to be utilized in the country as the cost of infrastructure is very high and the region is dominated by low velocity flow, which translates to power output per unit for each turbine. Unlike the UK, average tidal current velocity in the Philippines range from 0.40-0.80m/s with a maximum of about 1.4-1.6m/s [4]. Nonetheless, resource assessment for tidal current continues and it is determined that the highest annual available energy in the Northern Philippines, in the Luzon Strait, reaches up to 2.60MWh/m^2 [4], making it a suitable site for initial deployment of tidal turbines.

However, there is an apparent lack of a suitable turbine design that may harness energy in low velocity flows. Current studies in the Philippines usually involve the adoption of existing turbine technologies with a cut-in speed that matches the average range of tidal velocities [4]. This is misleading as existing technologies are not specifically designed for low velocity flow. Thus, a design for tidal turbines operating in low velocity flows is done to enable the capture of tidal energy in regions such as the Philippines.

Methods

BEMT is used to analyze the torque and the thrust on the blades. A code written in Matlab [5] and Python is used to implement BEM methods on a steady state low velocity flow of 0.4 to 1.0 m/s. Two blade profiles are analysed, the NREL S814 and the NACA 63-8XX series blades. These blade profiles are chosen due to the occurrence of their peak Cp at different TSRs – at low (TSR = 4) and high (TSR = 6) TSRs respectively. The comparison is done to determine how a low-tip speed ratio and high-tip speed ratio blade would fair in a low velocity environment; and which would be more suitable to use for low velocity tidal flows.

The BEM method is then incorporated into the blade design methodology to come up with an optimized blade profile for low velocity flow. Gracie-Orr [6] developed a blade design methodology for overspeed regulation which limits the operation of turbines at low TSRs. This methodology serves as a basis for developing the appropriate blade profile for low velocity flows and the TSR region is determined by the initial comparison of the high and low TSR blades. It is worth noting that cavitation becomes an issue on high TSRs when a turbine is used in high velocity flow [6]. This effect is reduced for turbines operating in low velocity flows since higher TSRs do not result in angular speeds as high as the ones achieved for higher TSRs at high flow velocity.

In addition to the blade design, generator specifications and speed control measures are also investigated as to how they could be used to optimize the performance of the whole turbine in terms of converting the flow energy and delivering power.

Results

The Cp-λ and Ct-λ curves for each of the blades are obtained and shown in Figures 1 and 2. It is apparent that the lower loads are present in the peak Cp of the high tip speed ratio blade NACA 63-8XX with a value of less than 0.5 while the NREL S814 has a Ct value of 0.8.

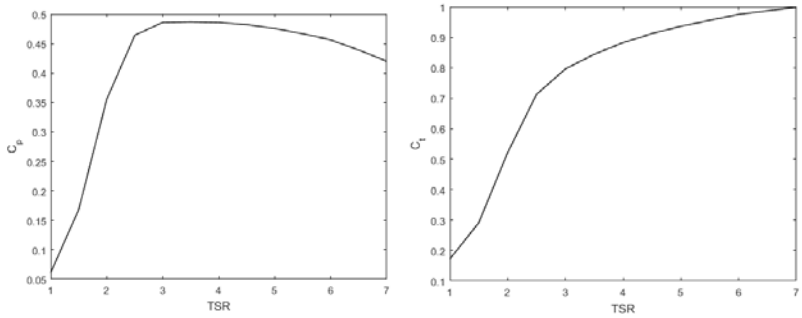

Figure 1. Cp-λ and Ct-λ curves for NREL S814

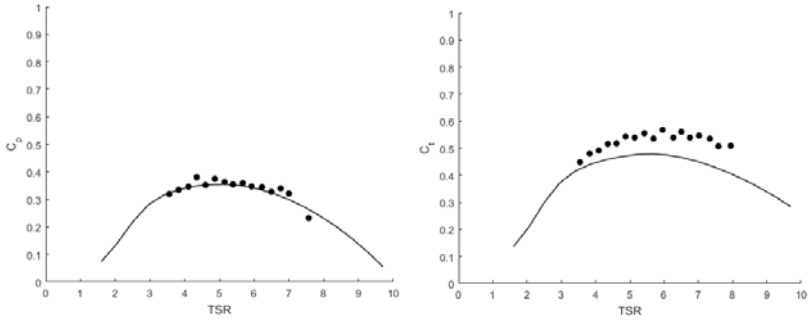

Figure 2. Cp-λ and Ct-λ curves for NACA 63-8XX

For a low velocity site, it is important to consider the loads that are experienced by the blade since any reduction in load will translate to a reduction in cost. As previously discussed, the lower energy present in low velocity tidal flow poses a problem if an expensive turbine is used. This brings up the LCOE and would result in an economically infeasible adoption of the technology. Thus, it is shown that high tip speed ratio blades are very much attractive in low velocity situations because of the lower loading. These blade can be used since cavitation is reduced as compared to using high tip speed ratio blades at high velocity flows.

Conclusions

The results show a possible characteristic of optimized blades operating in low velocity flow. The lower values of Ct would result in lower thrust loads and thus, less expensive material may be used in manufacturing. The higher tip speed ratio blades can be used since cavitation is reduced in lower velocity flows.

References:

[1] Posadas, J.C. (2017). Philippine Energy Plan 2017-2040. Presentation to ACD Conference toward Energy Security, Sustainability and Resiliency
[2] Delos Santos, A.S.A (2011). Renewable Energy in the Philippines. Presentation. International renewable Energy Agency.
[3] Abundo, M.L.S (2016). Marine Renewable Energy for Island Micro-Grids in South East Asia. OceanPixel
[4] M.D. Bausas., O.D.G. de Luna and M.R.C.O Ang. Tidal In-stream Energy Resource and Conversion Device Suitability Analysis in the Northern Philippines. Proceedings on Asian Conference on Remote Sensing. 2016.
[5] Nevalainen, T (2016). The effect of unsteady sea conditions on tidal stream turbine loads and durability. PhD thesis. University of Strathclyde
[6] Gracie-Orr, K (2017). A blade design methodology for overspeed power regulation of horizontal axis tidal turbines. PhD thesis. University of Strathclyde

Measuring marine turbulence kinetic energy with 4- and 5-beam ADCPs

Michael Togneri*, Dale Jones, Ian Masters
College of Engineering, Swansea University

Matt Lewis, Simon Neill, Sophie Ward, Marco Piano
School of Ocean Sciences, Bangor University

Summary: Acoustic Doppler current profilers (ADCPs) are instruments that are frequently used to measure flow properties at energetic tidal sites. Conventional ADCPs employ four-beams in a so-called Janus configuration, but since 2014 devices with an additional fifth vertical beam have become more commonplace. This fifth beam is typically employed to measure wave properties, but its measurements can also be used to supplement turbulence measurements taken with the off-vertical beams. In this presentation, we discuss the advantages and disadvantages of this approach, using a dataset from the West Anglesey Tidal Demonstration Zone that exhibits both strong tidal currents and significant wave activity.

Introduction

Turbulence in marine currents is a significant determinant of tidal energy converter (TEC) survivability and reliability, so being able to accurately characterise it is a matter of concern for device developers [1,2]. Any consideration of marine turbulence, at least in the relatively shallow waters in which TECs are deployed, should also take account of the influence of the ocean surface as an upper bound, where surface waves can increase turbulence by their interactions with the mean flow [3].

ADCPs are a widely-used instrument for measuring marine flow properties, including those related to turbulence. They use Doppler shift in the echoes of acoustic pings to measure flow velocities along 'beams' transmitted from the instrument. At TEC sites, ADCPs are typically deployed on the seabed looking upward. Conventional ADCPs use three or four beams inclined away from the vertical, but more recent models add a fifth vertical beam. The work presented here examines how the extra measurements made possible by this fifth beam might be used to improve estimation of turbulent parameters [4].

All measurements used in this study were taken from a deployment of an RDI Sentinel V five-beam device near the West Anglesey Tidal Demonstration Zone (DZ) between 19th September and 19th November 2014. Concurrent measurement of wave height, period and direction were taken from a buoy approximately 2km to the south of the ADCP. A detailed description of the deployment is available in [5].

Methods

As ADCPs measure single components of velocity at spatially-separated locations, it is not in general possible to have direct knowledge of turbulence properties at a single point. Instead, a variety of methods are employed to infer knowledge of turbulence characteristics from the measured beam velocities. Here, we rely primarily on the variance method, which relates the autocovariance of the in-beam velocity components to turbulence properties such as the turbulent kinetic energy (TKE), k. The formulation of this relationship differs in the four- and five-beam ADCP layouts.

Using B_i to denote the velocity in the ith beam of the ADCP, and B_i' the corresponding fluctuation velocity (i.e., the difference between the instantaneous beam velocity and its mean value), we can express the autocovariance of the ith beam as $\langle B_i'^2 \rangle$, with angle brackets denoting a suitable time-average. For a four-beam ADCP, this gives an estimate for k (which we denote k_4 to distinguish it from five-beam estimates) of:

$$k_4 = \frac{\sum_{i=1}^{4} \langle B_i'^2 \rangle}{4 \sin^2 \theta (1 - \xi(1 - \cot^2 \theta))}$$

Here, θ is the angle between the beam direction and the vertical, and ξ parametrises the proportion of TKE contained in vertical fluctuations. The value of ξ cannot be measured directly, and is instead assumed from semi-

* Corresponding author.
Email address: M.Togneri@swansea.ac.uk

empirical models of open-channel flow. With a five-beam ADCP, however, this additional assumption is not required. Using B_5 to refer to the fifth, vertical beam, we can estimate TKE from a five-beam device as:

$$k_5 = \frac{\sum_{i=1}^{4}\langle B_i'^2\rangle}{4\sin^2\theta} + \left(\frac{1}{2} - \cot^2\theta\right)\langle B_5'^2\rangle$$

Both of the above expressions for TKE estimates neglect the effect of instrument noise. We are particularly interested in how this affects the variance of the TKE estimate. Since both estimates take the form $k = \sum_i c_i \langle B_i'^2\rangle$, to determine $\mathrm{Var}(k)$ we can find their variances by a sum of weighted random variables: $\mathrm{Var}(k) = \Sigma_i c_i'^2 \mathrm{Var}(\langle B_i'^2\rangle)$. These variances of variances are calculated using bootstrapping.

Results

We find that adding the data from the fifth beam has very little effect on the estimated value of k in the bottom half of the water column, as can be seen in figure 1. This suggests that any improvement in TKE estimates from adding a vertical beam will be very minor. For the results shown in figure 1, four- and five-beam estimates differ by only 3.6% on average.

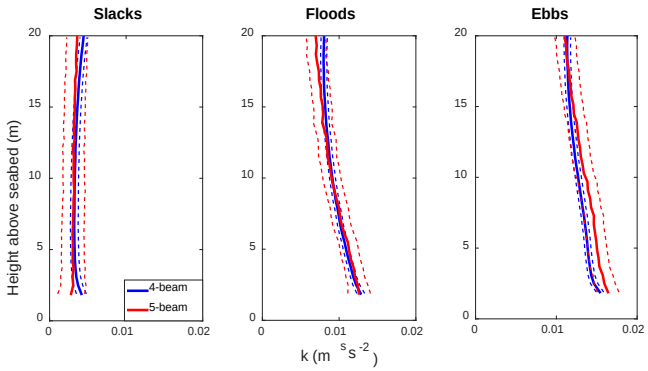

Fig. 1. Comparison of four- and five-beam TKE estimates for the deepest 20m of the deployment site. Solid lines show mean profiles, dashed lines show one standard deviation above and below mean value.

However, it is also clear from this figure that variance in the five-beam estimate is significantly higher – by a factor of 8 on average. This is due to a combination of the higher noise in the vertical beam and its relatively high weighting in the calculation of k_5.

Nearer the surface, however, there is an additional complication due to wave action. The variance method cannot distinguish between velocity fluctuations caused by turbulence and those caused by wave action. This means that the estimated TKE values become very high near the surface, particularly at times when there are strong waves. This tendency is less pronounced in the k_5 estimate of TKE than the k_4 estimate, as can be seen in figure 2. This shows that as we move towards the surface, and therefore the part of the water column where wave action is more important, k_4 tends to exceed k_5 by an increasing margin. Thus, although there is a general tendency for five-beam estimates to be more uncertain than four-beam estimates, in cases where significant wave action is expected a five-beam configuration will reduce contamination of turbulence measurements by waves compared to a four-beam configuration.

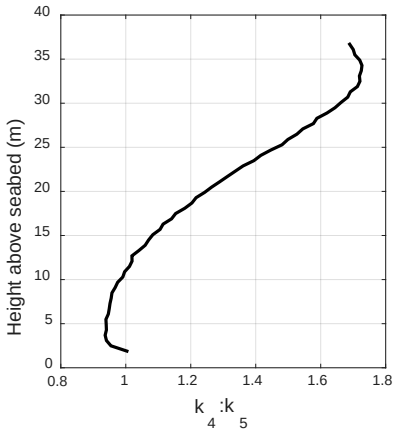

Fig. 2. Average ratio of four-beam to five-beam estimates of TKE throughout water column

References:

[1] Val, D. V., Chernin, L., Yurchenko, D. V. (2014). Reliability analysis of rotor blades of tidal stream turbines. *Reliab. Eng. Syst. Safe.* **121**, 26-33

[2] Sellar, B. G., Wakelam, G., Sutherland, D. R. J., Ingram, D. M., Venugopal, V. (2018). Characterisation of Tidal Flows at the European Marine Energy Centre in the Absence of Ocean Waves. *Energies.* **11**(1), 176.

[3] Lewis, M. J., Neill, S. P., Hashemi, M. R., Reza, M. (2014) Realistic wave conditions and their influence on quantifying the tidal stream energy resource. *Appl. Energ.* **136** 495-508.

[4] Togneri, M., Jones, D., Neill, S., Lewis, M., Ward, S., Piano, M. (2017). Comparison of 4- and 5-beam acoustic Doppler current profiler configurations for measurement of turbulent kinetic energy. *Energ. Proced.* **125**, 260-267

[5] Piano, M., Neill, S. P., Lewis, M. J., Robins, P. E., Hashemi, M. R., Davies, A. G., Ward, S. L., Roberts, M. J. (2017). Tidal stream resource assessment uncertainty due to flow asymmetry and turbine yaw misalignment. *Renew. Energ.* **114**(B), 1363-1375

Recent developments to compute turbines interactions in an ambient turbulent flow

Clément Carlier[o,*], Camille Choma Bex[o,*], Grégory Pinon[*,1], Grégory Germain[o], Elie Rivoalen[*,#]

[*] *Laboratoire Ondes et Milieux Complexes - Normandie Univ, UNIHAVRE, CNRS, LOMC, 76600 Le Havre, France*
[o] *IFREMER, Centre Manche Mer du Nord, 150 quai Gambetta, BP 699, 62321 Boulogne-sur-Mer, France*
[#] *Laboratoire de Mécanique de Normandie - Normandie Univ, INSA ROUEN, LMN, 76600 Rouen, France.*

Summary: This paper presents the recent developments performed in a Lagrangian Vortex Method software to account for ambient turbulence. Once validated, results on wake behind a 3 bladed tidal turbine will be presented and discussed.

Introduction

The development of marine current turbines arrays has been an active research topic for some years. However, many studies are still necessary in order to fully understand the behaviour of such arrays. One of these studies is the impact of ambient turbulence on the behaviour of tidal turbines. Indeed recent studies have shown that ambient turbulence intensity highly modifies the behaviour of interacting turbines [3]. Consequently, numerical simulations must represent the ambient turbulence or at least its effects on the turbines performance and wake. This paper presents the latest numerical developments carried out at LOMC in collaboration with IFREMER in order to take into account the effects of ambient turbulence [1] and wake interaction [4].

Synthetic-Eddy-Method applied in the framework of Vortex Method

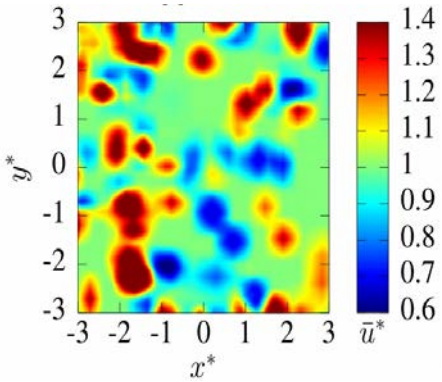

Fig. 1. Example of ambient turbulent flow generated with the Synthetic-Eddy-Method.

A new module based on the Synthetic-Eddy-Method initially proposed by Jarrin et al. [2] was implemented in the numerical code in order to represent the ambient turbulence. The general characteristics of the Synthetic-Eddy-Method will be presented together with its integration in the framework of a 3D unsteady Lagrangian Vortex method [5], which is accomplished by adding a perturbation component to the constant velocity. This ambient turbulence model is capable of reproducing a perturbed flow of any given turbulence intensity I_∞ and any anisotropic ratio (σ_u:σ_v:σ_w). This has been verified in the absence of turbines, with turbulent intensities ranging from 0% to 15% as well as typical anisotropic ratios given by Milne et al. [6]. As shown in Fig. 2, after some additions to the original model a satisfying reproduction of experimental power spectral density has been achieved. The ambient turbulence model has been further validated by comparing wakes computed for individual turbines with test data from IFREMER, carried out with turbulence intensities of either 3% (low turbulence) or 15% (high turbulence). These validations will be presented together with first results.

Results obtained in terms of wake computations

The final goal of this study is the computation of an entire farm of marine current turbines for any turbulent intensity. This hard challenge is however treated step by step, and the recent communication of Mycek et al. [4]

1 Corresponding author.
Email address: gregory.pinon@univ-lehavre.fr

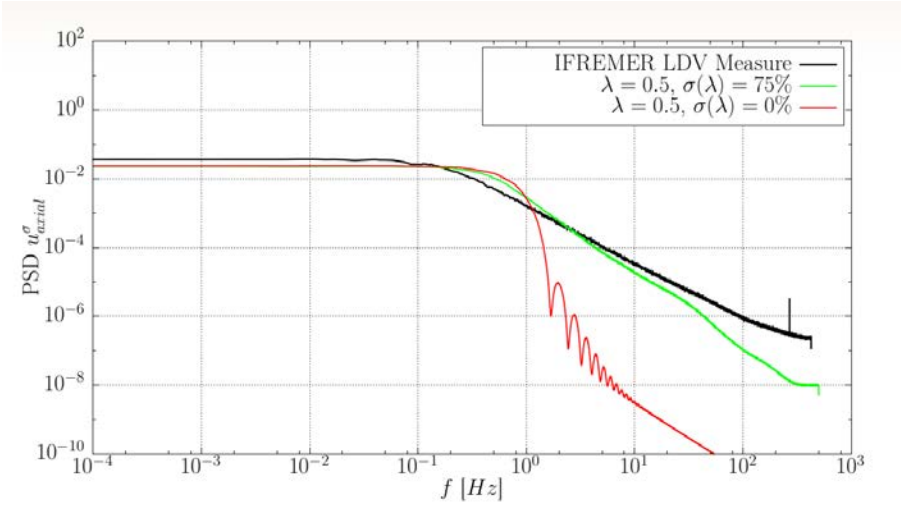

Fig. 2. Power spectral densities generated with the Synthetic-Eddy-Method compared to experimental results.

presents the numerical treatment of turbines in a farm. Computations of various configurations of 3 interacting turbines have been carried out in order to compare the results with the latest experimental trials performed at IFREMER, with turbulence intensities of either 3 or 15%. Once this configuration has been tested and validated, more complex configurations will be computed taking into account more than 3 turbines and different levels of ambient turbulence.

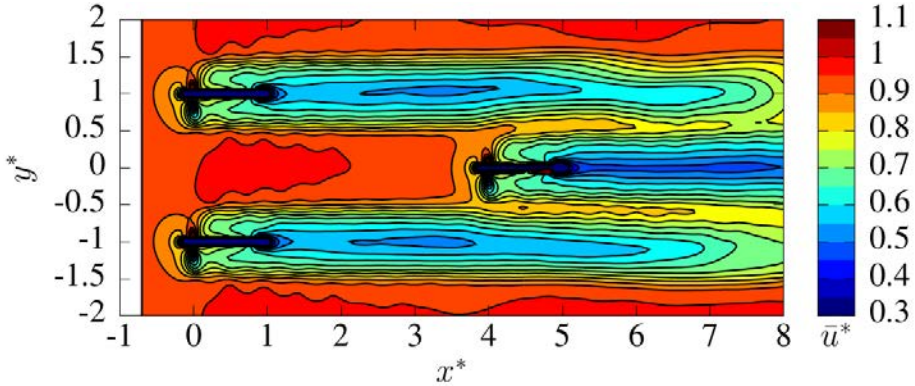

Fig. 3. Example of 3 interacting turbines.

Acknowledgements:

Clément Carlier would like to thank the Normandy Regional Council and IFREMER for the financial supports for his Ph.D. grant. Camille Choma Bex acknowledges the financial support of IFREMER for her Ph.D. grant. The authors would like to thank the CPER-ERDF program NEPTUNE financed by the Normandy Regional Council. The Normandy regional project called SEMARIN also contributed to this research. Finally the authors wish to thank the CRIANN (Centre des Ressources Informatiques et Applications Numérique de Normandie) for their numerical computation resources.

References:

[1] C. Carlier, G. Pinon, B. Gaurier, G. Germain, and E. Rivoalen. A synthetic eddy-method to represent the ambient turbulence in numerical simulation of marine current turbine. In 10th European Wave and Tidal Energy Conference (EWTEC), 6-11th Sept. 2015. Nantes, France.

[2] N. Jarrin, S. Benhamadouche, D. Laurence, and R. Prosser. A synthetic- eddy-method for generating inflow conditions for large-eddy simulations. International Journal of Heat and Fluid Flow, 27:585–593, 2006.

[3] P. Mycek, B. Gaurier, G. Germain, G. Pinon, and E. Rivoalen. Experimental study of the turbulence intensity effects on marine current turbines behaviour. part II: Two interacting turbines. Renewable Energy, 68(0):876 – 892, 2014.

[4] P. Mycek, G. Pinon, C. Lothodé, A. Dezotti, and C. Carlier. Iterative solver approach for turbine interactions: application to wind or marine current turbine farms. Applied Mathematical Modelling, 41:331 – 349, 2017.

[5] G. Pinon, P. Mycek, G. Germain, and E. Rivoalen. Numerical simulation of the wake of marine current turbines with a particle method. Renewable Energy, 46(0):111 – 126, 2012.

[6] I. A. Milne, R. N. Sharma, R. G. J. Flay, and S. Bickerton. Characteristics of the turbulence in the flow at a tidal stream power site. Philosophical Transactions of the Royal Society A : Mathematical, Physical and Engineering Sciences, 371(1985) , 2013.

6th Oxford Tidal Energy Workshop (OTE 2018)

Participants

Tom Adcock	University of Oxford
Federico Zilic de Arcos	University of Oxford
Federico Attene	University of Lancaster
Paul Bonar	University of Edinburgh
Alistair Borthwick	University of Edinburgh
Alice Goward Brown	Bangor University
Byron Byrne	University of Oxford
Jose Manuel Rivera Camacho	University of Strathclyde
Bowen Cao	University of Oxford
Lei Chen	University of Oxford
Camille Choma Bex	Laboratoire Ondes et Milieux Complexes, Le Havre
Ian Corder	
Matt Edmunds	Swansea University
Job Immanuel Encarnacion	University of Strathclyde
Xingya Feng	University of Oxford
Esteban Ferrer	Universidad Politécnica de Madrid
Ahmad Firdaus	University of Oxford
Zoe Goss	Imperial College
Ross Gwenter	Swansea University
Guy Houlsby	University of Oxford
Jack Hughes	Swansea University
Monika Kreitmair	University of Edinburgh
Thomas Lake	Swansea University
Matt Lewis	Bangor University
Qian Ma	University of Oxford
Ian Masters	Swansea University
James McNaughton	University of Oxford
Tulio Moreira	University of Oxford
Hannah Mullings	University of Manchester
Takafumi Nishino	Cranfield University
Mohamad Hasif Bin Osman	University of Oxford
Pablo Ouro	Cardiff University
Grégory Payne	University of Strathclyde
Grégory Pinon	Normandie Univ, CNRS, LOMC, Le Havre

Esther Quaintmere	University of Hull
Peyman Razi	University of North Carolina at Charlotte
Hannah Ross	University of Washington
Gabriel Scarlett	University of Edinburgh
Andrea Schnabl	University of Oxford
Robert Hudson Von Shuker	Shuker & Sons
Richard Simons	University College, London
Amanda Smyth	University of Cambridge
Timothy Stallard	University of Manchester
Vance Tan	University of Oxford
Michael Togneri	Swansea University
Merel Verbeek	Delft University of Technology
Ignazio Maria Viola	University of Edinburgh
Christopher Vogel	University of Oxford
Sophie Ward	Bangor University
Richard Willden	University of Oxford
Alison Williams	Swansea University
Aidan Wimshurst	University of Oxford
Anna Young	University of Cambridge
Ruiwen Zhao	University of Edinburgh
Xiaowei Zhao	University of Warwick